Ancient introgression between highly divergent fungal sister species

A genomic analysis of

Trichaptum abietinum and *Trichaptum fuscoviolaceum*

Vilde Bruhn Kinneberg

Master Thesis
Ecology and Evolution
60 credits

Department of Biosciences
Faculty of Mathematics and Natural Sciences

UNIVERSITY OF OSLO

August / 2021

2021

Ancient introgression between highly divergent fungal sister species – a genomic analysis of *Trichaptum abietinum* and *Trichaptum fuscoviolaceum*

Author: Vilde Bruhn Kinneberg

http://www.duo.uio.no/

Print: Reprosentralen, Universitetet i Oslo

Ancient introgression between highly divergent fungal sister species

A genomic analysis of *Trichaptum abietinum* and *Trichaptum fuscoviolaceum*

Acknowledgements

To my supervisors: Thank you, Inger for being such a wonderful, intelligent, and kind supervisor. You gave me the best introduction to academia that I could possibly get. Thank you, Dabao for your patient guidance, help and friendship. The way you seemingly float through life is mindboggling. Thank you, Peris for your advice and for letting me struggle with bioinformatic problems for hours when you could have shown me the solutions in a few minutes (it has taught me a lot). I hope you have found a good academic home in Oslo Mycology Group.

Mark, thank you for your invaluable help and for taking the time to discuss results and approaches with me. Thank you, Inger, Dabao, Dr. David Malloch, Dr. Stephen R. Clayden, M.Sc. Amanda Bremner and Dr. Carolina Grometta for collecting samples included in my thesis. To the fungal masters: Ine, Sondre, Eivind, Markus, and Erik, thank you for the last two years. The master experience has truly become one to remember because of you. I hope The Lounge will live on without us. Malin, thank you for introducing me to the world of Oslo Mycology Group. Trond, thank you for introducing me to Inger. Thank you, Cecilie and Chiara for your help and for solving all my lab emergencies (like putting out ethanol fires in the safety cabinet). To everyone at Oslo Mycology Group: Thank you for constituting such a brilliant collection of people. To my parents: Thank you for teaching me independence and letting me explore all my interests before ending up with biology.

And lastly, thank you Markus, for always being there. You mean the universe to me.

Abstract

The evolutionary past of lineages can be intricate despite well-resolved phylogenies. When speciation occurs on a continuous scale, reproductive barriers can remain incomplete and give way to introgression. If species have diverged over large time spans, the signs of introgression can get blurred by recombination and genetic drift, leaving only small traces of admixture in the genomes. The kingdom of Fungi originated over a billion years ago, and it might contain many species exhibiting signs of ancient introgression. In this study, I investigate introgression between two fungal sister species, *Trichaptum abietinum* and *T. fuscoviolaceum*. The species constitute monophyletic taxa but are morphologically and ecologically similar, with overlapping habitats. I aimed at investigating the possibility of introgression between these species by conducting whole genome sequencing of individuals from populations in North America and Europe. I applied divergence analyses (F_{ST} and d_{XY}) to assess the genome wide nucleotide differences between the species, and ABBA-BABA analyses (D and f statistics) to investigate introgression. This study is one of few conducting such analyses to examine introgression among mushroom-forming fungi. I also performed crossing experiments to assess reproductive barriers between the species. The results reveal *T. abietinum* and *T. fuscoviolaceum* to be highly divergent sister species with genome wide high F_{ST} and d_{XY} values. The crossing experiments further show the species incompatible in vitro. Despite the large genetic differences and incompatibility, the species show signs of introgression with small regions of high or low f_{dM} values scattered throughout the genomes. Ghost populations (both unsampled extant and extinct populations) may be involved in the introgression. Moreover, the introgression is most likely ancient and might have affected the evolutionary trajectory of the species. This study demonstrates that ancient introgression can be found among mushroom-forming fungi, but the implications of gene transfer across species and possible retention of introgressed genes from extinct lineages remain unknown.

Table of contents

1 Introduction

Classifying organisms into groups, or taxa, has been an interest of humans for ages, from the concept of essentialism in ancient Greek, through the binomial taxonomy of Linnaeus and the evolutionary concept of species presented by Darwin and Wallace, to modern species concepts rooted in genetics (Zachos, 2016). The process of how new species evolve, called speciation, is still an active field of research. This mainly stems from the difficulty of understanding the intricacies of the speciation process. The boundary between populations and species is hard to define, but research on speciation can nevertheless give insight into the mechanisms that impact the evolutionary trajectory of taxa (Chandler and Gromko, 1989).

Speciation can occur rapidly, changing the course of evolution in a single event, or over a long period of time with gradual shifts from semi-compatible populations to complete divergence (Nosil et al., 2017). When speciation occurs on a continuous scale, barriers to gene exchange do not arise immediately and gene flow between divergent populations can sustain (Ravinet et al., 2018). When populations diverge into species, but complete barriers have not yet evolved, reproduction between species can yield hybrid individuals (Harrison and Larson, 2014). If these hybrids backcross into the parental species, a scenario dubbed introgression (Anderson and Hubricht, 1938), it can result in unique genetic combinations (Stukenbrock, 2016). The amalgamation of genes across lineages can also contribute to the strengthening of barriers to gene exchange, a process known as reinforcement (Butlin, 1987). Reinforcement occurs because hybrids often have detrimental gene combinations, resulting in poorer fitness compared to the parental species (Abbott et al., 2013). Consequently, hybridization is a double-edged sword; it can both give rise to beneficial gene combinations which selection can act upon, and at the same time accelerate the divergence process by reinforcing reproductive barriers (Abbott et al., 2010).

Hybridization is now established as a common event in nature and have been recognized as a central mechanism of speciation in several taxa (Abbott et al., 2013; Mallet, 2008), including plants (e.g., *Senecio* ssp.; Hegarty and Hiscock, 2005; Wood et al., 2009), animals (e.g., *Heliconius* butterflies; Mavárez et al., 2006), and certain fungal groups such as yeasts (e.g., *Saccharomyces* sp.; Langdon et al., 2019) and pathogenic fungi (e.g., *Zymoseptoria pseudotritici*; Stukenbrock et al., 2012). Even though hybridization among fungal pathogens has been studied comprehensively in recent years due to its role in the emergence of new pathogens (e.g., Hessenauer et al., 2020), research on hybridization, and more specifically introgression, among other fungal taxa such as the Agaricomycotina (mushroom-forming fungi) is meagre. There are a few examples from genera including *Pleurotus* (Bresinsky et al., 1987), *Heterobasidion* (Garbelotto et al., 1996; Giordano et al., 2018; Stenlid and Karlsson, 1991), *Armillaria* (Baumgartner et al., 2012) and *Microbotryum*

(Devier et al., 2010), indicating that hybridization might be a common but understudied mechanism of speciation and gene exchange among taxa in this branch of the tree of life.

The subphylum Agaricomycotina is an old and diverse taxon, with about 20 000 species described worldwide and age estimates ranging from 380 – 960 million years (Hibbet, 2006). With old taxa, it can be difficult to discover if hybridization has occurred, because genomic signs of introgression can get blurred over macroevolutionary time. The evolutionary history of a genus can be complex even though current investigations recover clear and resolved phylogenies (Keuler et al., 2020). With modern technology, signs of ancient introgression have been possible to detect using high-throughput sequencing and statistical models (e.g., Crowl et al., 2019; Ravinet et al., 2018). Regions of ancient introgression might constitute small parts of otherwise divergent genomes, due to the erosion of linkage by recombination coupled with a long period of mostly independent evolution (Ravinet et al., 2018). The retention of these regions can be a corollary of adaptational benefits, but the patterns of introgression can also be difficult to distinguish from mechanisms such as incomplete lineage sorting (i.e., preservation of ancestral polymorphisms; Platt et al., 2019). Methods have been developed to circumvent confounding signals (e.g., ABBA-BABA statistics) and theoretically it is possible to bioinformatically separate introgression from other evolutionary processes (Martin, Davey and Jiggins, 2014). Research on introgression between divergent species can reveal important contributions to the evolutionary history of these taxa (e.g., ecological adaptations) and increase our understanding of how life evolves.

An interesting case appears in the fungal sister species *Trichaptum fuscoviolaceum* (Ehrenb.) Ryvarden and *Trichaptum abietinum* (Dicks.) Ryvarden (Figure 1 and 2). These agaricomycetes are saprotrophic, white rot fungi growing on conifers across the northern hemisphere. They are phylogenetically well separated species (Seierstad et al., 2020) but look very similar apart from the hymenium; *T. abietinum* is poroid and *T. fuscoviolaceum* is irpicoid (Figure 2). Studies of *T. abietinum* indicate that the species has a clear population structure, where reproductive barriers occur between both populations of different and the same geographic area. This pattern is particularly obvious in North America, where two populations referred to as the Circumboreal North American and the North American population occur in sympatry and are reproductively isolated (i.e., form intersterility groups; Kauserud and Schumacher, 2003; Ko and Jung, 2002; Macrae, 1967; Seierstad et al., 2020). Such intersterility groups have not been detected among populations of *T. fuscoviolaceum* (Macrae, 1967; Seierstad et al., 2020). Reproductive barriers have been documented between *T. abietinum* and *T. fuscoviolaceum* in vitro (Macrae, 1967). However, putative introgression between the sister species have been suggested in previous research based on ribosomal genetic markers (Kauserud and Schumacher, 2003; Seierstad et al., 2020).

In this study, I investigate collections of *T. fuscoviolaceum* individuals from Canada (the Canadian population; Figure 1) and Italy (the Italian population; Figure 1), together with individuals from two *T. abietinum* populations from Canada (the North American and the

Circumboreal North American population; Figure 1). The aims of the study are: (1) To explore potential introgression by conducting large-scale whole-genome sequencing of different populations of *T. abietinum* and *T. fuscoviolaceum*. Should introgression be discovered, I aim at identifying whether it occurred between extant species or as an ancient introgressive event among ancestral populations. (2) To assess the possibility of current gene flow by testing compatibility across species through crossing experiments.

Based on previous research, I hypothesize that *T. fuscoviolaceum* and *T. abietinum* do not hybridize frequently due to a well resolved phylogeny where *T. abietinum* and *T. fuscoviolaceum* form monophyletic groups. Earlier crossing experiments by Macrae (1967) have also shown the species incompatible. However, due to their overlapping habitat and similar ecology, I hypothesize that the sister species might have a shared history that involves introgression, possibly having occurred among ancient populations.

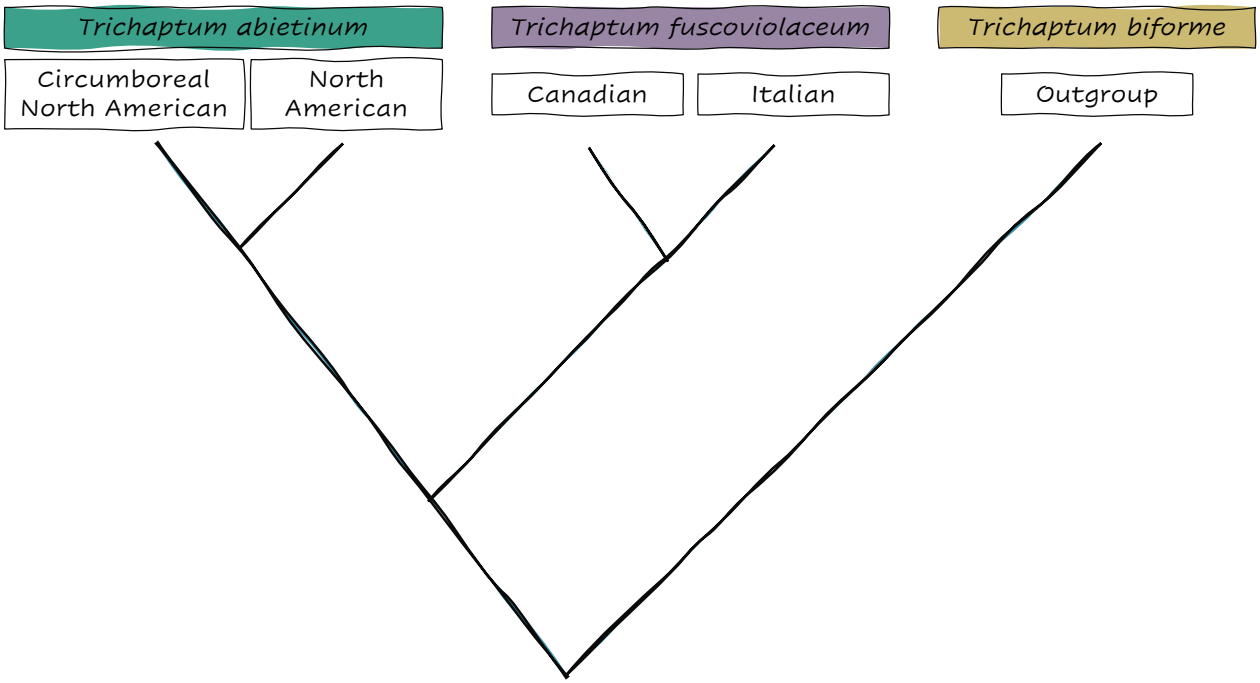

Figure 1, ***The phylogenetic relationship of species and populations used in the study.*** *The sketch depicts the phylogenetic relationship between* Trichaptum abietinum *and* T. fuscoviolaceum *together with the outgroup* T. biforme*. Species are presented in colored boxes and populations and the outgroup are denoted in white boxes. The phylogeny is based on results from Seierstad et al. (2020). The figure was made in Microsoft® PowerPoint for Mac v16.50.*

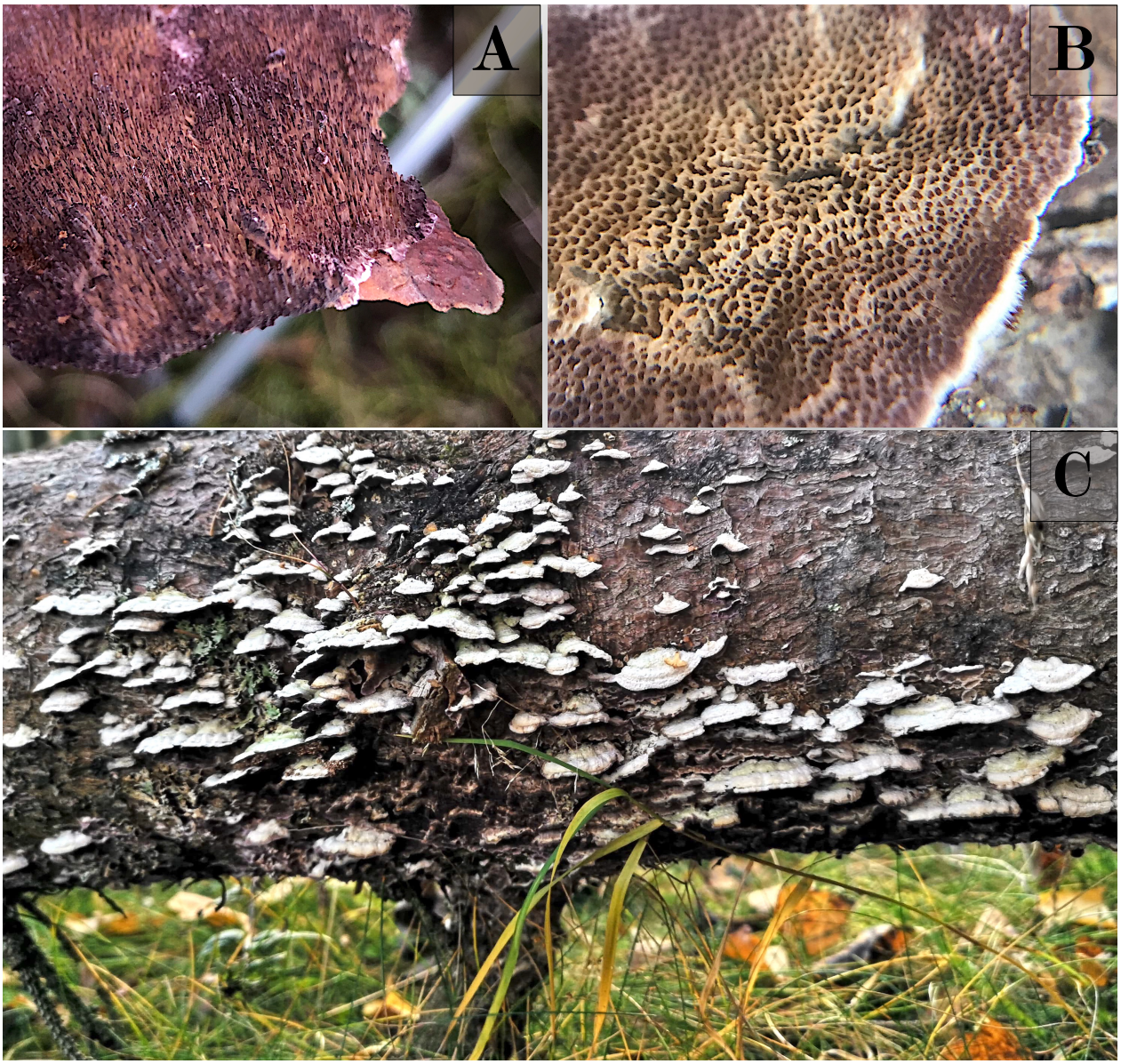

Figure 2, Trichaptum abietinum *and* Trichaptum fuscoviolaceum *in the field.* *(A) The irpicoid ("toothed") hymenium of* T. fuscoviolaceum*. (B) The poroid hymenium of* T. abietinum*. (C) Sporocarps from above. The species have similar white and green (due to algae) sporocarps. The shade of purple of the hymenium can vary. Photographs of hymenia by Inger Skrede and photograph of sporocarps by Malin Stapnes Dahl.*

2 Material and Methods

2.1 Sampling

Individuals of *T. abietinum* and *T. fuscoviolaceum* were collected in New Brunswick, Canada and Pavia, Italy during the autumn of 2018 (Figure 3). For all collection sites, ten individuals were sampled from separate logs, or two meters apart on the same log, within one square kilometer. For every individual, a cluster of sporocarps about 3 x 3 cm was collected and placed in separate paper bags. Notes on host substrate, GPS coordinates and locality were made for all individuals, and they were given a collection ID according to collection site and species identification based on morphology. The sporocarps were dried at room temperature for 2 – 3 days, or in a dehydrator at 30 °C, and later stored in an arid room at room temperature. Individuals used in this study are presented in Table S1. Due to misidentification and poor growth of some individuals, downstream analyses do not include all individuals originally collected.

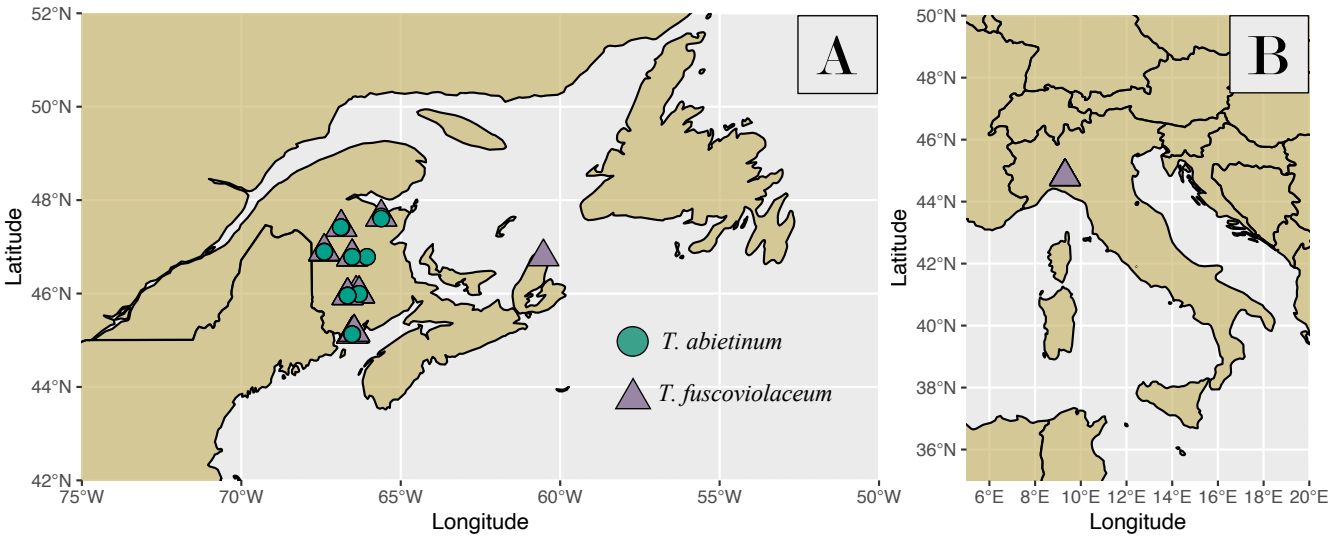

Figure 3, ***The collection sites of individuals in the study.*** *(A) The collection sites of* Trichaptum fuscoviolaceum *and* T. abietinum *individuals in New Brunswick, Canada. (B) The collection site of* T. fuscoviolaceum *individuals in Pavia, Italy.* Trichaptum abietinum *collection sites are represented by green circles and* T. fuscoviolaceum *collections are in purple triangles. Points are mapped from GPS coordinates in Table S1. The figure is made in R v4.0.2 GUI 1.72 Catalina build using RStudio v1.3.1073 and the packages rnaturalearth (South, 2017), sp (Pebesma and Bivand, 2005; Bivand, Pebesma and Gomez-Rubio, 2013), ggplot2 (Wickham, 2016) and wesanderson (Ram and Wickham, 2018).*

2.2 Culturing

Since haploid sequences are bioinformatically convenient to work with, I isolated monokaryotic mycelia for sequencing by culturing collected *Trichaptum* individuals as follows (illustrated in Figure 4): (A) To revive dried individuals for spore shooting, wet sporocarps were placed in a moist paper towel and left in the fridge until soaked through (about 3 hours). (B) While working in a safety cabinet (Labculture® ESCO Class II Type A2 BSC, Esco Micro Pte. Ltd., Singapore), sporocarps were attached, hymenium facing media, with silicon grease from Merck Millipore (Darmstadt, Germany) to the lid of a petri dish containing 3% malt extract agar (MEA), with antibiotics and fungicides (10 mg/l Tetracycline, 100 mg/l Ampicillin, 25 mg/l Streptomycin and 1 mg/l benomyl) to avoid contamination. The sporocarps were left for a minimum of one hour for spores to shoot onto the MEA plates. Subsequently, the sporocarps were removed to minimize spore shooting and the petri dish was sealed off with Parafilm M® (Neenah, WI, USA). The cultures were left for approximately one week, or until hyphal patches were starting to show, at 20 °C in a dark incubator (Termaks AS KB8400/KB8400L, Bergen, Norway). (C) Working in a safety cabinet, single, germinated spores were picked with a sterile scalpel and placed onto new MEA dishes with antibiotics and fungicides. The new cultures were left in a dark incubator at 20 °C for a few days until a mycelial patch could be observed. (D) The hyphae were checked for clamp connections in a Nikon Eclipse 50i light microscope (Tokyo, Japan) using 0.1% Cotton Blue to accentuate cells (examples in Figure S4). Clamps indicate a dikaryotic hyphae and I proceeded with the cultures lacking clamps (i.e., monokaryotic hyphae). (E) Monokaryotic cultures were replated onto new MEA dishes without antibiotics and fungicides (the mycelia grow better without these substances and the cultures were now free from contaminants) and placed in an incubator at 19 °C impending sequencing and experiments. All cultures were replated onto new MEA dishes every month to prevent the mycelia from dying.

For every individual, I used two sporocarps for step (A) and (B). To ensure monokaryotic cultures in step (D), seeing that some are usually dikaryotic or contaminated, I made three replicates for all sporocarps in step (C). After confirmation of monokaryotic mycelia, three replicates were chosen for each individual in step (E), labeled M1, M2 and M3.

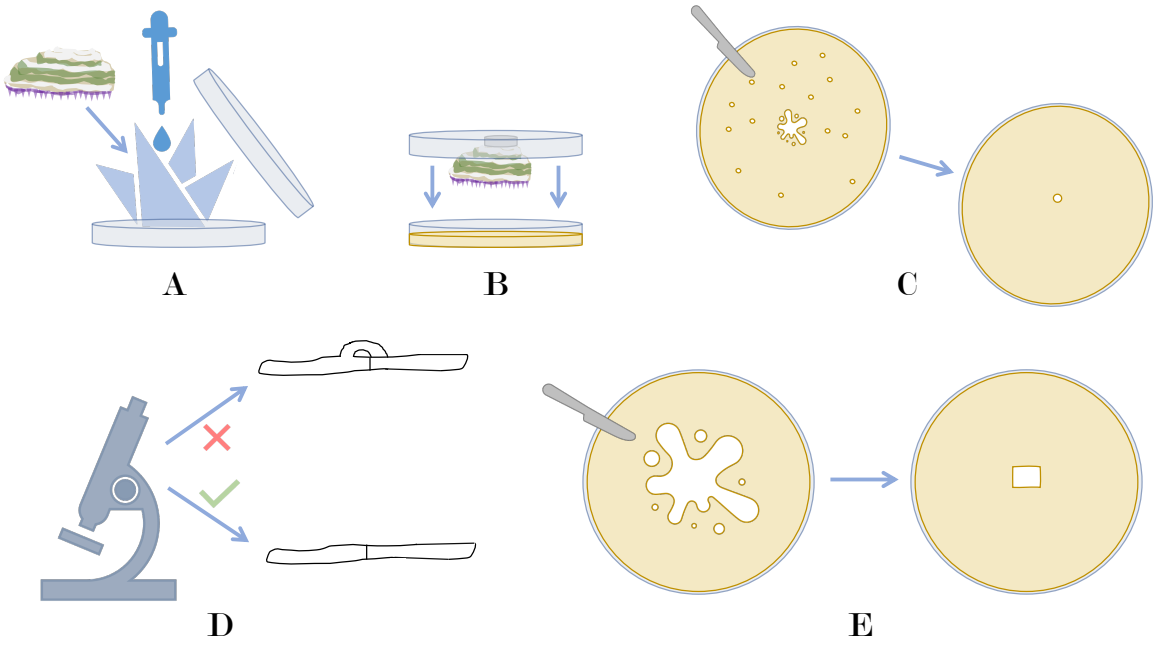

Figure 4, *Procedure for culturing monokaryotic fungal individuals.* *(A) A sporocarp is placed in a wet paper towel onto a petri dish. (B) The sporocarp is glued to the lid of the petri dish to allow for spore shooting onto agar. (C) Hyphae from single spores are picked with a scalpel and placed onto new agar. (D) Microscopy of hyphae to confirm monokaryotic cultures. Hypha with clamp connection is indicated with a red cross and hypha without clamp connection is indicated with a green check symbol. (E) Mycelium from the new culture made in (C) is cut out with a scalpel and placed onto new agar. The figure was made in Microsoft® PowerPoint for Mac v16.50.*

2.3 Species identification

2.3.1 PCR and Sanger sequencing

Cultures can be contaminated by different fungal species living on the sporocarp of collected individuals or in the laboratory. It is nearly impossible to identify fungal species by mycelial morphology and I therefore used Sanger sequencing (Sanger, Nicklen and Coulson, 1977) of the internal transcribed spacer (ITS), a region which is commonly used as a barcode for species identification in fungi, to confirm correct species designation of the cultures produced in section 2.2.

For amplification of fungal DNA, I performed polymerase chain reaction (PCR; Mullis et al., 1986) on all cultures using the Thermo Scientific™ Phire Plant Direct PCR Kit (Waltham, USA). Tissue was collected from the cultures by scraping off mycelia with a pipette tip, which was subsequently dipped in one well of a Multiply® PCR strip (Nümbrecht, Germany) containing

20 µl dilution buffer (Phire Plant Direct PCR Kit) and stirred for release of tissue from the tip. The strip with collected tissue was spun down. One µl of the DNA template (mycelia and dilution buffer) was added to one well of a new PCR strip containing the master mix: 10 µl buffer (Phire Plant Direct PCR Kit), 2 µl forward primer (5 µM), 2 µl reverse primer (5 µM), 4.8 µl milliQ H_2O (Merck Millipore, Darmstadt, Germany) and 0.2 µl enzyme (Phire Hot start II DNA polymerase). I used the ITS1 (5' – TCCGTAGGTGAACCTGCGG – 3'; White et al., 1990) region as forward primer and ITS4 (5' – TCCTCCGCTTATTGATATGC – 3'; White et al., 1990) as reverse primer. The PCR reaction was run in either the Eppendorf AG's Eppendorf Mastercycler nexus GSX1 (Hamburg, Germany) or MJ Research PTC-200 Peltier Thermal Cycler (Marshall Scientific, Hampton, NH, USA), using a cycling protocol of 98 °C initial denaturation for 5 minutes, followed by 40 cycles of 98 °C denaturation for 5 seconds, 54 °C annealing for 5 seconds and 72 °C extension for 20 seconds, finishing off with 1 minute on 72 °C final extension before a 10 °C forever hold. To check if the PCR was successful, I performed a 1% agarose gel electrophoresis prepared with SeaKem® LE Agarose from Lonza (BioNordika, Oslo, Norway) and GelRed™ (Biotium, VWR International, Oslo, Norway) nucleic acid stain (3 µl/100 ml gel) before loading with Thermo Scientific™ Gel Loading Dye 6X (~ 5 µl PCR product mixed with 1 µl dye) and Thermo Scientific™ FastRuler Low Range DNA Ladder (5 µl).

PCR products with band of correct size (700 – 1000 bp) were further purified for Sanger sequencing using the ExoProStar 1-Step from GE Healthcare (Chicago, USA) to remove primers and deoxyribonucleotide triphosphates (dNTPs). For each sample, 10 × diluted ExoProStar 1-Step solution was mixed with 5 µl of PCR product. The samples were placed in the same thermocyclers as for the PCR reaction at 37 °C for 15 minutes then 80 °C for 15 minutes before a 10 °C forever hold. The solutions were further diluted by adding 45 µl of milliQ H_2O to each tube before transferring 5 µl of the diluted samples to two 1.5 ml Eppendorf Tubes® (Hamburg, Germany), one containing 5 µl of the forward primer and the other containing 5 µl of the reverse primer (the primers are separated to enable both forward and reverse sequencing). The samples were sent to Eurofins Scientific (Hamburg, Germany) for Sanger sequencing.

I assessed, trimmed, and aligned the resulting forward and reverse sequences to consensus sequences using Geneious Prime v2020.1.2 (https://www.geneious.com). To verify species designation of cultures, the consensus sequences were checked with the Basic local alignment search tool (BLAST; Altschul et al., 1990) in the National Centre of Biotechnology Information (NCBI) database (U.S. National Library of Medicine, Bethesda, MD, USA). I kept cultures identified as *T. fuscoviolaceum* or *T. abietinum* and updated *Trichaptum* cultures with incorrect initial species designation based on sporocarp morphology. Where possible, I chose approximately five individuals of *T. fuscoviolaceum* from each collection site and five individuals of *T. abietinum* corresponding to the same sites for DNA extraction and Illumina sequencing, including one individual of *T. biforme* as an outgroup. I only had one population from Italy since the Italian

collection was not originally planned to be included. Therefore, nine individuals were chosen from this population to compensate for lack of collections from this region.

2.4 Whole genome sequencing

2.4.1 DNA extraction

Before performing DNA extraction on the selected individuals, I replated the cultures onto new MEA dishes with an autoclaved (HV-25L, HMC Europe, Tüssling, Germany) nylon sheet, which makes it easier to remove the mycelium without including agar. When the individuals had grown to cover at least 25% of the petri dish, I performed DNA extraction using the E.Z.N.A.® Fungal HP DNA Kit (Omega Bio-Tek, Norcross, GA, USA). Mycelium was scraped off with a sterile scalpel and put into 2 ml Lysing Matrix E tubes with 1.4 mm ceramic spheres, 0.1 mm silica spheres and one 4 mm glass sphere (MP Biomedicals™, Santa Ana, CA, USA). In each tube, 600 µl CSPL buffer (E.Z.N.A.® Fungal HP DNA Kit) and 30 µl RNase (Qiagen, Hilden, Germany) was added before the solutions were crushed and homogenized in FastPrep-24 (MP Medicals, Santa Ana, CA, USA) for 2 × 20 seconds at 4.5 m/s, followed by an incubation on heat blocks (Eppendorf Thermomixer comfort, VWR International, Oslo, Norway) at 65 °C for at least 30 minutes, ensuring degradation of proteins. The samples cooled at room temperature and were spun down before further processing.

Working in a fume hood (Labflex, Skive, Denmark), 600 µl of chloroform was added to each tube, vortexed and centrifuged with an Eppendorf Centrifuge 5415 D (VWR International, Oslo, Norway) at 10 000 × g for 10 minutes. Leaving the lower layer untouched to avoid contamination by organic matter (DNA is in the aqueous phase), 450 µl of the upper layer of the solutions was carefully aspirated into new 1.5 ml Eppendorf Tubes®. Subsequently, 225 µl CXD Buffer (E.Z.N.A.® Fungal HP DNA Kit) and 450 µl 96% ethanol was added and the solutions vortexed to homogenize the mix. HiBind® DNA Mini Columns (E.Z.N.A.® Fungal HP DNA Kit) were inserted into 2 ml Collection Tubes (E.Z.N.A.® Fungal HP DNA Kit). To activate the HiBind® DNA Mini Columns for DNA binding, 100 µl 3M NaOH was added and the columns were left for 4 minutes at room temperature before centrifugation on maximum speed for 20 seconds to remove excess solution. The filtrate was then discarded and samples from the Eppendorf Tubes® were transferred to the HiBind® DNA Mini Columns and centrifuged at 10 000 × g for 1 minute. The centrifuged columns were inserted into new 2 ml Collection Tubes and the old tubes were discarded. Samples were transferred in two rounds due to limited space in the HiBind® DNA Mini Columns.

To remove contaminants from the solution, 650 µl DNA Wash Buffer (E.Z.N.A.® Fungal HP DNA Kit) was added to the HiBind® DNA Mini Columns containing DNA from the transferred

samples and the columns were centrifuged at 10 000 × g for 1 minute. This step was performed twice and, as a final step to remove excess solution, the empty columns were centrifuged at maximum speed for 2 minutes. The HiBind® DNA Mini Columns were then transferred to new 1.5 ml Eppendorf Tubes® and 50 µl of preheated (65 °C) Elution Buffer (E.Z.N.A.® Fungal HP DNA Kit) was added. The tubes were then placed on a heating block for 5 minutes on 65 °C, allowing the enzymes to work. After heating, the tubes were centrifuged at maximum speed for 1 minute to release DNA from the HiBind® DNA Mini Columns into the Eppendorf Tubes®. Lastly, the elution step was repeated with 20 µl Elution Buffer to obtain a second extraction.

2.4.2 Illumina sequencing

Before preparing the samples for whole genome sequencing, I assessed the quality and concentration of the extracted DNA (section 2.4.1) using NanoDrop® ND-1000 Spectrophotometer (Saveen & Werner AB, Limhamn, Sweden), Thermo Scientific™ Invitrogen™ Qubit® fluorometer (Q32857) with the Qubit™ dsDNA BR Assay Kit, and 1% agarose gel electrophoresis (same substances as in section 2.3.1, except from the ladder, which was changed to Thermo Scientific™ FastRuler High Range DNA Ladder).

Approximately 20 ng/µl of each sample was delivered to the Norwegian Sequencing Center (NSC; Oslo, Norway) for Illumina whole genome sequencing. Libraries were prepared by NSC. They used 1 µl of extracted DNA from each sample, which was fragmented using 96 microTUBE-50 AFA Fiber plates (Covaris Inc., Woburn, MA, USA) on a Covaris E220 system (Covaris Inc., Woburn, MA, USA). The target size was 300-400 bp. The resulting gDNA was washed with a small volume Mosquito liquid handler (TTP Labtech) with 1:1 ratio Kapura Pure beads (Roche, Basel, Switzerland) eluted in Tris-CL with pH 8.0. The library preparations used 500 ng fragmented DNA, applying the Kapa Hyper library prep kit (Roche, Basel Switzerland). Barcodes were attached using the Illumina UD 96 index 490 kit (Illumina) and PCR-amplification was conducted by running 5 cycles with Kapa HIFI PCR kit (Roche, Basel, Switzerland). Subsequently, the libraries were checked with regular library quality control and the standard sensitivity NGS Fragment kit (Agilent, Santa Clara, CA, USA). A qPCR with Kapa Library quantification Kit (Roche, Basel, Switzerland) was used for quantification and sequencing generated 2 × 150 paired end Illumina reads. Samples were sequenced on either the Illumina Hiseq 4000 or the Illumina Novaseq I.

2.5 Crossing experiments

I performed crossing experiments to assess mating compatibility between species (i.e., between individuals of *T. abietinum* and *T. fuscoviolaceum*) in addition to compatibility between individuals of *T. fuscoviolaceum* from the Canadian and the Italian population. I used cultures produced as explained in section 2.2. The crosses between *T. abietinum* and *T. fuscoviolaceum* individuals were also part of experiments in Peris et al. (in prep.). Therefore, some of the *T. abietinum* individuals are European (see Peris et al., in prep. for details on these individuals). The crossing set-ups were planned according to a mating compatibility scheme based on mating loci (*MAT*) found in Peris et al. (in prep.). Briefly, they located *MAT* genomic regions in the reference genomes of *T. abietinum* and *T. fuscoviolaceum* by searching conserved flanking genes. Delimitation of mating genes were performed by blasting towards *Pyrrhoderma noxium* (a high-quality genome of a species in the Hymenochaetales, the same order as *Trichaptum*) homeodomains and pheromone receptors (Chung et al., 2017). Introns and exons of each mating gene were annotated using FGENESH (Solvyev et al., 2006) and a blastx in NCBI was run to confirm the gene designation. Lastly, they phylogenetically inferred allelic class for each mating gene and the mating type designation using a collection of 181 *Trichaptum* specimens from both *T. abietinum* and *T. fuscoviolaceum* individuals. Tetrapolar fungi, like *Trichaptum*, are only compatible when the two *MAT* loci (called *MATA* and *MATB*) are different. I crossed individuals that were both expected and not expected to mate based on their mating type (i.e., dissimilar or similar allelic classes on both *MAT* loci). Individuals used for the experiment are presented in Table 1. Three replicates were made for all crosses to strengthen the confidence in the observations.

Pairs of monokaryotic individuals were plated on petri dishes containing 3% MEA, 4 cm to opposite sides of the center. The mycelium was cut out with a scissored 1 ml pipette tip to ensure the same starting conditions for both individuals. The petri dishes were placed in a dark incubator at 19 °C until the individual mycelia had grown together (about 2 weeks). To investigate if the crossing experiments were successful, I assessed the presence or absence of clamp connections using a Zeiss Axioplan 2 imaging light microscope (Güttingen, Germany) with Zeiss AxioCam HRc (Güttingen, Germany) in addition to photographing the cultures using a Nikon D600 Digital Camera (Tokyo, Japan). Microscopy photographs of hyphae were taken at 400 and 630 × magnification.

Table 1, *Individuals used in the crossing experiments.* *The table includes cross name (ID), monokaryotic individuals crossed (Mate pairs), mating loci differences and similarities between the crosses (Mating type (*MAT*)), populations crossed (Populations) and expected mating compatibility (Prediction). Dist. = distinct, ident. = identical, TA =* Trichaptum abietinum*, TF =* T. fuscoviolaceum*, It = Italian, Eu = European, NAm = North American and CNAm = Circumboreal North American.*

T. abietinum* × *T. fuscoviolaceum				
ID	**Mate pairs**	**Mating type (*MAT*)**	**Populations**	**Prediction**
TFTAX1	TF10147M9 × TA10264M3	Ident. *MATA*, dist. *MATB*	It × Eu	Incompatible
TFTAX2	TF10147M9 × TA10058M1	Ident. *MATA*, dist. *MATB*	It × NAm	Incompatible
TFTAX3	TF101410M1 × TA10355M3	Dist. *MATA*, ident. *MATB*	It × Eu	Incompatible
TFTAX4	TF10141M2 × TA10139M1	Dist. *MATA*, ident. *MATB*	It × CNAm	Incompatible
TFTAX5	TF101410M1 × TA10264M3	Dist. *MAT*s	It × Eu	Compatible
TFTAX6	TF101410M1 × TA10139M1	Dist. *MAT*s	It × CNAm	Compatible
TFTAX7	TF101410M1 × TA10058M1	Dist. *MAT*s	It × NAm	Compatible
TFTAX8	TF10034M2 × TA10139M1	Dist. *MAT*s	NAm × CNAm	Compatible
TFTAX9	TF10034M2 × TA10264M3	Dist. *MAT*s	NAm × Eu	Compatible
TFTAX11	TF10034M2 × TA10058M1	Dist. *MAT*s	NAm × NAm	Compatible
T. fuscoviolaceum* × *T. fuscoviolaceum				
ID	**Mate pairs**	**Mating type (*MAT*)**	**Populations**	**Prediction**
TFX1	TF10147M1 × TF10147M1	Ident. *MAT*	It × It	Incompatible
TFX2	TF10147M1 × TF10147M9	Dist. α *MATA* and *MATB*	It × It	Compatible
TFX3	TF10147M1 × TF10143M3	Dist. α *MATA,* ident. *MATB*	It × It	Incompatible
TFX4	TF10147M9 × TF10141M2	Dist. β *MATA* and *MATB*	It × It	Compatible
TFX5	TF10032M1 × TF10135M2	Dist. β *MATA* and *MATB*	NAm × NAm	Compatible
TFX7	TF10091M1 × TF10135M2	Dist. α *MAT* and *MATB*	NAm × NAm	Compatible
TFX9	TF10034M2 × TF10091M1	Dist. *MATA*, ident. *MATB*	NAm × NAm	Incompatible
TFX10	TF10122M1 × TF10147M1	Dist. β *MATA* and *MATB*	It × NAm	Compatible
TFX11	TF101410M1 × TF10122M1	Dist. α *MATA* and *MATB*	It × NAm	Compatible
TFX12	TF10141M2 × TF10122M1	Dist. *MATA*, ident. *MATB*	It × NAm	Incompatible

2.6 Bioinformatic analyses

2.6.1 Preprocessing and search for hybrids

To preprocess the Illumina raw sequences, I first used Trim Galore! v0.6.2 (https://www.bioinformatics.babraham.ac.uk/projects/trim_galore/; Krueger, 2015) to remove sequences with a Phred quality score less than 30. The quality of the sequences was assessed before and after trimming with FastQC (Andrews, 2010) and MultiQC (Ewels et al., 2016). After preprocessing, I used BWA v0.7.17 (Li and Durbin, 2009) to map the sequences to two different reference genomes. One *T. fuscoviolaceum* reference produced by Peris et al. (in prep.), and one combined reference of both *T. fuscoviolaceum* and *T. abietinum*. The combined reference was constructed by merging the *T. abietinum* and *T. fuscoviolaceum* reference genomes produced by Peris et al. (in prep.) with the wrapper sppIDer (Langdon et al., 2019). I further applied SAMtools v1.9 (Li et al., 2009) to sort the resulting files. I searched for hybrids by mapping Illumina reads from *T. fuscoviolaceum* to the combined reference genome, using the sppIDer. No hybrids were revealed among the *T. fuscoviolaceum* individuals in the sppIDer analysis (Figure 5). All *T. fuscoviolaceum* individuals mapped with greater depth to the *T. fuscoviolaceum* part of the combined reference genome than the *T. abietinum* part, implying *T. fuscoviolaceum* origin of all genomes of individuals investigated. Since there were no hybrid individuals and I could only use one reference for further analyses, I chose to continue with the *T. fuscoviolaceum* reference genome.

2.6.2 Re-mapping with Stampy

To improve mapping of *T. abietinum*, *T. biforme* and the Italian *T. fuscoviolaceum* to the reference genome (based on a Canadian *T. fuscoviolaceum* individual), the raw sequences were mapped with Stampy v1.0.32 (Lunter and Goodson, 2011), which is known to be more sensitive to divergent sequences (Lunter and Goodson, 2011), before continuing with further analyses. Based on nucleotide divergence estimates found in Peris et al. (in prep.) by conversion of average nucleotide identity using FastANI (Jain et al., 2018), the substitution rate flag was set to 0.23 for *T. biforme* mapped to the reference, 0.067 for the Italian *T. fuscoviolaceum* mapped to the reference, and 0.157 for *T. abietinum* mapped to the reference. The raw sequences were not trimmed before mapping due to limitations on hard clipping in Stampy (i.e., sequences are sometimes too short for Stampy to work with), but I filtered away bad sequences at a later stage (section 2.6.3).

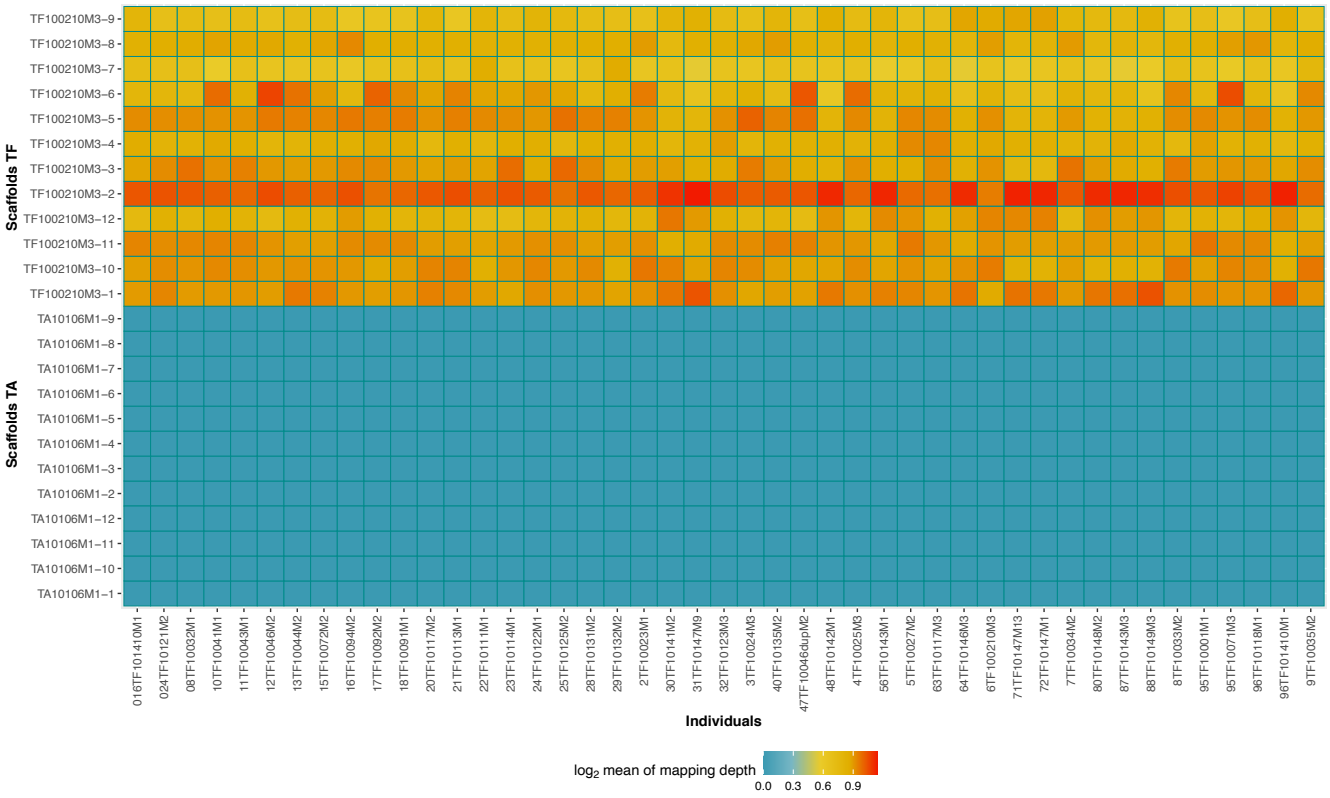

Figure 5, ***The sppIDer analysis did not detect hybrid individuals.*** *On the y-axis are scaffolds (chromosomes) of the* Trichaptum fuscoviolaceum *(TF) and* T. abietinum *(TA) combined reference genome. The x-axis shows* T. fuscoviolaceum *individuals mapped to the combined reference genome. The legend on the bottom shows a color gradient for the* log_2 *mean of the mapping depth. Cooler colors indicate poor mapping, while warmer colors indicate good mapping. The figure is made in R v4.0.2 GUI 1.72 Catalina build using Rstudio v1.3.1073 and the packages ggplot2 (Wickham, 2016), wesanderson (Ram and Wickham, 2018), viridis (Garnier, 2018), readtext (Benoit and Obeng, 2020), data.table (Dowle and Srinivasan, 2020) and hrbrthemes (Rudis, 2020).*

2.6.3 SNP calling and filtering

To obtain a dataset with single nucleotide polymorphisms (SNPs), I first used GATK HaplotypeCaller v4.1.4. (McKenna et al., 2010). To create the dictionary files and regroup the mapped files before SNP calling, I used Picard v2.21.1 (https://broadinstitute.github.io/picard/) and reference index files were made using SAMtools faidx. I ran HaplotypeCaller in haploid mode with otherwise default settings. Subsequently, I used the resulting Variant Call Format (VCF) files in GATK GenomicsDBImport (McKenna et al., 2010) to create a database used as input for GATK GenotypeGVCF (McKenna et al., 2010), which creates one VCF file containing SNPs for all individuals. GenomicsDBImport was used with default settings together with the java options ('--java-options') '-Xmx4g' and '-Xms4g' and an interval text file ('--intervals') containing names of

the different scaffolds. GenotypeGVCF was used with default settings. To remove indels, bad SNPs, and individuals with high missingness, I filtered the resulting VCF file with GATK VariantFiltration (McKenna et al., 2010) and BCFtools v1.9 filter (Danecek and Bonfield, 2021). I used GATK's hard filtering recommendations (https://gatk.broadinstitute.org/hc/en-us/articles/360035890471-Hard-filtering-germline-short-variants) together with the Phred quality score option of removing SNPs with a score less than 30.0 ('QUAL < 30.0'). With BCFtools filter, I removed indels and poor SNPs using these options: minimum read depth (DP) < 3, genotype quality (GP) < 3 and '-v snps'. I also used BCFtools filter to remove multiallelic SNPs ('view -M2'), SNPs close to indels ('--SnpGap 10'), variants with a high number of missing genotypes ('-e 'F_MISSING > 0.2''), minimum allele frequency ('MAF <= 0.05') and monomorphic SNPs ('-e 'AC==0 || AC==AN''). I made one dataset where monomorphic SNPs were removed and the MAF filter was applied (Dataset 1 with 2 040 885 SNPs) and two datasets, one with the outgroup and one without, not applying these filters (Dataset 2 with 3 065 109 SNPs; Dataset-O 2 with 3 118 957 SNPs, where O = Outgroup), because monomorphic sites are required to calculate some divergence statistics. After filtering, some individuals had been removed due to high missingness or high heterozygosity (i.e., dikaryons). The final datasets consisted of 32 individuals from the Canadian *T. fuscoviolaceum* population, 9 individuals from the Italian *T. fuscoviolaceum* population, 30 individuals from the Circumboreal North American *T. abietinum* population, and 6 individuals from the North American *T. abietinum* population. In total 77 individuals.

2.6.4 Principal component and divergence analyses

To explore the data and investigate population groupings, I performed a principal component analysis (PCA; Pearson, 1901; Hotelling, 1933; Jolliffe, 2002) with PLINK v2.00-alpha (www.cog-genomics.org/plink/2.0/; Chang et al., 2015). To prepare the input file, I linkage pruned Dataset 1 in PLINK, using the flags '--vcf $vcf_file', '--double-id', '--allow-extra-chr', '--set-missing-var-ids @:#', --out $out_file' and '--indep-pairwise 50 10 0.1', retaining 56 046 SNPs. The '--indep-pairwise' flag performs the linkage pruning, where '50' denotes a 50 Kb window, '10' sets the window step size to 10 bp, and '0.1' denotes the r^2 (or linkage) threshold. A PCA was subsequently performed on the pruned VCF file, using the flags, '--vcf $vcf_file', '--double-id', '--allow-extra-chr', '--set-missing-var-ids @:#', '--extract $prune.in_file', '--make-bed', '--pca', and '--out $out_file' (both linkage pruning and PCA flags were based on the Physalia tutorial by Mark Ravinet and Joana Meier; https://speciationgenomics.github.io/pca/).

To investigate the divergence between populations, I applied a sliding window approach on Dataset 2 to calculate the fixation index (F_{ST}) and absolute divergence (d_{XY}) along the genome. I also performed a sliding window analysis to calculate within population divergence (π). The analyses were performed using Simon Martin's script popgenWindows.py (https://github.com/simonhmartin/genomics_general#diversity-and-divergence-analyses-in-

sliding-windows) with Python v3.8 (Van Rossum and Drake, 2009). I sat the window size to 20 000 bp ('-w 20000'), step to 10 000 bp ('-s 10000') and the minimum number of SNPs in each window to 10 ('-m 10').

2.6.5 Introgression analyses

To investigate introgression between populations, I used the R package admixr (Petr, 2020) and Dataset-O 2 to calculate the *D*, f_3 and f_4-ratio statistics between different populations with *T. biforme* as outgroup (based on recommendations from the Physalia tutorial by Mark Ravinet and Joana Meier: https://speciationgenomics.github.io/ADMIXTOOLS_admixr/, and the tutorial by Martin Petr: https://bodkan.net/admixr/articles/tutorial.html#f4-ratio-statistic-1). To prepare the input file from VCF to Eigenstrat format, I used the conversion script convertVCFtoEigenstrat.sh by Joana Meier (https://github.com/speciationgenomics/scripts), which utilizes VCFtools v0.1.16 (Danecek et al., 2011) and EIGENSOFT v7.2.1 (Patterson, 2006; Price, 2006). The script has a default recombination rate of 2.0 cM/mb, which I changed to 2.5 cM/mb based on earlier findings in the class Agaricomycetes, where *Trichaptum* belongs (Heinzelmann et al., 2020).

I further used another Python script developed by Simon Martin, ABBABABAwindows.py, for a sliding window ABBA-BABA analysis on Dataset-O 2 to calculate the proportion of introgression (f_{dM}) with a window size of 20 000 ('-w 20000') no step size and minimum number of SNPs to 100 ('-m 100'), together with '--minData 0.5' to specify that at least 50% of the individuals in each population must have data for a site to be included (based on recommendations from the Physalia tutorial by Mark Ravinet and Joana Meier: https://speciationgenomics.github.io/sliding_windows/). I used *T. biforme* as outgroup and tested introgression between the Canadian *T. fuscoviolaceum* and the *T. abietinum* populations in addition to the Italian *T. fuscoviolaceum* and the *T. abietinum* populations (the phylogenetic topology was based on results from the f_3 analysis). The 99.7% outlier windows (3 standard deviations) were extracted from the result using R v4.0.2 GUI 1.72 (https://cran.r-project.org/bin/macosx/). The outliers were considered significant outputs. Annotated genes in these outlier windows were retrieved from the annotated *T. fuscoviolaceum* reference genome. The reference genome was annotated using RepeatModeler (Flynn et al., 2019), RepeatMasker (Smit et al., 2013-2015) and MAKER2 (Holt and Yandell, 2011). Functional annotation and protein domain annotations of detected coding sequences and the encoded proteins were performed using blastp (Altschul et al., 1990), against a local UniProt database, and InterProScan (Jones et al., 2014), respectively. All annotations were encoded in a General Feature Format (GFF) file, which was used to match the significant windows and extract the genes.

3 Results

3.1 Crossing experiments

I did not observe clamp connections in the crosses between individuals of *T. fuscoviolaceum* and *T. abietinum*, neither for mate pairs that were predicted to mate based on mating type alleles nor those that were not (Table 2; Figure S1 and S3). All crosses within and between *T. fuscoviolaceum* populations were as predicted, and clamp connections were observed for the compatible individuals (Table 2; Figure S2 and S4). It was difficult to observe compatible crosses by investigating the cultures macroscopically, but there was often a sharper line between individuals on the petri dish when the crosses were incompatible (Figure S1 and S2).

Table 2, Trichaptum fuscoviolaceum *individuals mated as predicted, while* T. abietinum *crossed with* T. fuscoviolaceum *individuals did not.* *The table includes cross name (ID), expected outcome (Prediction) and actual outcome by observation (Yes) or not observation (No) of clamp connections (Clamps). See Table 1 in section 2.5 for more details on individuals and populations crossed.*

T. abietinum* × *T. fuscoviolaceum			***T. fuscoviolaceum* × *T. fuscoviolaceum***		
ID	**Prediction**	**Clamps**	**ID**	**Prediction**	**Clamps**
TFTAX1	Incompatible	No	TFX1	Incompatible	No
TFTAX2	Incompatible	No	TFX2	Compatible	Yes
TFTAX3	Incompatible	No	TFX3	Incompatible	No
TFTAX4	Incompatible	No	TFX4	Compatible	Yes
TFTAX5	Compatible	No	TFX5	Compatible	Yes
TFTAX6	Compatible	No	TFX7	Compatible	Yes
TFTAX7	Compatible	No	TFX9	Incompatible	No
TFTAX8	Compatible	No	TFX10	Compatible	Yes
TFTAX9	Compatible	No	TFX11	Compatible	Yes
TFTAX11	Compatible	No	TFX12	Incompatible	No

3.2 Bioinformatic analyses

3.2.1 Principal component and divergence analyses

The PCA indicated clear groupings of the different *T. fuscoviolaceum* and *T. abietinum* populations, with PC1 and PC2 explaining 57.5% and 12.2% of the observed variation, respectively (Figure 6). The Italian and Canadian *T. fuscoviolaceum* populations placed closer to each other than to the Circumboreal North American and the North American *T. abietinum* population on PC1, and the two *T. abietinum* populations placed nearer each other than to the *T. fuscoviolaceum* populations. The gap between the *T. fuscoviolaceum* populations was larger than between the *T. abietinum* populations on PC1. PC2 positioned the Italian *T. fuscoviolaceum* population and the North American *T. abietinum* population at opposite ends of the axis, while the Canadian *T. fuscoviolaceum* and the Circumboreal North American *T. abietinum* population were placed denser amidst the PC2 variation.

The clear distinction spotted in the PCA was corroborated by the fixation index (F_{ST}), which showed a high degree of divergence both between populations of different species (Figure S5A and S5B), with a mean from 0.6 – 0.8 (measured in proportion of heterozygosity, where 0 is complete sharing of alleles while 1 is complete divergence; Chang et al., 2019), and between populations of the same species (Figure S5C), with a mean around 0.4. The divergence between the two *T. fuscoviolaceum* populations was higher than between the *T. abietinum* populations (mean F_{ST} between *T. fuscoviolaceum* populations was ~ 0.5, while mean F_{ST} between *T. abietinum* populations was ~ 0.3). I observed some regions of lower F_{ST} (e.g., scaffold 4 and 5). There were also regions of higher F_{ST} between populations of the same species (Figure S5C). For example, in *T. fuscoviolaceum* a region in the second half of scaffold 5 had very high F_{ST}, while for *T. abietinum* this was observed in the first half of scaffold 5. These elevated F_{ST} regions, compared to the mean, are not as distinct in the between species analyses (Figure S5A and S5B).

The absolute between populations divergence (d_{XY}) echoed the patterns of the PCA and F_{ST} scan, with generally high divergence both between populations of different species and between populations within species (Figure S6). The mean d_{XY} values between populations of different species were about 0.4 (measured in average proportion of dissimilarities between all sequence pairs between populations; Nei and Miller, 1990; Figure S6A and S6B), while the values between populations of same species were slightly less than 0.2 (Figure S6C). Regions of low divergence values (e.g., scaffold 4 and 5) and the patterns in scaffold 5 found in the F_{ST} analyses were also observed in the d_{XY} analyses.

The within population variation calculated by the nucleotide diversity, π, had a mean value of about 0.05 for all populations (measured in average proportion of dissimilarities between all sequence pairs within populations; Nei and Li, 1979; Figure S7). The pattern of π was, for the most

part, opposite of F_{ST} and d_{XY}; in low F_{ST} and d_{XY} regions, for example scaffold 4 and 5, π was high. Generally, the within population variations were moderate (disregarding the scaffold tails).

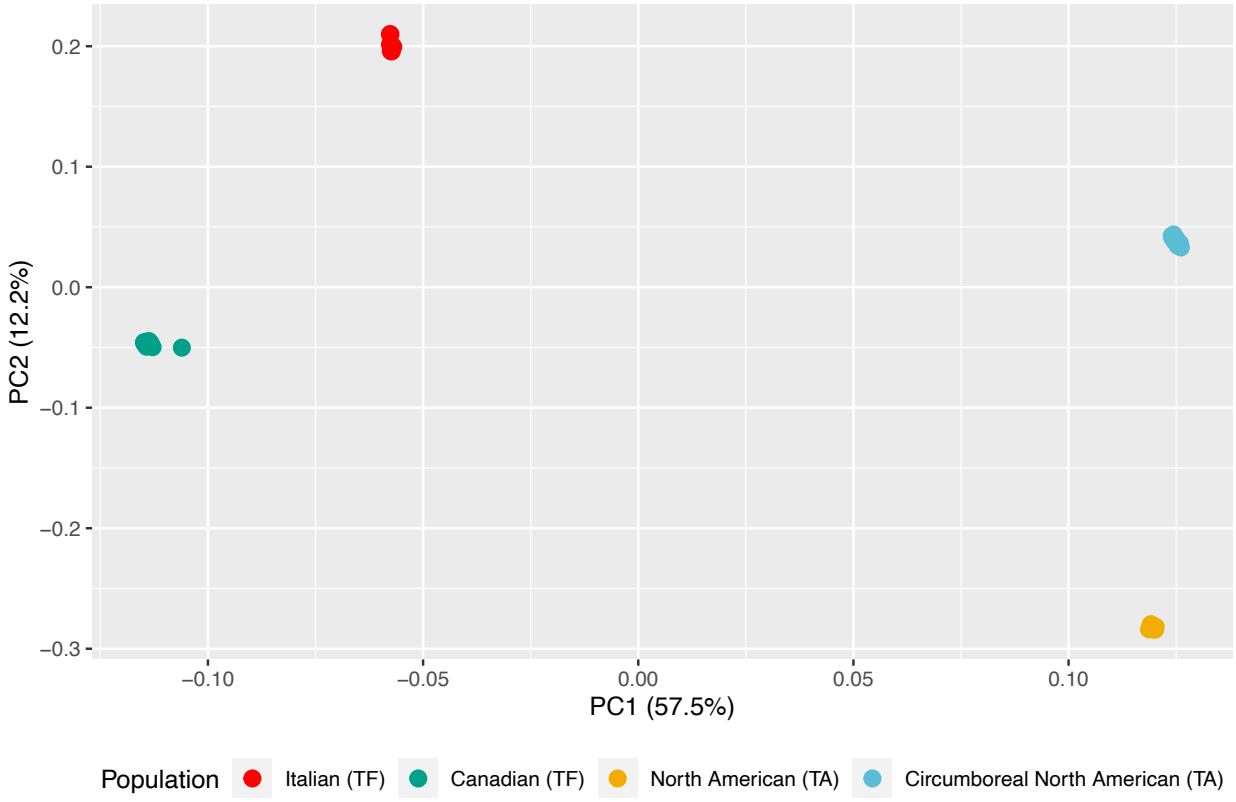

Figure 6, ***Clear groupings according to species and populations in the principal component analysis (PCA).*** *The PCA is based on a single nucleotide polymorphism (SNP) dataset of 2 040 885 SNPs linkage pruned to 56 046 SNPs. The x and y-axes represent PC1 and PC2, respectively, with percentage of variance explained in parentheses. Points are individuals colored by population as indicated in the legend. TF =* Trichaptum fuscoviolaceum *and TA =* T. abietinum. *The figure is made in R v4.0.2 GUI 1.72 Catalina build using Rstudio v1.3.1073 and the packages ggplot2 (Wickham, 2016) and wesanderson (Ram and Wickham, 2018).*

3.2.2 Introgression analyses

The *D* statistic (or ABBA-BABA statistic), used to detect signs of introgression across the genome, gave significant *D* values (|z-score| > 3) between the Italian *T. fuscoviolaceum* and both the *T. abietinum* populations (Table 3), indicating introgression between the Italian *T. fuscoviolaceum* and the *T. abietinum* populations. The test of introgression between the *T. abietinum* populations and either of the *T. fuscoviolaceum* populations did not reveal significant positive or negative *D*-values. There was also a larger discrepancy between ABBA and BABA sites in the significant topologies (Table 3, row three and four), than in the nonsignificant topologies (Table 3, row one and two).

Table 3, *The* D *statistic indicates introgression.* *The analysis is performed on a single nucleotide polymorphism (SNP) dataset of 3 118 957 SNPs. The* D *statistic is based on a phylogenetic tree hypothesis of (((W, X), Y), Z) in Newick tree format and tests introgression between Y and X (negative* D*) and Y and W (positive* D*). Z is the outgroup. The table includes the* D *value (*D*), standard error (std error), significance of the* D *values (z-score; an absolute z-score larger than 3 is considered significant), the number of SNPs shared between Y and W (BABA), the number of SNPs shared between Y and X (ABBA), the number of SNPs used for the comparison (n SNPs). Significant introgression between populations is highlighted in bold. Can TF = Canadian* Trichaptum fuscoviolaceum*, It TF = Italian* T. fuscoviolaceum*, CNAm TA = Circumboreal North American* T. abietinum*, Nam TA = North American* T. abietinum*, and TB =* T. biforme*.*

***D* statistics**									
W	**X**	**Y**	**Z**	***D***	**std error**	**z-score**	**BABA**	**ABBA**	**n SNPs**
CNAm TA	Nam TA	Can TF	TB	-0.0041	0.004744	-0.868	9142	9217	662894
Nam TA	CNAm TA	It TF	TB	0.0060	0.005929	1.018	9706	9590	662712
Can TF	**It TF**	**Nam TA**	TB	-0.2257	0.008558	-26.376	8072	12776	662712
It TF	Can TF	**CNAm TA**	TB	0.2287	0.009069	25.221	12810	8041	664963

The four-population *f*-statistic (f_4 ratio), used to test proportion of introgression, resulted in a violation of the statistical model (i.e., negative alpha values; valid values are proportions between 0 and 1) when placing *T. abietinum* and *T. fuscoviolaceum* as sister groups with the Canadian *T. fuscoviolaceum* or the Circumboreal North American *T. abietinum* at the X position (Table 4). Reversing the positions at X resulted in a positive alpha value, which did not violate the model. The alpha value indicated ~ 5.7% shared ancestry between the *T. abietinum* populations and the Italian *T. fuscoviolaceum* population (Table 4, row three and four). The small amount of shared ancestry (0.1 – 0.2%) between the North American *T. abietinum* and the two *T. fuscoviolaceum* populations did not show a significant z-score (< 3; Table 4, row seven and eight).

Further investigation of introgression with the three-population *f*-statistic (f_3), which estimates shared genetic drift (or branch length), revealed that the *T. abietinum* populations split later (share more genetic drift) than the *T. fuscoviolaceum* populations (Figure S8). As with the f_4 ratio analysis, the Italian *T. fuscoviolaceum* population exhibited slightly more shared genetic drift with the *T. abietinum* populations than the Canadian *T. fuscoviolaceum* population. Nevertheless, the difference between the two *T. fuscoviolaceum* populations was miniscule. The f_3 analysis indicated a phylogenetic topology where the *T. fuscoviolaceum* populations diverged earlier than the *T. abietinum* populations. It was then natural to test introgression from the *T. abietinum* populations into each of the *T. fuscoviolaceum* populations in the subsequent sliding window introgression analyses (i.e., a (((Circumboreal North American *T. abietinum*, North American *T. abietinum*), *T. fuscoviolaceum* population), *T. biforme*) phylogenetic topology).

Table 4, *The four-population* f-*statistic* (f_4) *show further signs of introgression.* *The analysis is based on a single nucleotide polymorphism (SNP) dataset of 3 118 957 SNPs. The table shows the different configurations tested from a hypothesis of the phylogenetic relationship presented as (((A, B), (X, C)), O) in Newick tree format, where X is the introgressed population and C its sister population, with the B population as the source of introgression and A as its sister population. O is the outgroup (*Trichaptum biforme*). The alpha value indicates proportion of gene flow with standard error (std error) and significance (z-score; considered significant when larger than 3). Negative alpha values are due to violation of the statistical model. Significant introgression between populations is highlighted in bold. Nam = North American, CNAm = Circumboreal North American, Can = Canadian, It = Italian, TF =* T. fuscoviolaceum *and TA =* T. abietinum.

F_4 ratio							
A	**B**	**X**	**C**	**O**	**alpha**	**std error**	**z-score**
Nam TA	CNAm TA	Can TF	It TF	*T. biforme*	-0.061072	0.003619	-16.878
CNAm TA	Nam TA	Can TF	It TF	*T. biforme*	-0.060432	0.003553	-17.010
CNAm TA	**Nam TA**	**It TF**	Can TF	*T. biforme*	0.057001	0.003160	18.038
Nam TA	**CNAm TA**	**It TF**	Can TF	*T. biforme*	0.057569	0.003215	17.906
It TF	Can TF	CNAm TA	Nam TA	*T. biforme*	-0.002591	0.002536	-1.022
Can TF	It TF	CNAm TA	Nam TA	*T. biforme*	-0.001535	0.001703	-0.902
Can TF	It TF	Nam TA	CNAm TA	*T. biforme*	0.001536	0.001697	0.905
It TF	Can TF	Nam TA	CNAm TA	*T. biforme*	0.002592	0.002522	1.028

The sliding window proportion of introgression, f_{dM}, calculated across the genome revealed small regions of possible introgression (Figure 7). The mean f_{dM} value was around zero for the test of introgression from the *T. abietinum* populations into the Canadian *T. fuscoviolaceum* population and the *T. abietinum* populations into the Italian *T. fuscoviolaceum* population. Yet, the mean was slightly positive, which would indicate more sharing of derived polymorphisms than expected between either of the *T. fuscoviolaceum* populations tested and the North American *T. abietinum* population. Nonetheless, the deviation from zero was infinitesimal. There were some points of high positive and high negative (e.g., more shared derived polymorphisms than expected between the *T. fuscoviolaceum* population tested and the Circumboreal North American *T. abietinum* population) f_{dM} values, which suggests introgression (99.7 % outliers are marked in Figure 7 and presented in Table S2). The 99.7% outlier genes coded for many unknown proteins and proteins similar to those found in humans or common model organisms such as *Saccharomyces* sp. There were also some genes coding for proteins found in other fungi such as *Amanita muscaria*, *Heterobasidion annosum*, and *Coprinopsis cinerea* (Table S2). The genes with similarity to other organisms are annotated to many different functions (i.e., there are genes involved in oxidoreductases, hydrolases, polyketidesynthases, DNA repair mechanism and transport, among others; The UniProt Consortium, 2021). About the same number of outlier genes were detected for the test of introgression between the Canadian *T. fuscoviolaceum* and the *T. abietinum* populations as for introgression between the Italian *T. fuscoviolaceum* and *T. abietinum* populations.

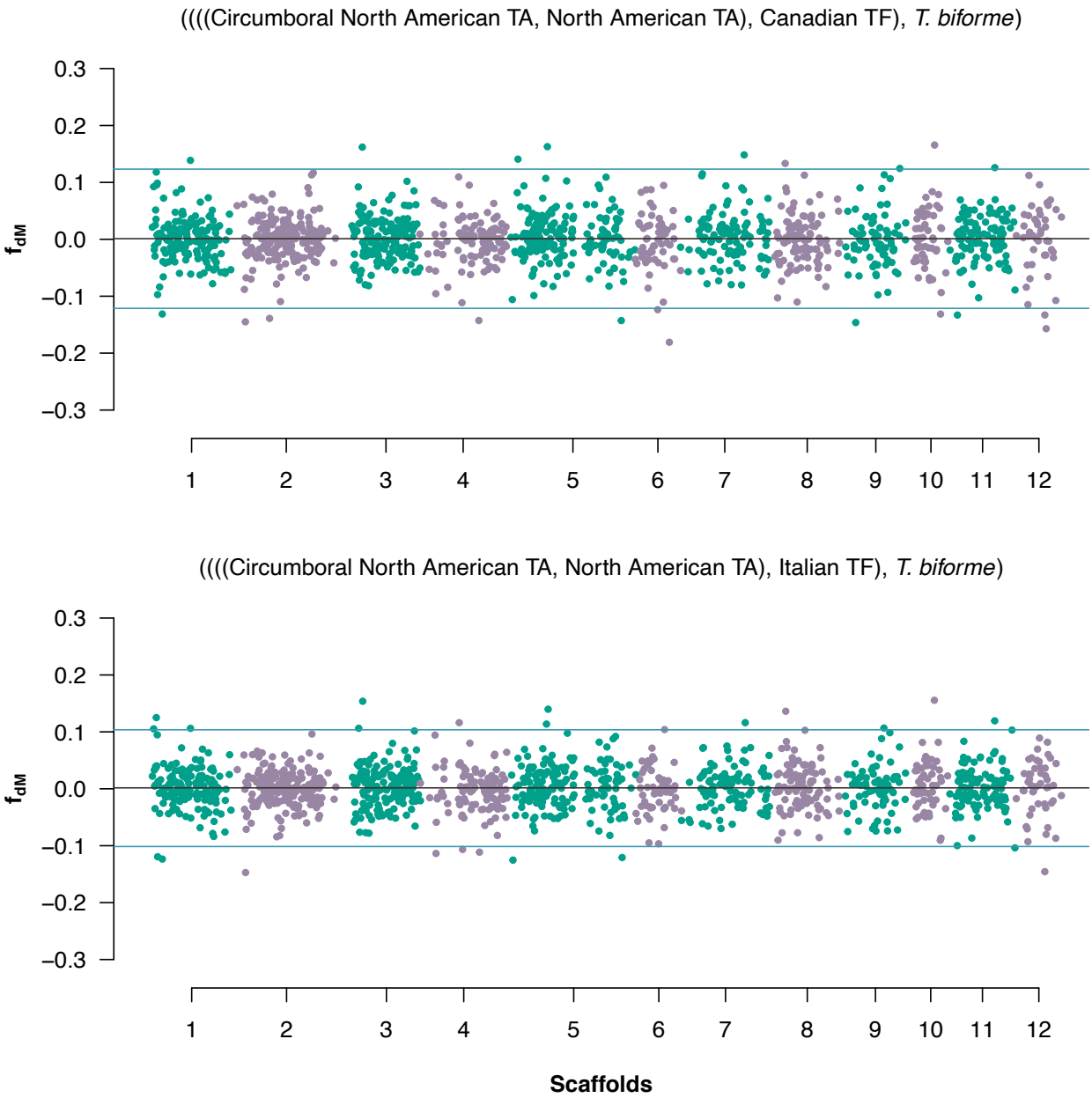

Figure 7, *Signs of scattered introgression throughout the genome*. *A proportion of introgression (f_{dM}) sliding window analysis based on a single nucleotide polymorphism (SNP) dataset of 3 118 957 SNPs where windows with at least 100 SNPs are included. Y-axes show the f_{dM} value, x-axes represent scaffolds (alternating between green and purple), and the black horizontal lines are the mean f_{dM} values. Headers depict the phylogenetic hypothesis in Newick tree format, ((((P1, P2), P3), O), where P1, P2 and P3 are populations investigated for introgression and O is the outgroup. Each point is the f_{dM} value of a window (window size = 20 000 base pairs). A positive value indicates more shared derived polymorphisms than expected between P2 and P3, while a negative value indicates the same for P1 and P3. The points below (negative) or above (positive) the blue lines are the 99.7% outlier windows. Annotated genes in the outlier windows can be found in Table S2. TA =* Trichaptum abietinum *and TF =* T. fuscoviolaceum*. The figure is made in R v4.0.2 GUI 1.72 Catalina build using Rstudio v1.3.1073 and the packages qqman (Turner, 2017), tidyverse (Wickham et al., 2019) and wesanderson (Ram and Wickham, 2018).*

4 Discussion

4.1 Divergent sister species show signs of introgression

The PCA and divergence analyses indicate that *T. abietinum* and *T. fuscoviolaceum* are clearly separated as distinct groups (observed in the PCA and by the elevated F_{ST} and d_{XY} values). High divergence values are prevalent throughout the genomes, disregarding regions in scaffold tails (which can have low values due to conservation of telomeric regions (Mirabello et al., 2012) or bioinformatic handling, e.g., the assembly process). The large genetic differences between the species can be a result of mechanisms such as reproductive isolation (Nei, Maruyama and Wu, 1983) or simply random events over time (i.e., genetic drift; Watterson, 1985). The fungi make up an ancient and diverse kingdom that originated over a billion years ago (Berbee et al., 2020), with the oldest fungal-like fossil dating back to 2.4 billion years ago (Bengtson et al., 2017) and an estimate of 2 – 5 million extant species (Li et al., 2021). The divergence of the order Hymenochaetales, which *Trichaptum* belongs to, dates to the Jurassic, about 167 million years ago (Varga et al., 2019). There are no estimates of the age of *Trichaptum* but seeing the old age of Hymenochaetales, time might be a reasonable explanation for the genome wide high divergence between *T. fuscoviolaceum* and *T. abietinum*, assuming the sister species are old lineages. If this is the case, the morphological similarities between the species are even more interesting. Either because they have been conserved through large periods of time (i.e., morphological stasis; Lee and Frost, 2002), or because the species are converging on similar morphology even though their genomes are largely different (i.e., morphological convergence; Kelly and Motani, 2015). There are several possible explanations as to why the sister species are genetically very divergent. One explanation could be that the genus *Trichaptum* underwent a diversification event during its evolutionary history due to a sudden increase in available hosts (e.g., divergence of conifers), resulting in the emergence of many new species with similar ecologies (Janz, Nylin and Wahlberg, 2006). Over time, several species might have been outcompeted and gone extinct, as they had specialized on the same niche (i.e., exclusion principle; Zaret and Rand, 1971).

Today, *Trichaptum abietinum* and *T. fuscoviolaceum* occur in the same habitat, with similar morphology and ecology, acting as early saprotrophs on newly deceased conifers in the northern hemisphere (Kauserud and Schumacher, 2003). There are 37 accepted species in the genus (Index Fungorum, 2021). The species can grow on the same host, but *T. fuscoviolaceum* is usually found on pine (*Pinus*) and fir (*Abies*; most individuals in this study is collected on balsam fir; *A. balsamea*), while *T. abietinum* is more common on spruce (*Picea*) and larch (*Larix*). Even though habitats overlap, the crossing experiments corroborate previous results (Macrae, 1967) that *T.*

abietinum and *T. fuscoviolaceum* do not hybridize in vitro, and the genomic analyses suggest that this does not happen in situ either. The barriers to gene exchange might have arisen over time as a consequence of sympatric speciation, where gene flow is upheld while populations keep diverging due to for example host specialization (Smith, 1966). This can explain why these sister species are genetically very dissimilar while still occupying the same habitat and ecology today (i.e., they specialized on slightly different host species with some overlap). If such a scenario is true, speciation in sympatry might have lengthened the period of gene exchange. This can again have made it possible for individuals to hybridize because reproductive barriers can remain incomplete in the face of gene flow (Rutherford et al., 2018).

The crossing experiments between *T. fuscoviolaceum* individuals of different populations demonstrate that individuals can still mate successfully even though the divergence analyses exhibit high F_{ST} and d_{XY} values. This could be due to geographic separation of the Italian and Canadian population, reducing reinforcement. Compatibility is not observed among all populations of *T. abietinum*, where intersterility is detected between some populations that occur in sympatry (Macrae, 1967; Kauserud and Schumacher, 2003; Peris et al., in prep.). The genus *Trichaptum* consist of tetrapolar fungi, which means individuals are compatible only when they have different alleles on both of the two mating loci (*MATA* and *MATB*; Fraser et al., 2007). Previous studies have shown that fungal mating loci are diverse and maintained by balancing selection (May et al., 1999; James et al., 2004), which has recently been observed in *Trichaptum* as well (Peris et al., in prep.). In *T. abietinum*, additional reproductive barriers other than incompatible mating loci are at play, causing the formation of intersterility groups. This because the intersterility groups have compatible mating types but still exhibit incompatibility in crossing experiments (Macrae et al., 1967). However, such barriers can, as previously explained, remain incomplete. If other reproductive barriers were incomplete during the divergence of *T. abietinum* and *T. fuscoviolaceum*, and they diverged mostly due to genetic drift, conserved diversity on the mating loci over time can have allowed for introgression by maintaining compatibility across species.

Whether the species diverged due to sympatric speciation, genetic drift, or other mechanisms is difficult to untangle based on my results. However, the *D* and *f*-statistics do show signs of introgression between *T. abietinum* and *T. fuscoviolaceum*. Based on the *D* statistic, it seems like the Italian *T. fuscoviolaceum* have been more involved with the *T. abietinum* populations than the Canadian *T. fuscoviolaceum* (Figure 8). Which might seem odd, as it is the Canadian *T. fuscoviolaceum* population that currently occur in sympatry with the collected *T. abietinum* populations. The f_4 ratio test further corroborates these results, indicating that the Italian *T. fuscoviolaceum* share a longer evolutionary history with the *T. abietinum* populations than the Canadian *T. fuscoviolaceum* (Figure 8). The violation of the statistical model for some topologies with *T. abietinum* and *T. fuscoviolaceum* populations as sister species in the f_4 ratio test can be due to lack of data from populations not sampled (i.e., ghost populations; Beerli, 2004), suggesting a

more intricate evolutionary history of *Trichaptum* than the collected data can disclose. It is difficult to tell based on the results when and between which populations introgression occurred. One scenario can be that a *T. fuscoviolaceum* ghost population introgressed with *T. abietinum* populations and that this ghost population was more closely related to the Italian than the Canadian *T. fuscoviolaceum*. Another possibility can be that the Canadian *T. fuscoviolaceum* hybridized with a ghost population, becoming more dissimilar to the *T. abietinum* populations than the Italian *T. fuscoviolaceum*. Based on the high divergence and similar proportion of introgression between the Italian *T. fuscoviolaceum* and both *T. abietinum* populations in the f_4 ratio test (similar values also observed in the *D* statistic), it seems more probable that an introgression event is placed further back in time. This is corroborated by the f_3 result where *T. abietinum* populations diverged later than the *T. fuscoviolaceum* populations (the *T. abietinum* populations are also positioned closer on PC1 in the PCA than the *T. fuscoviolaceum* populations). Accordingly, the introgression most likely occurred between the ancestral population that gave rise to the Circumboreal North American and the North American *T. abietinum* and a *T. fuscoviolaceum* population related to the Italian one (Figure 8). The f_{dM} analysis give similar number of introgressed genes for both the Italian and the Canadian *T. fuscoviolaceum* population tested against the *T. abietinum* populations, which further suggests that ancestral, and not current, populations of *T. abietinum* and *T. fuscoviolaceum* hybridized (Figure 8). The small regions of scattered introgression in the f_{dM} sliding window analysis also imply ancient introgression. This follows similar patterns with highly divergent genomes and localized regions of introgression as found in analyses of three-spined stickleback species pairs in the Japanese archipelago (Ravinet et al., 2018) and *Heliconius* butterflies in Brazil (Zhang et al., 2016).

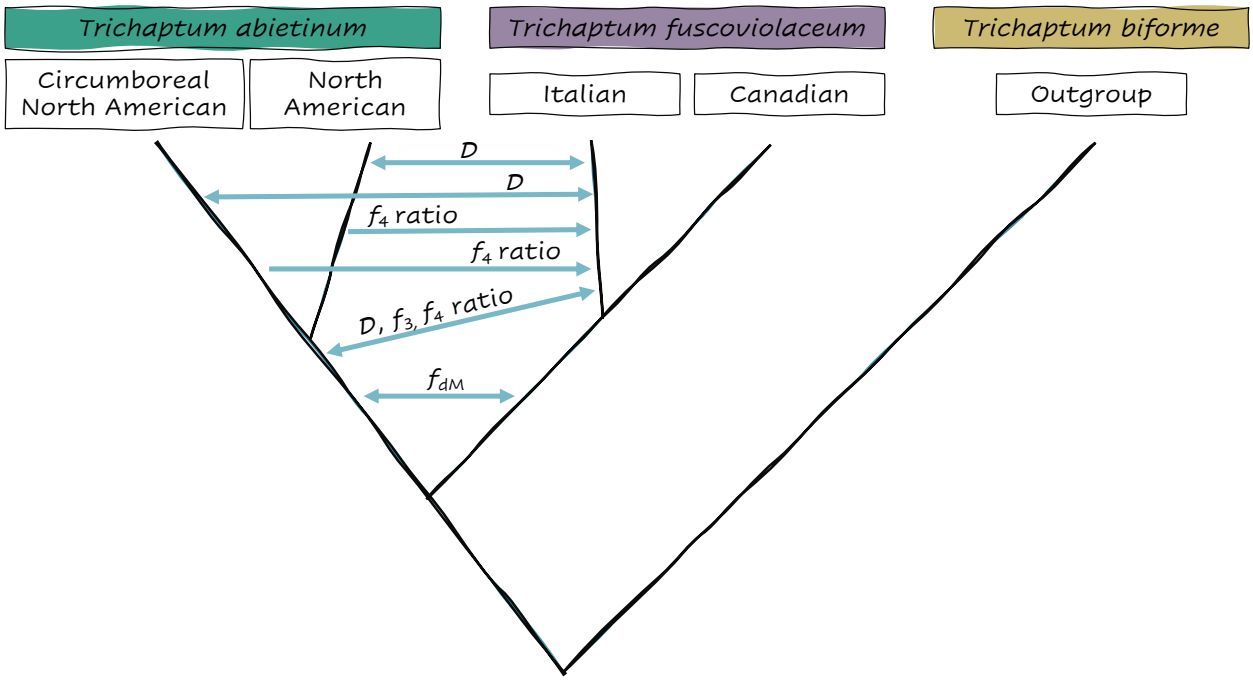

Figure 8, ***The source, direction, and time of introgression is indecisive.*** *A sketch of the possible introgression events based on results from the* D *statistic,* f_4 *ratio statistic,* f_3 *statistic and* f_{dM} *analysis. The figure was made in Microsoft® PowerPoint for Mac v16.50.*

4.2 Ancient introgression and its implications

As the species are highly divergent, it is possible that several *Trichaptum* lineages have gone extinct (populations or species) leading up to the current taxa. The signs of introgression observed in the *D* and *f*-statistics could then be a case of introgression from extinct lineages. Ancient introgression has previously been detected from extinct cave bears in the genomes of brown bears (*Ursus arctus*; Barlow et al., 2018), through phenotype analyses of beak sizes in one of Darwin's finches (*Geospiza fortis*; Grant and Grant, 2021), and in the mitochondrial genome of the intermediate horseshoe bat (*Rhinolophus affinis*; Mao et al., 2012). Genes from extinct lineages can in this way persist in extant species and might impose adaptive benefits (The *Heliconius* Genome Consortium et al., 2013). It is difficult to say if this is the case with *T. abietinum* and *T. fuscoviolaceum*, but genes found in outlier windows of the f_{dM} analysis can represent putatively adaptive genes with an ancient introgression origin. Many of the genes code for proteins of unknown function, which is common in non-model organisms due to limited research. The genes with similarity to other functional annotated genes are involved in several different functions in organisms (e.g., oxidoreductases and hydrolases partake in numerous enzymatic reactions; The UniProt Consortium, 2021), but whether any of these genes are involved in adaptive introgression cannot be concluded based on the f_{dM} analysis alone. Thus, this question remains inconclusive until further analyses are conducted (see section 4.5).

Genes transferred through introgression can lead to an expansion of a species' distribution range as seen in cypress species (*Cupressus* sp.) at the eastern Qinghai-Tibet Plateau, where ancient introgression has been found to be related to habitat adaptation and possibly adaptation to cooler and drier weather at higher altitudes (Ma et al., 2019). The divergence of many of the taxa in the family Pinaceae, which includes the current host species of *T. fuscoviolaceum* and *T. abietinum*, is dated to the Jurassic (< ~185 million years ago; Ran et al., 2018), the same period as the divergence of Hymenochaetales. There are several examples where research on cryptic diversity in fungi has revealed high divergence and old divergence times when species initially were thought to be closely related (summarized in Skrede, 2021), which might also be the case for *T. fuscoviolaceum* and *T. abietinum*. My results cannot conclude on adaptive introgression but based on the large nucleotide discrepancies and possibly old divergence, one could speculate that introgression has facilitated adaption to a larger host range of *T. fuscoviolaceum* and *T. abietinum* as conifers diverged and expanded across the northern hemisphere. More research is needed to say anything certain about the implications of introgression between *T. fuscoviolaceum* and *T. abietinum*.

Since ancient introgression can have impacts on the evolutionary trajectory of a species, it is an important mechanism to consider when investigating the evolutionary history of taxa. Ancient introgression is not vastly examined in fungi. There are some studies that indicate adaptive ancient introgression and host specialization in parasitic fungi (e.g., *Microbotryum violaceum*; Le Gac et al., 2007), but research within the Agaricales has not been conducted to my knowledge. My results indicate that ancient introgression can be found among mushroom-forming fungi, especially regarding the old age of many species in this part of the tree of life (Varga et al., 2019). Even though the phylogenetic relationship between *T. fuscoviolaceum* and *T. abietinum* is well-defined (Seierstad et al., 2020), signals of introgression lingering in their genomes suggest that the evolutionary history of these species is more complex than the current phylogenies can reveal.

4.3 Methodological aspects and future perspectives

To investigate my research questions, I settled on a restricted set of experimental and analytical methods doable within the time limits and scope of my thesis. The divergence and ABBA-BABA (*D* and *f* statistics) analyses are relatively new statistical tools to implement when working with whole-genome sequences and research questions regarding speciation and more specifically introgression. There are also only a few examples of the application of ABBA-BABA statistics in studies of fungi (e.g., Maxwell et al., 2018; Sillo et al., 2021). The tools are accessible and suited my aims, dataset, and time limit. The original *D* statistics had also been updated to fit sliding window analyses (Martin, Davey and Jiggins, 2014), which I had planned to perform. If the time limit had been less stringent, I could preferably have conducted additional analyses to dig deeper

into the direction and implications of introgression. I could have coupled my analyses with other statistical tools such as positive selection analyses, admixture analyses, and graph approaches (e.g., TreeMix), together with a hidden Markov-model approach as a more unbiased way to find genomic windows with significant introgression, as used in Ravinet et al. (2018). It would also have been interesting to test other reference genomes than the *T. fuscoviolaceum* reference used in this study. In this way, I could be more certain that some of my results are not artifacts of the reference genome I used (e.g., the slight differences between the Italian and the Canadian *T. fuscoviolaceum* population in the f_3 analysis).

The sampling scheme of *T. fuscoviolaceum* and *T. abietinum* populations could have, in retrospect, been conducted more evenly, assuring an equal number of individuals in all populations, and covered a larger area of the species' distribution. As it is not possible to differentiate the sympatric Circumboreal North American and North American *T. abietinum* in the field, such a sampling scheme is difficult to implement, but I could have included additional collections to increase the number of individuals in the North American population compared to the Circumboreal North American. Regarding *T. fuscoviolaceum*, the individuals from Italy were not collected specifically for this study, resulting in only one collection site in Italy, compared to 14 in Canada. Whether the skewness of populations and number of individuals had an impact on the analyses is difficult to assess without increasing the sampling size. If the effective population sizes (i.e., the number of individuals needed to account for the same amount of genetic drift as in the original population; Lande and Barrowclough, 1987) are not largely diminished by the sampling scheme, the introgression analyses should exhibit similar results as in a bigger dataset, conserving the nucleotide diversity of the natural populations (Martin, Davey and Jiggins, 2014). The sliding window π analyses did not display specifically low amounts of within population variation, which could indicate that the individuals included in the dataset echoes the effective population sizes of the original populations. In future research, a wider collection, including more populations across the northern hemisphere (e.g., Asia, and throughout Europe, and North America), could possibly capture ghost populations and help untangling the intricate evolutionary history of *T. abietinum* and *T. fuscoviolaceum*.

My results cannot conclude on adaptive introgression or impacts of introgression on the distribution range of the sister species. In future research, it would be possible to conduct biogeography studies to reveal the place of origin of the genus *Trichaptum* and subsequent migration routes and connections to host species. Thus, the signs of introgression found in this study could possibly be linked to historical events increasing insight into the mechanisms governing speciation and adaptation in these species. To be more certain about divergence times within the genus, a molecular dating analyses could be conducted. The lack of fungal specimens in the fossil record makes it hard to perform a primary calibration, but by using the few fossils available and molecular clock models, a calibration should be doable (Berbee et al., 2020; dos Reis, Donoghue and Yang, 2016; Varga et al., 2019). It would also be possible to estimate the time

of introgression using a multispecies coalescent model with introgression (Flouri et al., 2020). The divergence and introgression times could then be investigated in concert with the biogeography analyses to possibly reveal connections to for example adaptations, distribution expansion, or host shifts.

I discovered several unknown proteins in the outlier windows of the sliding window introgression analysis. It would be interesting to reveal the function of these proteins to better understand the implications of the introgression events and if there are any adaptational benefits linked to these genomic regions or if the regions have been retained in the genomes due to mechanisms such as high recombination rate (Ravinet et al., 2018) or genetic drift. It would also be possible to conduct an enrichment analysis to reveal if there are more unknown proteins in the introgressed regions compared to the rest of the genome and in this way assess the probability of the genes being preserved due to chance or possibly adaptational benefits (Mostert-O'Neill et al., 2020). An enrichment analysis could also be applied to figure out if there are more genes with specific functions than what is expected by chance in the introgressed regions (as was done for genes under selection in Balasundaram et al., 2018). As genes coding for unknown proteins keep accumulating in studies on non-model organisms, more research into the function of these proteins is needed to better understand the adaptational implications they impose.

The kingdom of fungi remains an uncharted territory in many ways, with knowledge gaps including diversity, ecology, and life histories of the species it encompasses. Fungi can almost appear alien at times, with their unrelatable way of life; massive mycelial networks spreading through soil, symbiotic relationships forming lichens in extreme environments and mycorrhiza with plants, single celled yeasts fermenting bread and beverages, and colorful mushrooms developing overnight. The fungi are everywhere, even in the oceans. By studying the evolution of these successful organisms, we can better understand how life evolves on earth. My research is a tiny cut into a scarcely studied part of fungal evolution, but hopefully new research will answer unresolved questions from this study in the future.

4.4 Conclusion

My study corroborates earlier findings, indicating that *T. abietinum* and *T. fuscoviolaceum* do not hybridize in vitro. The results show that the sister species are highly divergent, exhibiting large genetic difference and are reproductively isolated. Nevertheless, introgression analyses display signs of previous admixture, with small regions of introgression occurring throughout their genomes. These signs points to a case of ancient introgression between ancestral populations of *T. abietinum* and *T. fuscoviolaceum*. Regardless of a well-resolved phylogeny, the evolutionary history of these species seems to be intricate, including transfer of genes across lineages with unknown implications. The study is the first investigation into ancient introgression among mushroom-forming fungi, expanding our knowledge on how these old taxa evolve and radiate. The ceaselessness of speciation will naturally leave traces of historical events in the genomes of extant organisms. Accounting for these events when investigating speciation and adaptation can give insight into how evolution proceeds and thus add a piece to the puzzle of life.

References

Abbott, R., Albach, D., Ansell, S., Arntzen, J. W., Baird, S. J. E., Bierne, N., Boughman, J., Brelsford, A., Buerkle, C. A., Buggs, R., Butlin, R. K., Dieckmann, U., Eroukhmanoff, F., Grill, A., Cahan, S. H., Hermansen, J. S., Hewitt, G., Hudson, A. G., Jiggins, C., Jones, J., Keller, B., Marczewski, T., Mallet, J., Martinez-Rodriguez, P., Möst, M., Mullen, S., Nichols, R., Nolte, A. W., Parisod, C., Pfennig, K., Rice, A. M., Ritchie, M. G., Seifert, B., Smadja, C. M., Stelkens, R., Szymura, J. M., Väinölä, R., Wolf, J. B. W. and Zinner, D. (2013). Hybridization and speciation, *Journal of Evolutionary Biology*, 26(2), pp. 229-246. https://doi.org/10.1111/j.1420-9101.2012.02599.x.

Abbott, R. J., Hegarty, M. J., Hiscock, S. J. and Brennan, A. C. (2010). Homoploid hybrid speciation in action, *Taxon*, 59(5), 1375-1386. https://doi.org/10.1002/tax.595005.

Altschul, S.F., Gish, W., Miller, W., Meyers, E. W. and Lipman, D. J. (1990). Basic local alignment search tool, *Journal of Molecular Biology*, 215(3), pp. 403-410. https://doi.org/10.1016/S0022-2836(05)80360-2.

Anderson, E. and Hubricht, L. (1938). Hybridization in *Tradescantia*. III. The evidence for introgressive hybridization, *Botany*, 25(6), pp. 396-402. https://doi.org/10.1002/j.1537-2197.1938.tb09237.x.

Andrews, S. (2010). *FastQC: A Quality Control Tool for High Throughput Sequence Data*. http://www.bioinformatics.babraham.ac.uk/projects/fastqc/.

Balasundaram, S. V., Hess, J., Durling, M. B., Moody, S. C., Thorbek, L., Progida, C., LaButti, K., Aerts, A., Barry, K., Grigoriev, I. V., Boddy, L., Högberg, N., Kauserud, H., Eastwood, D. C. and Skrede, I. (2018). The fungus that came in from the cold: dry rot's pre-adapted ability to invade buildings, *The ISME Journal*, 12(3), pp. 791-801. https://doi.org/10.1038/s41396-017-0006-8.

Barlow, A., Cahill, J. A., Hartmann, S., Theunert, C., Xenikoudakis, G., Fortes, G. G., Paijmans, J. L. A., Rabeder, G., Frischauf, C., Grandal-d'Anglade, A., García-Vázquez, A., Murtskhvaladze, M., Saarma, U., Anijalg, P., Skrbinšek, T., Bertorelle, G., Gasparian, B., Bar-Oz, G., Pinhasi, R., Slatkin, M., Dalén, L., Shapiro, B. and Hofreiter, M. (2018). Partial genomic survival of cave bears in living brown bears, *Nature Ecology & Evolution*, 2(10), pp.1563-1570. https://doi.org/10.1038/s41559-018-0654-8.

Baumgartner, K., Baker, B. R., Korhonen, K., Zhao, J., Hughes, K. W., Bruhn, J., Bowman, T. S. and Bergemann, S. E. (2012). Evidence of natural hybridization among homothallic members of the basidiomycete *Armillaria mellea* sensu stricto, *Fungal Biology*, 116(6), pp. 677-691. https://doi.org/10.1016/j.funbio.2012.03.006.

Beerli, P. (2004). Effect of unsampled populations on the estimation of population sizes and migration rates between sampled populations, *Molecular Ecology*, 13(4), pp. 827-836. https://doi.org/10.1111/j.1365-294X.2004.02101.x.

Bengtson, S., Rasmussen, B., Ivarsson, M., Muhling, J., Broman, C., Marone, F., Stampanoni, M. and Bekker, A. (2017). Fungus-like mycelial fossils in 2.4-billion-year-old vesicular basalt, *Nature Ecology and Evolution*, 1(6), Article number: 0141. https://doi.org/10.1038/s41559-017-0141.

Benoit, K. and Obeng, A. (2020). *Readtext: Import and Handling for Plain and Formatted Text Files. R package version 0.80*. https://CRAN.R-project.org/package=readtext.

Berbee, M.L., Strullu-Derrien, C., Delaux, P-M., Strother, P. K., Kenrick, P., Selosse, M-A. and Taylor, J. W. (2020). Genomic and fossil windows into the secret lives of the most ancient fungi, *Nature Reviews of Microbiology,* 18(12)**,** pp. 717–730. https://doi.org/10.1038/s41579-020-0426-8.

Bivand, R. S., Pebesma, E. and Gomez-Rubio, V. (2013). *Applied spatial data analysis with R*. 2nd ed. New York: Springer.

Bresinsky, A., Fischer, M., Meixner, B. and Paulus, W. (1987). Speciation in *Pleurotus, Mycologia*, 79(2), pp. 234-245. https://doi.org/10.1080/00275514.1987.12025703.

Butlin, R. (1987). Speciation by reinforcement, *Trends in Ecology & Evolution*, 2(1), pp. 8-13. https://doi.org/10.1016/0169-5347(87)90193-5.

Chandler, C. R. and Gromko, M. H. (1989). On the relationship between species concepts and speciation processes, *Systematic Zoology*, 38(2), pp. 116-125. https://doi.org/10.1093/sysbio/38.2.116.

Chang, C. C., Chow, C. C., Tellier, L. C., Vattikuti, S., Purcell, S. M. and Lee, J. J. (2015). Second generation PLINK: rising to the challenge of larger and richer datasets, *GigaScience*, 4(1). https://doi.org/10.1186/s13742-015-0047-8.

Chang, L-Y., Toghiani, S., Hay, E. H., Aggrey, S. E. and Rekaya, R. (2019). A Weighted Genomic Relationship Matrix Based on Fixation Index (FST) Prioritized SNPs for Genomic Selection, *Genes*, 10(11), pp. 922-931. https://doi.org/10.3390/genes10110922.

Chung, C-L., Lee, T. J., Akiba, M., Lee, H-H., Kuo, T-H., Liu, D., Ke, H-M., Yokoi, T., Roa, M. B., Lu, M-Y. J., Chang, Y-Y., Ann, P-J., Tsai, J-N., Chen, G-Y., Tzean, S-S., Ota, Y., Hattori, T., Sahashi, N., Liou, R. F., Kikuchi, T. and Tsai, I. J. (2017). Comparative and population genomic landscape of Phellinus noxius: A hypervariable fungus causing root rot in trees, *Molecular Ecology*, 26(22), pp. 6301-6316. https://doi.org/10.1111/mec.14359.

Crowl, A. A., Manos, P. S., McVay, J. D., Lemmon, A. R., Lemmon, E. M. and Hipp, A. L. (2019). Uncovering the genomic signature of ancient introgression between white oak lineages (*Quercus*), *New Phytologist*, 226(4), pp. 1158-1170. https://doi.org/10.1111/nph.15842.

Danecek, P., Auton, A., Abecasis, G., Albers, C. A, Banks, E., DePristo, M. A., Handsaker, R., Lunter, G., Marth, G., Sherry, S. T., McVean, G., Durbin, R. and 1000 Genomes Project Analysis Group. (2011). The variant call format and VCFtools, *Bioinformatics*, 27(15), pp. 2156-2158. https://doi.org/10.1093/bioinformatics/btr330.

Danecek, P., Bonfield, J. K., Liddle, J., Marshall, J., Ohan, V., Pollard, M. O., Whitwham, A., Keane, T., McCarthy, S. A., Davies, R. M. and Li, H. (2021). Twelve years of SAMtools and BCFtools, *GigaScience*, 10(2). https://doi.org/10.1093/gigascience/giab008.

Devier, B., Aguileta, G., Hood, M. E. and Giraud, T. (2010). Using phylogenies of pheromone receptor genes in the *Microbotryum violaceum* species complex to investigate possible speciation by hybridization, *Mycologia*, 102(3), pp. 689-696. https://doi.org/10.3852/09-192.

Dowle, M. and Srinivasan, A. (2020). *Data.table: Extension of `data.frame`. R package version 1.13.0.* https://CRAN.R-project.org/package=data.table.

Edgar, R. C. (2004). MUSCLE: a multiple sequence alignment method with reduced time and space complexity, *BMC Bioinformatics*, 5(113), Article number: 113. https://doi.org/10.1186/1471-2105-5-113.

Ewels, P., Magnusson, M., Lundin, S. and Käller, M. (2016). MultiQC: Summarize analysis results for multiple tools and samples in a single report, *Bioinformatics*, 32(19), pp. 3047-3048. https://doi.org/10.1093/bioinformatics/btw354.

Flouri, T., Jiao, X., Rannala, B. and Yang, Z. (2020). A Bayesian implementation of the multispecies coalescent model with introgression for phylogenomic analysis, *Molecular Biology and Evolution*, 37(4), pp. 1211–1223. https://doi.org/10.1093/molbev/msz296.

Flynn, J. M., Hubley, R., Goubert, C., Rosen, J., Clark, A. G., Feschotte, C. and Smit, A. F. (2020). RepeatModeler2 for automated genomic discovery of transposable element families, *Proceedings of the National Academy of Sciences of the United States of America*, 117(17), pp. 9451-9457. https://doi.org/10.1073/pnas.1921046117.

Fraser, J. A., Hsueh, Y-P., Findley, K. M. and Heitman, J. (2007). Evolution of the Mating-Type Locus: The Basidiomycetes, in Heitman, J., Kronstad, J. W., Taylor, J. W. and Casselton, L. A. (ed.) *Sex in Fungi*. Washington, D.C.: ASM Press, pp. 19-34. https://doi.org/10.1128/9781555815837.ch2.

Garbelotto, M., Ratcliff, A., Bruns, T. D., Cobb, F. W. and Otrosina, W. J. (1996). Use of taxon-specific competitive-priming PCR to study host specificity, hybridization, and intergroup gene flow in intersterility groups of *Heterobasidion annosum*, *Phytopathology*, 86(5), pp. 543-551. https://doi.org/10.1094/phyto-86-543.

Garnier, S. (2018). *Viridis: Default Color Maps from 'matplotlib'. R package version 0.5.1.* https://CRAN.R-project.org/package=viridis.

Giordano, L., Sillo, F., Garbelotto, M. and Gonthier, P. (2018). Mitonuclear interactions may contribute to fitness of fungal hybrids, *Scientific Reports*, 8(1), pp. 1706. https://doi.org/10.1038/s41598-018-19922-w.

Grant, P. R. and Grant, B. R. (2021). Morphological ghosts of introgression in Darwin's finch populations, *Proceedings of the National Academy of Sciences of the United States of America*, 118(31), Article number: e2107434118. https://doi.org/10.1073/pnas.2107434118.

Harrison, R. G. and Larson, E. L. (2014). Hybridization, introgression, and the nature of species boundaries, *Journal of Heredity*, 105(1), pp. 795–809. https://doi.org/10.1093/jhered/esu033.

Hegarty, M. J. and Hiscock, S. J. (2005). Hybrid speciation in plants: new insights from molecular studies, *New Phytologist*, 165(2), pp. 411-423. https://doi.org/10.1111/j.1469-8137.2004.01253.x.

Heinzelmann, R., Rigling, D., Sipos, G., Münsterkötter, M. and Croll, D. (2020). Chromosomal assembly and analyses of genome-wide recombination rates in the forest pathogenic fungus *Armillaria ostoyae*, *Heredity*, 124(6), pp. 699-713. https://doi.org/10.1038/s41437-020-0306-z.

The Heliconius Genome Consortium, Dasmahapatra, K. K., Walters, J., Briscoe, A. D., Davey, J. W., Whibley, A., Nadeau, N. J., Zimin, A. V., Hughes, D. S. T., Ferguson, L. C., Martin, S. H., Salazar, C., Lewis, J. J., Adler, S., Ahn, S-J., Baker, D. A., Baxter, S. W., Chamberlain, N. L., Chauhan, R., Counterman, B. A., Dalmay, T., Gilbert, L. E., Gordon, K., Heckel, D. G., Hines, H. M., Hoff, K. J., Holland, P. W. H., Jacquin-Joly, E., Jiggins, F. M., Jones, R. T., Kapan, D. D., Kersey, P., Lamas, G., Lawson, D., Mapleson, D., Maroja, L. S., Martin, A., Moxon, S., Palmer, W. J., Papa, R., Papanicolaou, A., Pauchet, Y., Ray, D. A., Rosser, N., Salzberg, S. L., Supple, M. A., Surridge, A., Trolander, A. T., Vogel, H., Wilkinson, P. A., Wilson, D., Yorke, J. A., Yuan, F., Balmuth, A. L., Eland, C., Gharbi, K., Thomson, M., Gibbs, R. A., Han, Y., Jayaseelan, J. C., Kovar, C., Mathew, T., Muzny, D. M., Ongeri, F., Pu, L-L., Qu, J., Thornton, R. L., Worley, K. C., Wu, Y-Q., Linares, M., Blaxter, M. L., Constant, R. H. F., Joron, M., Kronforst, M. R., Mullen, S. P., Reed, R. D., Scherer, S. E., Richards, S., Mallet, J., McMillan, W. O. and Jiggins, C. D. (2012). Butterfly genome reveals promiscuous exchange of mimicry adaptations among species, *Nature*, 487(7405), pp. 94-98. https://doi.org/10.1038/nature11041.

Hessenauer, P., Fijarczyk, A., Martin, H., Prunier, J., Charron, G., Chapuis, J., Bernier, L., Tanguay, P., Hamelin, R. C. and Landry, C. R. (2020). Hybridization and introgression drive genome evolution of Dutch elm disease pathogens, *Nature Ecology & Evolution*, 4(4), pp. 626–638. https://doi.org/10.1038/s41559-020-1133-6.

Hibbet, D. S. (2006). A phylogenetic overview of the Agaricomycotina, *Mycologia*, 98(6), pp. 917-925. https://doi.org/10.1080/15572536.2006.11832621.

Holt, C. and Yandell. M. (2011). MAKER2: an annotation pipeline and genome-database management tool for second-generation genome projects, *BMC Bioinformatics*, 12(1), Article number: 491. https://doi.org/10.1186/1471-2105-12-491.

Hotelling, H. (1933). Analysis of a complex of statistical variables into principal components. *Journal of Educational Psychology*, 24(6), pp. 414-441. https://doi.org/10.1037/h0071325.

Index Fungorum. (2021). Index Fungorum, *The Royal Botanic Gardens Kew*. www.indexfungorum.org.

Jain, C., Rodriguez-R, L.M., Phillippy, A.M., Konstantinidis, K. T. and Aluru, S. (2018). High throughput ANI analysis of 90K prokaryotic genomes reveals clear species boundaries, *Nature Communications*, 9(1), Article number: 5114. https://doi.org/10.1038/s41467-018-07641-9.

James, T. Y., Kües, U., Rehnerc, S. A. and Vilgalysa, R. (2004). Evolution of the gene encoding mitochondrial intermediate peptidase and its cosegregation with the A mating-type locus of mushroom fungi, *Fungal Genetics and Biology*, 41(3), pp. 381-390. https://doi.org/10.1016/j.fgb.2003.11.008.

Janz, N., Nylin, S. and Wahlberg, N. (2006). Diversity begets diversity: host expansions and the diversification of plant-feeding insects, *BMC Evolutionary Biology*, 6(1), Article number: 4. https://doi.org/10.1186/1471-2148-6-4.

Jolliffe, I. T. (2002). *Principal Component Analysis*. 2nd ed. New York: Springer.

Jones, P., Binns, D., Chang, H-Y., Fraser, M., Li, W., McAnulla, C., McWilliam, H., Maslen, J., Mitchell, A., Nuka, G., Pesseat, S., Quinn, A. F., Sangrador-Vegas, A., Scheremetjew, M., Yong, S-Y., Lopez, R. and Hunter, S. (2014). InterProScan 5: genome-scale protein function classification, *Bioinformatics*, 30(9), pp. 1236-40. https://doi.org/10.1093/bioinformatics/btu031.

Kauserud, H. and Schumacher, T. (2003). Ribosomal DNA variation, recombination and inheritance in the basidiomycete *Trichaptum abietinum*: implications for reticulate evolution, *Heredity*, 91(2), pp. 163-172. https://doi.org/10.1038/sj.hdy.6800294.

Kelley, N. P. and Motani, R. (2015). Trophic convergence drives morphological convergence in marine tetrapods, *Biological Letters*, 11(1), Article number: 20140709. http://dx.doi.org/10.1098/rsbl.2014.0709.

Keuler, R., Garretson, A., Saunders, T., Erickson, R. J., St. Andre, N., Grewe, F., Smith, H., Lumbsch, H. T., Huang, J-P, St. Clair, L. L. and Leavitt, S. D. (2020). Genome-scale data reveal the role of hybridization in lichen-forming fungi, *Scientific Reports*, 10(1), Article number: 1497. https://doi.org/10.1038/s41598-020-58279-x.

Ko, K. S. and Jung, H. S. (2002). Three nonorthologous ITS1 types are present in a polypore fungus *Trichaptum abietinum*, *Molecular Phylogenetics and Evolution*, 23(2), pp. 112-122. https://doi.org/10.1016/S1055-7903(02)00009-X.

Krueger, F. (2015). *Trim Galore!: A wrapper tool around Cutadapt and FastQC to consistently apply quality and adapter trimming to FastQ files*. http://www.bioinformatics.babraham.ac.uk/projects/trim_galore/.

Lande, R. and Barrowclough, G. F. (1987). Effective population size, genetic variation, and their use in population, in Soulé, M. E. (ed.) *Viable Populations for Conservation*. Cambridge: Cambridge University Press, pp. 87-124. https://doi.org/10.1017/CBO9780511623400.007.

Langdon, Q. K., Peris, D., Baker, E. C. P., Opulente, D. A., Nguyen, H-V., Bond, U., Gonçalves, P., Sampaio, J. P., Libkind, D. and Hittinger, C. T. (2019). Fermentation innovation through complex hybridization of wild and domesticated yeasts, *Nature Ecology & Evolution*, 3(11), pp. 1576-1586. https://doi.org/10.1038/s41559-019-0998-8.

Langdon, Q. K., Peris, D., Kyle, B., and Hittinger, C. T. (2018). sppIDer: A species identification tool to investigate hybrid genomes with high-throughput sequencing, *Molecular Biology and Evolution*, 35(11), pp. 2835-2849. https://doi.org/10.1093/molbev/msy166.

Le Gac, M., Hood, M. E., Fournier, E. and Giraud, T. (2007). Phylogenetic evidence of host-specific cryptic species in the anther smut fungus, *Evolution*, 61(1), pp. 15-26. https://doi.org/10.1111/j.1558-5646.2007.00002.x.

Lee, C. E. and Frost, B. W. (2002). Morphological stasis in the *Eurytemora affinis* species complex (Copepoda: Temoridae), *Hydrobiologia*, 480(1-3), pp. 111-128. https://doi.org/10.1023/A:1021293203512.

Li, H. and Durbin, R. (2009). Fast and accurate short read alignment with Burrows-Wheeler Transform, *Bioinformatics*, 25(14), pp. 1754-60. https://doi.org/10.1093/bioinformatics/btp324.

Li, H., Handsaker, B., Wysoker, A., Fennell, T., Ruan, J., Homer, N., Marth, G., Abecasis, G., Durbin, R. and 1000 Genome Project Data Processing Subgroup. (2009). The Sequence alignment/map (SAM) format and SAMtools, *Bioinformatics*, 25(16), pp. 2078-2079. https://doi.org/10.1093/bioinformatics/btp352.

Li, Y., Steenwyk, J. L., Chang, Y., Wang, Y., James, T. Y., Stajich, J. E., Spatafora, J. W., Groenewald, M., Dunn, C. W., Hittinger, C. T., Shen, X-X. and Rokas, A. (2021). A genome-scale phylogeny of the kingdom Fungi, *Current Biology*, 31(8), pp. 1653-1665.e5. https://doi.org/10.1016/j.cub.2021.01.074.

Lunter, G. and Goodson, M. (2011). Stampy: A statistical algorithm for sensitive and fast mapping of Illumina sequence reads, *Genome Research*, 21(6), pp. 961-973. http://doi.org/10.1101/gr.111120.110.

Ma, Y., Wang, J., Hu, Q., Li, J., Sun, Y., Zhang, L., Abbott, R. J., Liu, J. and Mao, L. (2019). Ancient introgression drives adaptation to cooler and drier mountain habitats in a cypress species complex, *Communications Biology*, 2(1), Article number: 213. https://doi.org/10.1038/s42003-019-0445-z.

Macrae, R. (1967). Pairing incompatibility and other distinctions among *Hirchiporus abietinus*, *H. fusco-violaceus*, and *H. laricinus*, *Canadian Journal of Botany*, 45(8), pp. 1371-1399. https://doi.org/10.1139/b67-144.

Mallet, J. (2008). Hybridization, ecological races and the nature of species: empirical evidence for the ease of speciation. *Philosophical transactions of the Royal Society of London, Series B, Biological sciences*, 363(1506), pp. 2971-2986. https://doi.org/10.1098/rstb.2008.0081.

Martin, S. H., Davey, J. W. and Jiggins, C. D. (2014). Evaluating the use of ABBA–BABA statistics to locate introgressed loci, *Molecular Biology and Evolution*, 32(1), pp. 244–257. https://doi.org/10.1093/molbev/msu269.

Mavárez, J., Salazar, C. A., Bermingham, E., Salcedo, C., Jiggins, C. D. and Linares, M. (2006). Speciation by hybridization in *Heliconius* butterflies, *Nature*, 441(7095), pp. 868-871. https://doi.org/10.1038/nature04738.

Maxwell, C. S., Mattox, K., Turissini, D. A., Teixeira, M. M., Barker, B. M. and Matute, D. R. (2018). Gene exchange between two divergent species of the fungal human pathogen, *Coccidioides*, *Evolution*, 73(1), pp. 42-58. https://doi.org/10.1111/evo.13643.

May, G., Shaw, F., Badrane, H. and Vekemans, X. (1999). The signature of balancing selection: Fungal mating compatibility gene evolution, *Proceedings of the National Academy of Sciences of the United States of America*, 96(16), pp. 9172–9177. https://doi.org/10.1073/pnas.96.16.9172.

McKenna, A., Hanna, H., Banks, E., Sivachenko, A., Cibulskis, K., Kernytsky, A., Garimella, K., Altshuler, D., Gabriel, S., Daly, M. and DePristo, M. A. (2010). The Genome Analysis Toolkit: A MapReduce framework for analyzing next-generation DNA sequencing data, *Genome Research*, 20(9), pp. 1297-1303. http://doi.org/10.1101/gr.107524.110.

Mirabello, L., Yeager, M., Chowdhury, S., Qi, L., Deng, X., Wang, Z., Hutchinson, A. and Savage, S. A. (2012). Worldwide genetic structure in 37 genes important in telomere biology, *Heredity*, 108(2), pp. 124–133. https://doi.org/10.1038/hdy.2011.55.

Mostert-O'Neill, M.M., Reynolds, S. M., Acosta, J. J., Lee, D. J., Borevitz, J. O. and Myburg, A. A. (2020). Genomic evidence of introgression and adaptation in a model subtropical tree species, *Eucalyptus grandis*, *Molecular Ecology*, 30(3), pp. 625-638. https://doi.org/10.1111/mec.15615.

Mullis, K., Faloona, F., Scharf, S., Saiki, R., Horn, G. and Erlich, H. (1986). Specific enzymatic amplification of DNA in vitro: the polymerase chain reaction, *Cold Spring Harbor Symposia on Quantitative Biology*, 51(1), pp. 263-273. https://doi.org/10.1101/SQB.1986.051.01.032.

Nei, M. and Li, W-H. (1979). Mathematical model for studying genetic variation in terms of restriction endonucleases, *Proceedings of the National Academy of Sciences of the United States of America*, 76(10), pp. 5269-5273. https://doi.org/10.1073/pnas.76.10.5269.

Nei, M., Maruyama, T. and Wu, C-I. (1983). Models of evolution of reproductive isolation, *Genetics*, 103(3), pp. 557-579. https://doi.org/10.1093/genetics/103.3.557.

Nei, M. and Miller, J. C. (1990). A simple method for estimating average number of nucleotide substitutions within and between populations from restriction data, *Genetics*, 125(4), pp. 873-879. https://doi.org/10.1093/genetics/125.4.873.

Nosil, P., Feder, J. L., Flaxman, S. M. and Gompert, Z. (2017). Tipping points in the dynamics of speciation, *Nature Ecology & Evolution*, 1(2), article number: 0001. https://doi.org/10.1038/s41559-016-0001.

Patterson, N., Price, A. L. and Reich, D. (2006). Population structure and eigenanalysis, *PLoS Genetics*, 2(12), pp. 2074-2093. https://doi.org/10.1371/journal.pgen.0020190.

Pearson, K. F.R.S. (1901). LIII. On lines and planes of closest fit to systems of points in space, *The London, Edinburgh, and Dublin Philosophical Magazine and Journal of Science*, 2(11), pp. 559-572. https://doi.org/10.1080/14786440109462720.

Pebesma, E. J. and Bivand, R. S. (2005). Classes and methods for spatial data in R, *R News*, 5(2), pp. 9-13. https://CRAN.R-project.org/doc/Rnews/.

Peris, D., Lu, D. S., Kinneberg, V. B., Methlie, I-S., Dahl, M. S., James, T., Kauserud, H. and Skrede, I. (in prep.). Long-term balancing selection in two highly dynamic mating loci generates trans-species polymorphisms in fungi.

Petr, M. (2020). *admixr: An Interface for Running 'ADMIXTOOLS' Analyses. R package version 0.9.1.* https://CRAN.R-project.org/package=admixr.

Platt R. N., II, McDew-White, M., Clec'h, W. L., Chevalier, F. D., Allan, F., Emery, A. M., Garba, A., Hamidou, A. A., Ame, S. M., Webster, J. P., Rollinson, D., Webster, B. L. and Anderson, T. J. C. (2019). Ancient hybridization and adaptive introgression of an invadolysin gene in schistosome parasites, *Molecular Biology and Evolution*, 36(10), pp. 2127–2142. https://doi.org/10.1093/molbev/msz154.

Price, A. L., Patterson, N. J., Plenge, R. M., Weinblatt, M. E., Shadick, N. A. and Reich, D. (2006). Principal components analysis corrects for stratification in genome-wide association studies, *Nature Genetics*, 38(8), pp. 904-909. https://doi.org/10.1038/ng1847.

Ram, K. and Wickham, H. (2018*). wesanderson: A Wes Anderson Palette Generator. R package version 0.3.6.* https://CRAN.R-project.org/package=wesanderson.

Ravinet, M., Yoshida, K., Shigenobu, S., Toyoda, A., Fujiyama, A. and Kitano, J. (2018). The genomic landscape at a late stage of stickleback speciation: High genomic divergence interspersed by small localized regions of introgression, *PLoS Genetics*, 14(5), Article number: e1007358. https://doi.org/10.1371/journal.pgen.1007358.

Dos Reis, M., Donoghue, P. and Yang, Z. Bayesian molecular clock dating of species divergences in the genomics era, *Nature Reviews Genetics*, 17(2), pp. 71–80. https://doi.org/10.1038/nrg.2015.8.

Rudis, B. (2020). *hrbrthemes: Additional Themes, Theme Components and Utilities for 'ggplot2'. R package version 0.8.0*. https://CRAN.R-project.org/package=hrbrthemes.

Rutherford, S., Rossetto, M., Bragg, J. G., McPherson, H., Benson, D., Bonser, S. P. and Wilson, P. G. (2018). Speciation in the presence of gene flow: population genomics of closely related and diverging *Eucalyptus* species, *Heredity*, 121(2), pp. 126–141. https://doi.org/10.1038/s41437-018-0073-2.

Sanger, F., Nicklen, S. and Coulson, A. R. (1977). DNA sequencing with chain-terminating inhibitors, *Proceedings of the National Academy of Sciences of the United States of America*, 74(12), pp. 5463-5467. https://doi.org/10.1073/pnas.74.12.5463.

Seierstad, K. S., Fossdal, R., Miettinen, O., Carlsen, T., Skrede, I. and Kauserud, H. (2020). Contrasting genetic structuring in the closely related basidiomycetes *Trichaptum abietinum* and *Trichaptum fuscoviolaceum* (Hymenochaetales), *Fungal Biology*, 124(4), pp. 269-275. https://doi.org/10.1016/j.funbio.2020.11.001.

Sillo, F., Garbelotto, M., Giordano, L. and Gonthier, P. (2021). Genic introgression from an invasive exotic fungal forest pathogen increases the establishment potential of a sibling native pathogen, *NeoBiota*, 65(1), pp. 109-136. https://doi.org/10.3897/neobiota.65.64031.

Skrede, I. (2021). Chapter one - Diversity and distribution of ligninolytic fungi, in Morel-Rouhier M. and Sormani, R. (ed.) *Advances in Botanical Research*, *Wood Degradation and Ligninolytic Fungi*. Cambridge: Academic Press, pp. 1-36. https://doi.org/10.1016/bs.abr.2021.05.004.

Smit, A. F. A., Hubley, R. and Green, P. (2013-2015). *RepeatMasker Open-4.0*. http://www.repeatmasker.org.

Smith, J. M. (1966). Sympatric speciation, *The American Naturalist*, 100(916), pp. 637-650. https://doi.org/10.1086/282457.

Solovyev, V., Kosarev, P., Seledsov, I. and Vorobyev, D. (2006). Automatic annotation of eukaryotic genes, pseudogenes and promoters, *Genome Biology*, 7(S1), Article number: S10. https://doi.org/10.1186/gb-2006-7-s1-s10.

South, A. (2017). *rnaturalearth: World Map Data from Natural Earth. R package version 0.1.0.* https://CRAN.R-project.org/package=rnaturalearth.

Stamatakis, A. (2014). RAxML version 8: a tool for phylogenetic analysis and post-analysis of large phylogenies, *Bioinformatics*, 30(9), pp. 1312–1313. https://doi.org/10.1093/bioinformatics/btu033.

Stenlid, J. and Karlsson, J-O. (1991). Partial intersterility in *Heterobasidion annosum*, *Mycological research*, 95(10), pp. 1153-1159. https://doi.org/10.1016/S0953-7562(09)80004-X.

Stukenbrock, E. H. (2016). The role of hybridization in the evolution and emergence of new fungal plant pathogens, *Phytopathology*, 106(2), pp. 104-112. https://doi.org/10.1094/PHYTO-08-15-0184-RVW.

Stukenbrock, E. H., Christiansen, F. B., Hansen, T. T., Dutheil, J. Y. and Schierup, M. H. (2012). Fusion of two divergent fungal individuals led to the recent emergence of a unique widespread pathogen species, *Proceedings of the National Academy of Sciences of the United States of America*, 109(27), pp. 10954-10959. https://doi.org/10.1073/pnas.1201403109.

Turner, S. (2017). *qqman: Q-Q and Manhattan Plots for GWAS Data. R package version 0.1.4*. https://CRAN.R-project.org/package=qqman.

The UniProt Consortium. (2021). UniProt: the universal protein knowledgebase in 2021, *Nucleic Acids Research*, 49(D1), pp. D480–D489. https://doi.org/10.1093/nar/gkaa1100.

Van Rossum, G. and Drake, F. L. (2009). *Python 3 Reference Manual*. Scotts Valley, CA: CreateSpace.

Varga, T., Krizsán, K., Földi, C., Dima, B., Sánchez-García, M., Sánchez-Ramírez, S., Szöllősi, G. J., Szarkándi, J. G., Papp, V., Albert, L., Andreopoulos, W., Angelini, C., Antonín, V., Barry, K. W., Bougher, N. L., Buchanan, P., Buyck, B., Bense, V., Catcheside, P., Chovatia, M., Cooper, J., Dämon, W., Desjardin, D., Finy, P., Geml, J., Haridas, S., Hughes, K., Justo, A., Karasiński, D., Kautmanova, I., Kiss, B., Kocsubé, S., Kotiranta, H., LaButti, K. M., Lechner, B. E., Liimatainen, K., Lipzen, A., Lukács, Z., Mihaltcheva, S., Morgado, L., Niskanen, T., Noordeloos, M. E., Ohm, R. A., Ortiz-Santana, B., Ovrebo, C., Rácz, N., Riley, R., Savchenko, A., Shiryaev, A., Soop, K., Spirin, V., Szebenyi, C., Tomšovský, M., Tulloss, R. E., Uehling, J., Grigoriev, I. V., Vágvölgyi, C., Papp, T., Martin, F. M., Miettinen, O., Hibbett, D. S. and Nagy, L. G. (2019). Megaphylogeny resolves global patterns of mushroom evolution, *Nature Ecology & Evolution*, 3(4), pp. 668-678. https://doi.org/10.1038/s41559-019-0834-1.

Watterson, G. A. (1985). The genetic divergence of two populations, *Theoretical Population Biology*, 27(3), pp. 298-317. https://doi.org/10.1016/0040-5809(85)90003-6.

White, T. J., Bruns, T., Lee, S. and Taylor, J. W. (1990). Amplification and direct sequencing of fungal ribosomal RNA genes for phylogenetics, in Innis, M. A., Gelfand, D. H., Sninsky, J. J. and White, T. J. (ed.) *PCR Protocols: A Guide to Methods and Applications*. Academic Press, Inc., New York, pp. 315-322. https://doi.org/10.1016/b978-0-12-372180-8.50042-1.

Wickham, H. (2016). *ggplot2: Elegant Graphics for Data Analysis*. 2nd ed. New York: Springer.

Wickham, H., Averick, M., Bryan, J., Chang, W., McGowan, L. D., François, R., Grolemund, G., Hayes, A., Henry, L., Hester, J., Kuhn, M., Pedersen, T. L., Miller, E., Bache, S. M., Müller, K., Ooms, J., Robinson, D., Seidel, D. P., Spinu, V., Takahashi, K., Vaughan, D., Wilke, C., Woo, K. and Yutani, H. (2019). Welcome to the tidyverse, *Journal of Open Source Software*, 4(43), pp. 1686. https://doi.org/10.21105/joss.01686.

Wood, T. E., Takebayashi, N., Barker, M. S., Mayrose, I., Greenspoon, P. B. and Rieseberg, L. H. (2009). The frequency of polyploid speciation in vascular plants, *Proceedings of the National Academy of Sciences of the United States of America*, 106(33), pp. 13875–13879. https://doi.org/10.1073/pnas.0811575106.

Zachos, F.E. (2016) A Brief History of Species Concepts and the Species Problem, in *Species Concepts in Biology*. Cham: Springer, pp. 17-44. https://doi.org/10.1007/978-3-319-44966-1_2.

Zaret, T. M. and Rand, S. (1971). Competition in tropical stream fishes: Support for the competitive exclusion principle, *Ecology*, 52(2), pp. 336-342. https://doi.org/10.2307/1934593.

Zhang, W., Dasmahapatra, K. K., Mallet, J., Moreira, G. R. P. and Kronforst, M. R. (2016). Genome wide introgression among distantly related *Heliconius* butterfly species, *Genome Biology*, 17(1), Article number: 25. https://doi.org/10.1186/s13059-016-0889-0.

Supplementary information

Table S1, ***Overview of individuals collected and used for bioinformatic analyses.*** *The table includes information on name (collection ID), species designation (based on morphology, ITS sequence and Illumina sequence), collection site (area, longitude, latitude, and elevation), host substrate (substrate), name of collector and date of collection.* Trichaptum fuscoviolaceum *(TF) collections are in purple,* T. abietinum *(TA) in green, and the outgroup* T. biforme *(TB) in blue.*

Collection ID	Species morphology	Species ITS	Species Illumina	Area	Latitude	Longitude	Elevation	Substrate	Collector	Collection date
TF-1000-1-M1	*T. fuscoviolaceum*	*T. fuscoviolaceum*	*T. fuscoviolaceum*	CA, N.B., Charlotte County	45.13741 N	66.46785 W	120 m	*Abies balsamea*	David Malloch	09.10.2018
TF-1002-2-M1	*T. fuscoviolaceum*	*T. abietinum*	*T. abietinum*	CA, N.B., Charlotte County	45.129722 N	66.523889 W	50 m	*Abies balsamea*	Inger Skrede & Dabao Lu	09.10.2018
TF-1002-3-M1	*T. fuscoviolaceum*	*T. fuscoviolaceum*	*T. fuscoviolaceum*	CA, N.B., Charlotte County	45.126944 N	66.526944 W	50 m	*Abies balsamea*	Inger Skrede & Dabao Lu	09.10.2018
TF-1002-4-M3	*T. fuscoviolaceum*	*T. fuscoviolaceum*	*T. fuscoviolaceum*	CA, N.B., Charlotte County	45.128611 N	66.525000 W	50 m	*Abies balsamea*	Inger Skrede & Dabao Lu	09.10.2018
TF-1002-5-M3	*T. fuscoviolaceum*	*T. fuscoviolaceum*	*T. fuscoviolaceum*	CA, N.B., Charlotte County	45.126944 N	66.527222 W	50 m	*Abies balsamea*	Inger Skrede & Dabao Lu	09.10.2018
TF-1002-7-M2	*T. fuscoviolaceum*	*T. fuscoviolaceum*	*T. fuscoviolaceum*	CA, N.B., Charlotte County	45.130833 N	66.525000 W	50 m	*Abies balsamea*	Inger Skrede & Dabao Lu	09.10.2018
TF-1002-10-M3	*T. fuscoviolaceum*	*T. fuscoviolaceum*	*T. fuscoviolaceum*	CA, N.B., Charlotte County	45.12927 N	66.52469 W	50 m	*Abies balsamea*	Amanda Bremner	09.10.2018
TF-1003-2-M1	*T. fuscoviolaceum*	*T. fuscoviolaceum*	*T. fuscoviolaceum*	CA, N.B., Charlotte County	45.169444 N	66.459167 W	10 m	*Picea rubens*	Inger Skrede & Dabao Lu	09.10.2018
TF-1003-3-M2	*T. fuscoviolaceum*	*T. fuscoviolaceum*	*T. fuscoviolaceum*	CA, N.B., Charlotte County	45.169167 N	66.458889 W	10 m	*Picea rubens*	Inger Skrede & Dabao Lu	09.10.2018
TF-1003-4-M2	*T. fuscoviolaceum*	*T. fuscoviolaceum*	*T. fuscoviolaceum*	CA, N.B., Charlotte County	45.173611 N	66.465556 W	10 m	*Abies balsamea*	Inger Skrede & Dabao Lu	09.10.2018
TF-1003-5-M2	*T. fuscoviolaceum*	*T. fuscoviolaceum*	*T. fuscoviolaceum*	CA, N.B., Charlotte County	45.168611 N	66.461389 W	10 m	*Picea rubens*	Inger Skrede & Dabao Lu	09.10.2018
TF-1004-1-M1	*T. fuscoviolaceum*	*T. fuscoviolaceum*	*T. fuscoviolaceum*	CA, N.B., Sunbury County	45.993333 N	66.307500 W	80 m	*Abies balsamea*	Inger Skrede & Dabao Lu	10.10.2018
TF-1004-3-M1	*T. fuscoviolaceum*	*T. fuscoviolaceum*	*T. fuscoviolaceum*	CA, N.B., Sunbury County	45.992222 N	66.307222 W	80 m	*Abies balsamea*	Inger Skrede & Dabao Lu	10.10.2018

TF-1004-4-M2	*T. fuscoviolaceum*	*T. fuscoviolaceum*	*T. fuscoviolaceum*	CA, N.B., Sunbury County	45.992222 N	66.307222 W	80 m	*Abies balsamea*	Inger Skrede & Dabao Lu	10.10.2018
TF-1004-6-M2	*T. fuscoviolaceum*	*T. fuscoviolaceum*	*T. fuscoviolaceum*	CA, N.B., Sunbury County	46.00562 N	66.40087 W	130 m	*Abies balsamea*	Stephen R. Clayden	10.10.2018
TF-1004-6-dup-M2	*T. fuscoviolaceum*	*T. fuscoviolaceum*	*T. fuscoviolaceum*	CA, N.B., Sunbury County	45.991389 N	66.307500 W	80 m	*Abies balsamea*	Inger Skrede & Dabao Lu	10.10.2018
TF-1005-1-M1	*T. fuscoviolaceum*	*T. abietinum*	*T. abietinum*	CA, N.B., Sunbury County	46.035000 N	66.325000 W	130 m	*Picea mariana*	Inger Skrede & Dabao Lu	10.10.2018
TF-1007-1-M3	*T. fuscoviolaceum*	*T. fuscoviolaceum*	*T. fuscoviolaceum*	CA, N.B., Gloucester County	47.636944 N	65.610833 W	20 m	*Abies balsamea*	Inger Skrede & Dabao Lu	11.10.2018
TF-1007-2-M2	*T. fuscoviolaceum*	*T. fuscoviolaceum*	*T. fuscoviolaceum*	CA, N.B., Gloucester County	47.636944 N	65.610833 W	20 m	*Abies balsamea*	Inger Skrede & Dabao Lu	11.10.2018
TF-1009-1-M1	*T. fuscoviolaceum*	*T. fuscoviolaceum*	*T. fuscoviolaceum*	CA, N.B., Restigouche County	47.41611 N	66.868056 W	380 m	*Abies balsamea*	Inger Skrede & Dabao Lu	12.10.2018
TF-1009-2-M2	*T. fuscoviolaceum*	*T. fuscoviolaceum*	*T. fuscoviolaceum*	CA, N.B., Restigouche County	47.416111 N	66.866944 W	360 m	*Abies balsamea*	Inger Skrede & Dabao Lu	12.10.2018
TF-1009-3-M3	*T. fuscoviolaceum*	*T. fuscoviolaceum*	*T. abietinum*	CA, N.B., Restigouche County	47.418333	66.868889 W	240 m	*Abies balsamea*	Inger Skrede & Dabao Lu	12.10.2018
TF-1009-4-M2	*T. fuscoviolaceum*	*T. fuscoviolaceum*	*T. fuscoviolaceum*	CA, N.B., Restigouche County	47.418056 N	66.867778 W	290 m	*Abies balsamea*	Inger Skrede & Dabao Lu	12.10.2018
TF-1011-1-M1	*T. fuscoviolaceum*	*T. fuscoviolaceum*	*T. fuscoviolaceum*	CA, N.B., Victoria County	46.894167 N	67.398333 W	170 m	*Abies balsamea*	Inger Skrede & Dabao Lu	13.10.2018
TF-1011-3-M1	*T. fuscoviolaceum*	*T. fuscoviolaceum*	*T. fuscoviolaceum*	CA, N.B., Victoria County	46.893333 N	67.398333 W	170 m	*Abies balsamea*	Inger Skrede & Dabao Lu	13.10.2018
TF-1011-4-M1	*T. fuscoviolaceum*	*T. fuscoviolaceum*	*T. fuscoviolaceum*	CA, N.B., Victoria County	46.892778 N	67.398611 W	170 m	*Abies balsamea*	Inger Skrede & Dabao Lu	13.10.2018
TF-1011-7-M2	*T. fuscoviolaceum*	*T. fuscoviolaceum*	*T. fuscoviolaceum*	CA, N.B., Victoria County	46.892500 N	67.399167 W	170 m	*Picea sp.*	Inger Skrede & Dabao Lu	13.10.2018
TF-1011-8-M1	*T. fuscoviolaceum*	*T. fuscoviolaceum*	*T. fuscoviolaceum*	CA, N.B., Victoria County	46.902222 N	67.400556 W	170 m	*Abies balsamea*	Inger Skrede & Dabao Lu	13.10.2018

TF-1012-1-M2	*T. fuscoviolaceum*	*T. fuscoviolaceum*	*T. fuscoviolaceum*	CA, N.B., Northumberland County	46.783333 N	66.516667 W	390 m	*Abies balsamea*	Inger Skrede & Dabao Lu	13.10.2018
TF-1012-2-M1	*T. fuscoviolaceum*	*T. fuscoviolaceum*	*T. fuscoviolaceum*	CA, N.B., Northumberland County	46.783889 N	66.525556 W	390 m	*Abies balsamea*	Inger Skrede & Dabao Lu	13.10.2018
TF-1012-3-M3	*T. fuscoviolaceum*	*T. fuscoviolaceum*	*T. fuscoviolaceum*	CA, N.B., Northumberland County	46.784444 N	66.526111 W	400 m	*Abies balsamea*	Inger Skrede & Dabao Lu	13.10.2018
TF-1012-5-M2	*T. fuscoviolaceum*	*T. fuscoviolaceum*	*T. fuscoviolaceum*	CA, N.B., Northumberland County	46.785556 N	60.525278 W	380 m	*Abies balsamea*	Inger Skrede & Dabao Lu	13.10.2018
TF-1013-1-M2	*T. fuscoviolaceum*	*T. fuscoviolaceum*	*T. fuscoviolaceum*	CA, N.B., York County	45.9564 N	66.6668 W	50 m	*Abies balsamea*	Stephen R. Clayden	12.10.2018
TF-1013-2-M2	*T. fuscoviolaceum*	*T. fuscoviolaceum*	*T. fuscoviolaceum*	CA, N.B., York County	45.9564 N	66.6668 W	50 m	*Abies balsamea*	Stephen R. Clayden	12.10.2018
TF-1013-4-M2	*T. fuscoviolaceum*	*T. fuscoviolaceum*	*T. abietinum*	CA, N.B., York County	45.9564 N	66.6668 W	50 m	*Abies balsamea*	Stephen R. Clayden	12.10.2018
TF-1013-5-M2	*T. fuscoviolaceum*	*T. fuscoviolaceum*	*T. fuscoviolaceum*	CA, N.B., York County	45.9564 N	66.6668 W	50 m	*Abies balsamea*	Stephen R. Clayden	12.10.2018
TF-1013-8-M2	*T. fuscoviolaceum*	*T. fuscoviolaceum*	*T. fuscoviolaceum*	CA, N.B., York County	45.9564 N	66.6668 W	50 m	*Abies balsamea*	Stephen R. Clayden	12.10.2018
TF-1014-1-M2	*T. fuscoviolaceum*	*T. fuscoviolaceum*	*T. fuscoviolaceum*	ITL, Pavia, Menconico	44.80662 N	9.31246 E	–	*Pinus nigra*	Carolina Girometta	06.10.2018
TF-1014-2-M1	*T. fuscoviolaceum*	*T. fuscoviolaceum*	*T. fuscoviolaceum*	ITL, Pavia, Menconico	44.80744 N	9.31063 E	–	*Pinus nigra*	Carolina Girometta	06.10.2018
TF-1014-3-M1	*T. fuscoviolaceum*	*T. fuscoviolaceum*	*T. fuscoviolaceum*	ITL, Pavia, Menconico	44.80754 N	9.31042 E	–	*Pinus nigra*	Carolina Girometta	06.10.2018
TF-1014-6-M3	*T. fuscoviolaceum*	*T. fuscoviolaceum*	*T. fuscoviolaceum*	ITL, Pavia, Menconico	44.81126 N	9.30588 E	–	*Pinus nigra*	Carolina Girometta	06.10.2018
TF-1014-7-M1	*T. fuscoviolaceum*	*T. fuscoviolaceum*	*T. fuscoviolaceum*	ITL, Pavia, Menconico	44.81134 N	9.30589 E	–	*Pinus nigra*	Carolina Girometta	06.10.2018
TF-1014-7-M9	*T. fuscoviolaceum*	*T. fuscoviolaceum*	*T. fuscoviolaceum*	ITL, Pavia, Menconico	44.81134 N	9.30589 E	–	*Pinus nigra*	Carolina Girometta	06.10.2018
TF-1014-8-M2	*T. fuscoviolaceum*	*T. fuscoviolaceum*	*T. fuscoviolaceum*	ITL, Pavia, Menconico	44.81137 N	9.30661 E	–	*Pinus nigra*	Carolina Girometta	06.10.2018

TF-1014-9-M3	*T. fuscoviolaceum*	*T. fuscoviolaceum*	*T. fuscoviolaceum*	ITL, Pavia, Menconico	44.80795 N	9.30954 E	–	*Pinus nigra*	Carolina Girometta	06.10.2018
TF-1014-10-M1	*T. fuscoviolaceum*	*T. fuscoviolaceum*	*T. fuscoviolaceum*	ITL, Pavia, Menconico	44.80520 N	9.31298 E	–	*Pinus nigra*	Carolina Girometta	06.10.2018
TA-1002-8-M1	*T. abietinum*	*T. abietinum*	*T. abietinum*	CA, N.B., Charlotte County	45.129444 N	66.524167 W	50 m	*Abies balsamea*	Inger Skrede & Dabao Lu	09.10.2018
TA-1002-13-M2	*T. abietinum*	*T. abietinum*	*T. abietinum*	CA, N.B., Charlotte County	45.128611 N	66.524444 W	50 m	*Picea rubens*	Inger Skrede & Dabao Lu	09.10.2018
TA-1002-19-M1	*T. abietinum*	*T. abietinum*	*T. abietinum*	CA, N.B., Charlotte County	45.128611 N	66.524722 W	50 m	*Abies balsamea*	Inger Skrede & Dabao Lu	09.10.2018
TA-1002-27-M1	*T. abietinum*	*T. abietinum*	*T. abietinum*	CA, N.B., Charlotte County	45.128333 N	66.526111 W	50 m	*Picea rubens*	Inger Skrede & Dabao Lu	09.10.2018
TA-1002-35-M2	*T. abietinum*	*T. abietinum*	*T. abietinum*	CA, N.B., Charlotte County	45.128611 N	66.526389 W	50 m	*Picea rubens*	Inger Skrede & Dabao Lu	09.10.2018
TA-1003-1-M1	*T. abietinum*	*T. abietinum*	*T. abietinum*	CA, N.B., Sunbury County	45.991944 N	66.306944 W	60 m	*Abies balsamea*	Inger Skrede & Dabao Lu	10.10.2018
TA-1003-8-M1	*T. abietinum*	*T. abietinum*	*T. abietinum*	CA, N.B., Sunbury County	45.992778 N	66.306944 W	60 m	*Abies balsamea*	Inger Skrede & Dabao Lu	10.10.2018
TA-1003-17-M1	*T. abietinum*	*T. abietinum*	*T. abietinum*	CA, N.B., Sunbury County	45.990278 N	66.306667 W	60 m	*Abies balsamea*	Inger Skrede & Dabao Lu	10.10.2018
TA-1003-20-M2	*T. abietinum*	*T. abietinum*	*T. abietinum*	CA, N.B., Sunbury County	45.990278 N	66.307222 W	60 m	*Picea rubens*	Inger Skrede & Dabao Lu	10.10.2018
TA-1003-22-M2	*T. abietinum*	*T. abietinum*	*T. abietinum*	CA, N.B., Sunbury County	45.99056 N	66.30690 W	60 m	*Picea rubens*	Stepen R. Clayden	10.10.2018
TA-1007-1	*T. abietinum*	*T. abietinum*	*T. abietinum*	CA, N.B., Gloucester County	47.637500 N	65.610000 W	20 m	*Pinus cf. strobus*	Inger Skrede & Dabao Lu	11.10.2018
TA-1007-3	*T. abietinum*	*T. abietinum*	*T. abietinum*	CA, N.B., Gloucester County	47.631389 N	65.616111 W	20 m	*Picea cf. glauca*	Inger Skrede & Dabao Lu	11.10.2018
TA-1007-5	*T. abietinum*	*T. abietinum*	*T. abietinum*	CA, N.B., Gloucester County	47.637500 N	65.610556 W	30 m	*Picea cf. glauca*	Inger Skrede & Dabao Lu	11.10.2018
TA-1007-6	*T. abietinum*	*T. abietinum*	*T. abietinum*	CA, N.B., Gloucester County	47.649722 N	65.610833 W	30 m	*Picea cf. glauca*	Inger Skrede & Dabao Lu	11.10.2018

TA-1007-17	*T. abietinum*	*T. abietinum*	*T. abietinum*	CA, N.B., Gloucester County	47.603333 N	65.610833 W	30 m	*Abies balsamea*	Inger Skrede & Dabao Lu	11.10.2018
TA-1009-1-M3	*T. abietinum*	*T. abietinum*	*T. abietinum*	CA, N.B., Restigouche County	47.418056 N	66.866667 W	240 m	*Picea cf. glauca*	Inger Skrede & Dabao Lu	12.10.2018
TA-1009-4-M1	*T. abietinum*	*T. abietinum*	*T. abietinum*	CA, N.B., Restigouche County	47.417778 N	66.866944 W	330 m	*Picea cf. glauca*	Inger Skrede & Dabao Lu	12.10.2018
TA-1009-8-M3	*T. abietinum*	*T. abietinum*	*T. abietinum*	CA, N.B., Restigouche County	47.416944 N	66.867222 W	330 m	*Picea cf. glauca*	Inger Skrede & Dabao Lu	12.10.2018
TA-1009-12-M1	*T. abietinum*	*T. abietinum*	*T. abietinum*	CA, N.B., Restigouche County	47.417778 N	66.866111 W	340 m	*Picea sp.*	Inger Skrede & Dabao Lu	12.10.2018
TA-1009-19-M3	*T. abietinum*	*T. abietinum*	*T. abietinum*	CA, N.B., Restigouche County	47.418611 N	66.881389 W	220 m	*Picea sp*	Inger Skrede & Dabao Lu	12.10.2018
TA-1011-12-M2	*T. abietinum*	*T. abietinum*	*T. abietinum*	CA, N.B., Victoria County	46.894167 N	67.398333 W	170 m	*Picea cf. rubens*	Inger Skrede & Dabao Lu	13.10.2018
TA-1011-19-M1	*T. abietinum*	*T. abietinum*	*T. abietinum*	CA, N.B., Victoria County	46.892500 N	67.399444 W	170 m	*Picea cf. rubens*	Inger Skrede & Dabao Lu	13.10.2018
TA-1011-23-M1	*T. abietinum*	*T. abietinum*	*T. abietinum*	CA, N.B., Victoria County	46.900833 N	67.400278 W	170 m	*Picea sp.*	Inger Skrede & Dabao Lu	13.10.2018
TA-1011-26-M1	*T. abietinum*	*T. abietinum*	*T. abietinum*	CA, N.B., Victoria County	46.893611 N	67.400000 W	170 m	*Abies balsamea*	Inger Skrede & Dabao Lu	13.10.2018
TA-1011-31-M1	*T. abietinum*	*T. abietinum*	*T. abietinum*	CA, N.B., Victoria County	46.893333 N	67.401111 W	170 m	*Abies balsamea*	Inger Skrede & Dabao Lu	13.10.2018
TA-1012-3-M1	*T. abietinum*	*T. abietinum*	*T. abietinum*	CA, N.B., Northumberland County	46.783889 N	66.525556 W	390 m	*Picea rubens*	Inger Skrede & Dabao Lu	13.10.2018
TA-1012-5-M1	*T. abietinum*	*T. abietinum*	*T. abietinum*	CA, N.B., Northumberland County	46.784167 N	66.059444 W	390 m	*Abies balsamea*	Inger Skrede & Dabao Lu	13.10.2018
TA-1012-7-M1	*T. abietinum*	*T. abietinum*	*T. abietinum*	CA, N.B., Northumberland County	46.784167 N	66.059444 W	390 m	*Picea rubens*	Inger Skrede & Dabao Lu	13.10.2018

TA-1012-11-M1	*T. abietinum*	*T. abietinum*	*T. abietinum*	CA, N.B., Northumberland County	46.785556 N	66.525556 W	390 m	*Picea rubens*	Inger Skrede & Dabao Lu	13.10.2018
TA-1012-17-M1	*T. abietinum*	*T. abietinum*	*T. abietinum*	CA, N.B., Northumberland County	46.784722 N	66.524722 W	380 m	*Picea sp.*	Inger Skrede & Dabao Lu	13.10.2018
TA-1013-3-M2	*T. abietinum*	*T. abietinum*	*T. abietinum*	CA, N.B., York County	45.9564 N	66.6668 W	50 m	*Abies balsamea*	Stephen R. Clayden	12.10.2018
TA-1013-4-M1	*T. abietinum*	*T. abietinum*	*T. abietinum*	CA, N.B., York County	45.9564 N	66.6668 W	50 m	*Tsuga canadensis*	Stephen R. Clayden	12.10.2018
TA-1013-5-M1	*T. abietinum*	*T. abietinum*	*T. abietinum*	CA, N.B., York County	45.9564 N	66.6668 W	50 m	*Tsuga canadensis*	Stephen R. Clayden	12.10.2018
TA-1013-7-M1	*T. abietinum*	*T. abietinum*	*T. abietinum*	CA, N.B., York County	45.9564 N	66.6668 W	50 m	*Picea rubens*	Stephen R. Clayden	12.10.2018
TA-1013-9-M1	*T. abietinum*	*T. abietinum*	*T. abietinum*	CA, N.B., York County	45.9564 N	66.6668 W	50 m	*Picea rubens*	Stephen R. Clayden	12.10.2018
TB-1013-1-M2	*T. fuscoviolaceum*	*T. biforme*	*T. biforme*	CA, N. B., York County	45.9564 N	66.6668 W	50 m	*Abies balsamea*	Stephen R. Clayden	12.10.2018

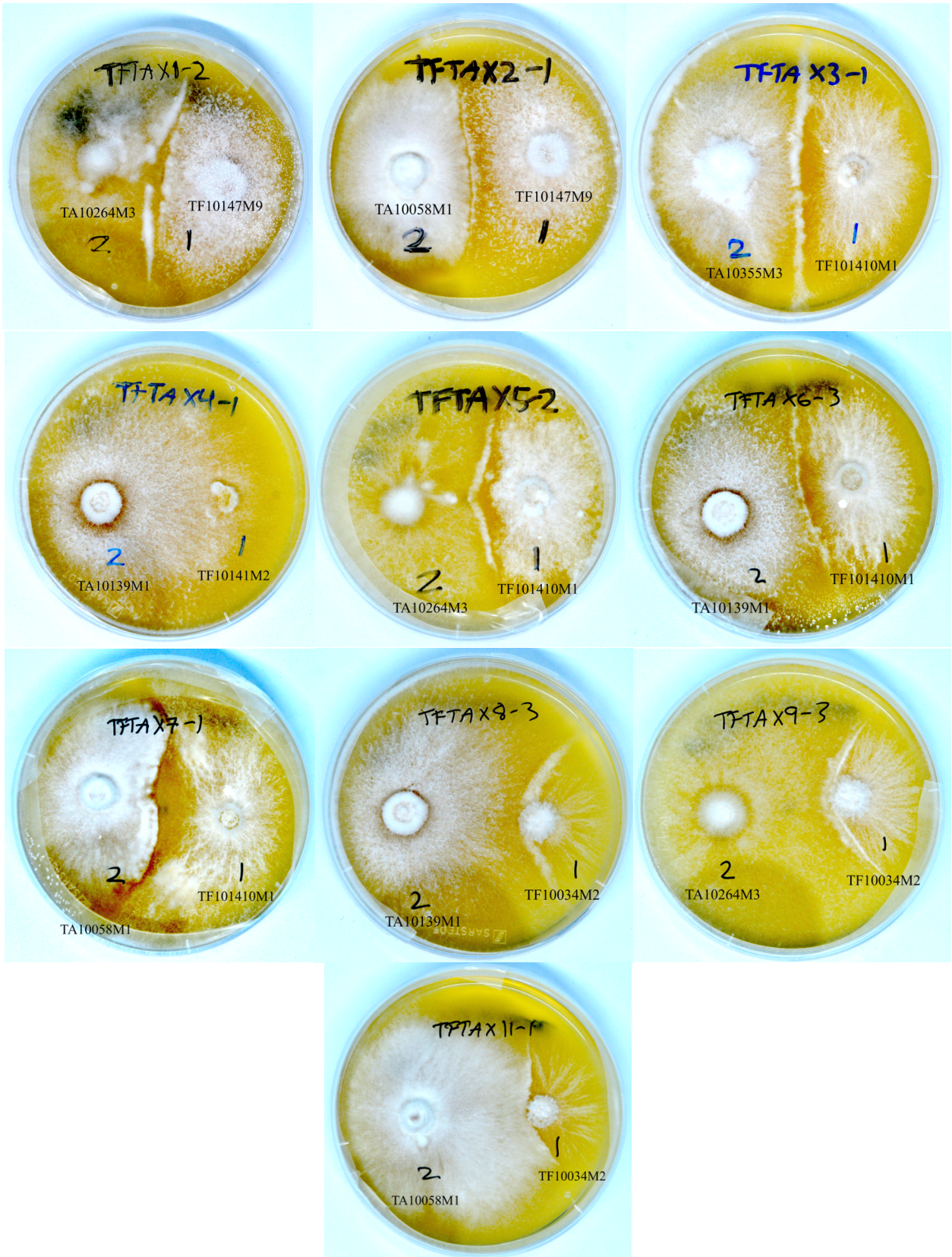

Figure S1, ***No successful crossings between*** **Trichaptum abietinum** ***and*** **T. fuscoviolaceum.** *Photographs of cultures from the crossing experiments (one of the three replicates for each cross). None of the crossings are successful. The cross name is indicated at the top (number after the dashed line indicates replicate number), and the individuals are noted on the bottom. TA* = T. abietinum *and TF* = T. fuscoviolaceum. *Photographs were taken with a Nikon D600 Digital Camera (Tokyo, Japan).*

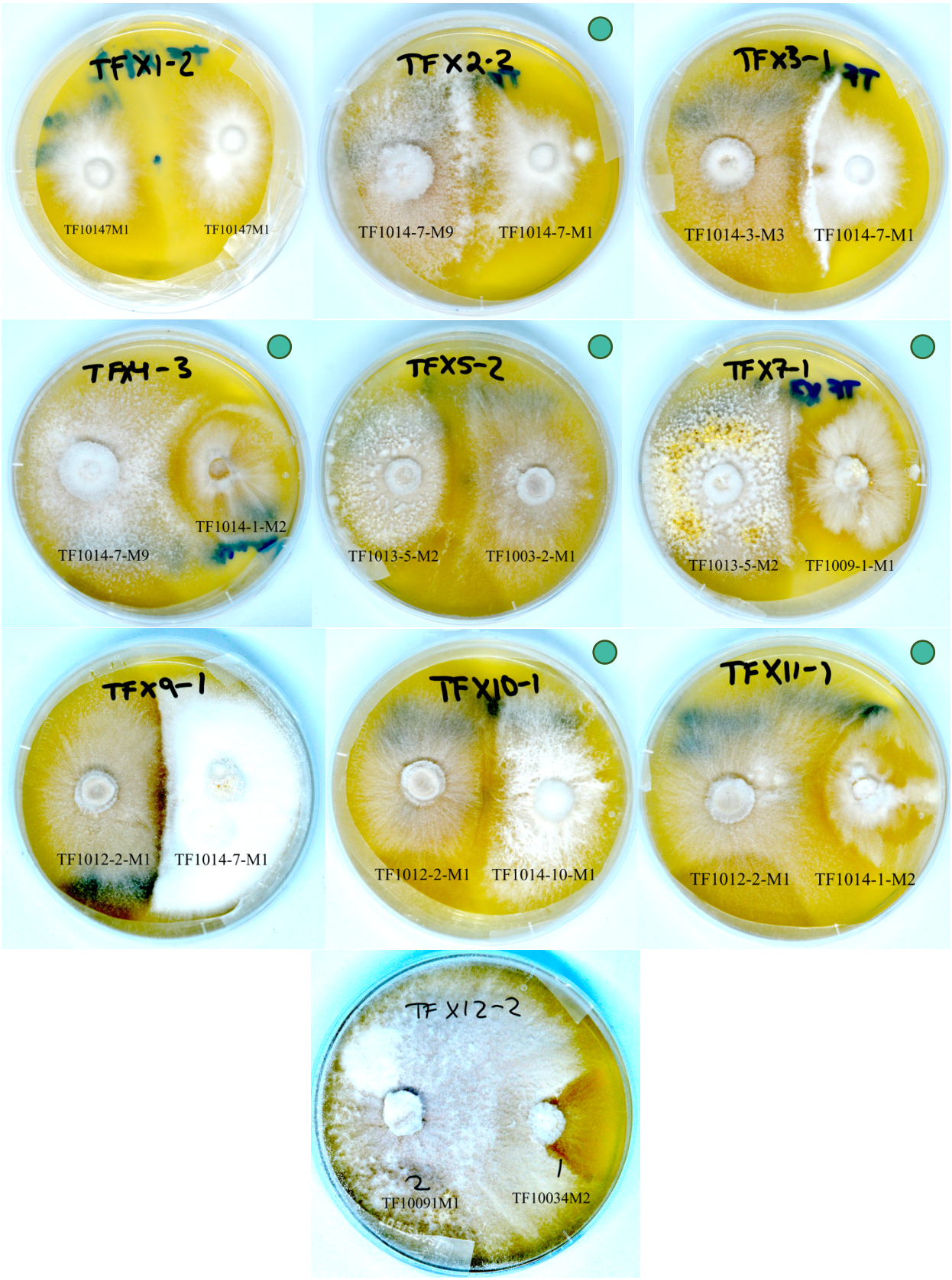

Figure S2, ***Crossings were as predicted between populations of*** **Trichaptum fuscoviolaceum.** *Photographs of cultures from the crossing experiments (one of the three replicates for each cross). Successful matings are marked with a green dot in the top right corner. The cross name is indicated at the top (number after the dashed line indicates replicate number), and the individuals are noted on the bottom. TF =* T. fuscoviolaceum. *Photographs were taken with a Nikon D600 Digital Camera (Tokyo, Japan).*

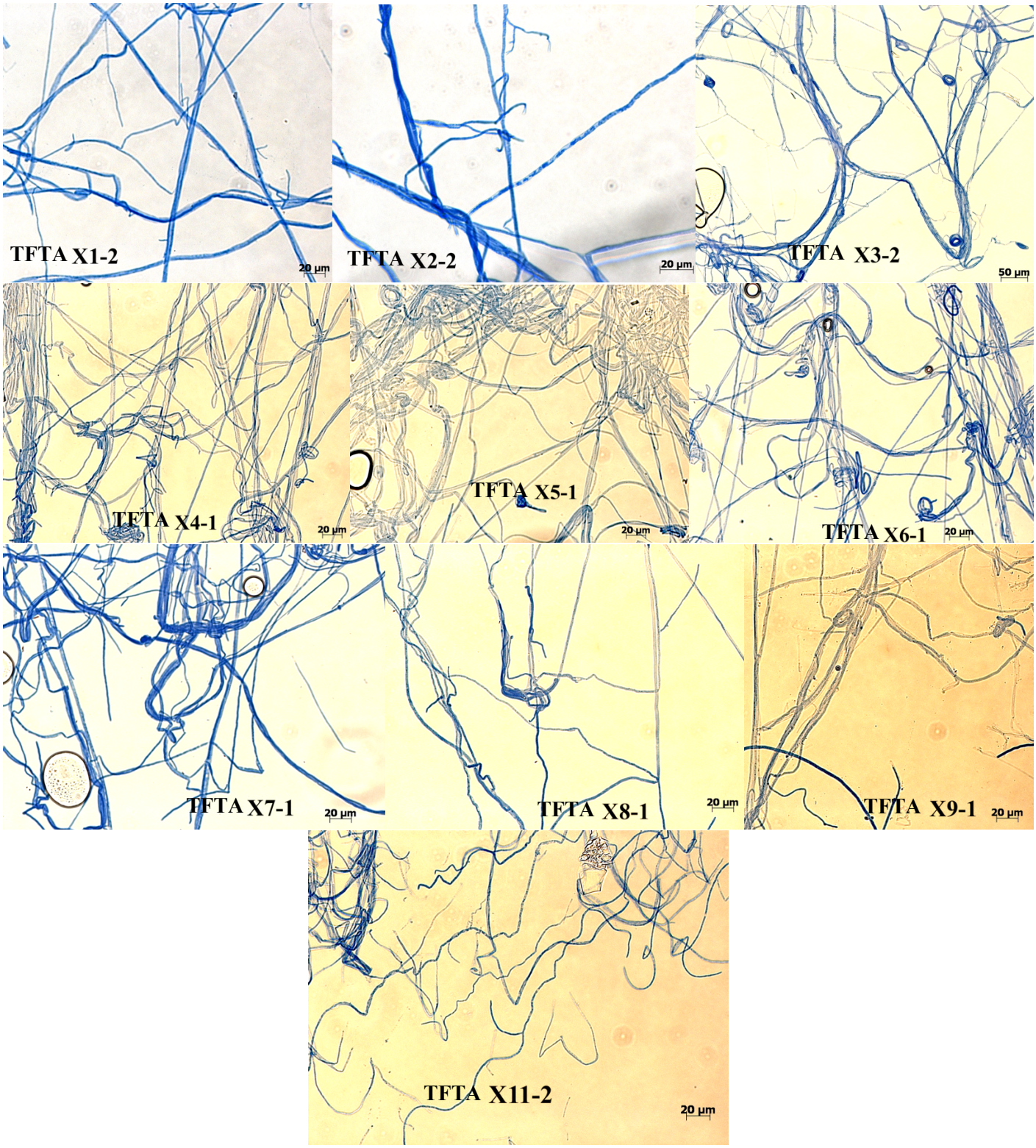

Figure S3, ***No clamp connections in the crossings between*** **Trichaptum abietinum** ***and*** **T. fuscoviolaceum.** *Microscope photographs of the crossing experiments. Cross names are indicated at the bottom of the pictures and the number after the dashed lines indicate replicate number. A scale bar is positioned at the bottom right of every picture. Photographs were taken using Zeiss Axioplan 2 imaging light microscope (Güttingen, Germany) with Zeiss AxioCam HRc (Güttingen, Germany).*

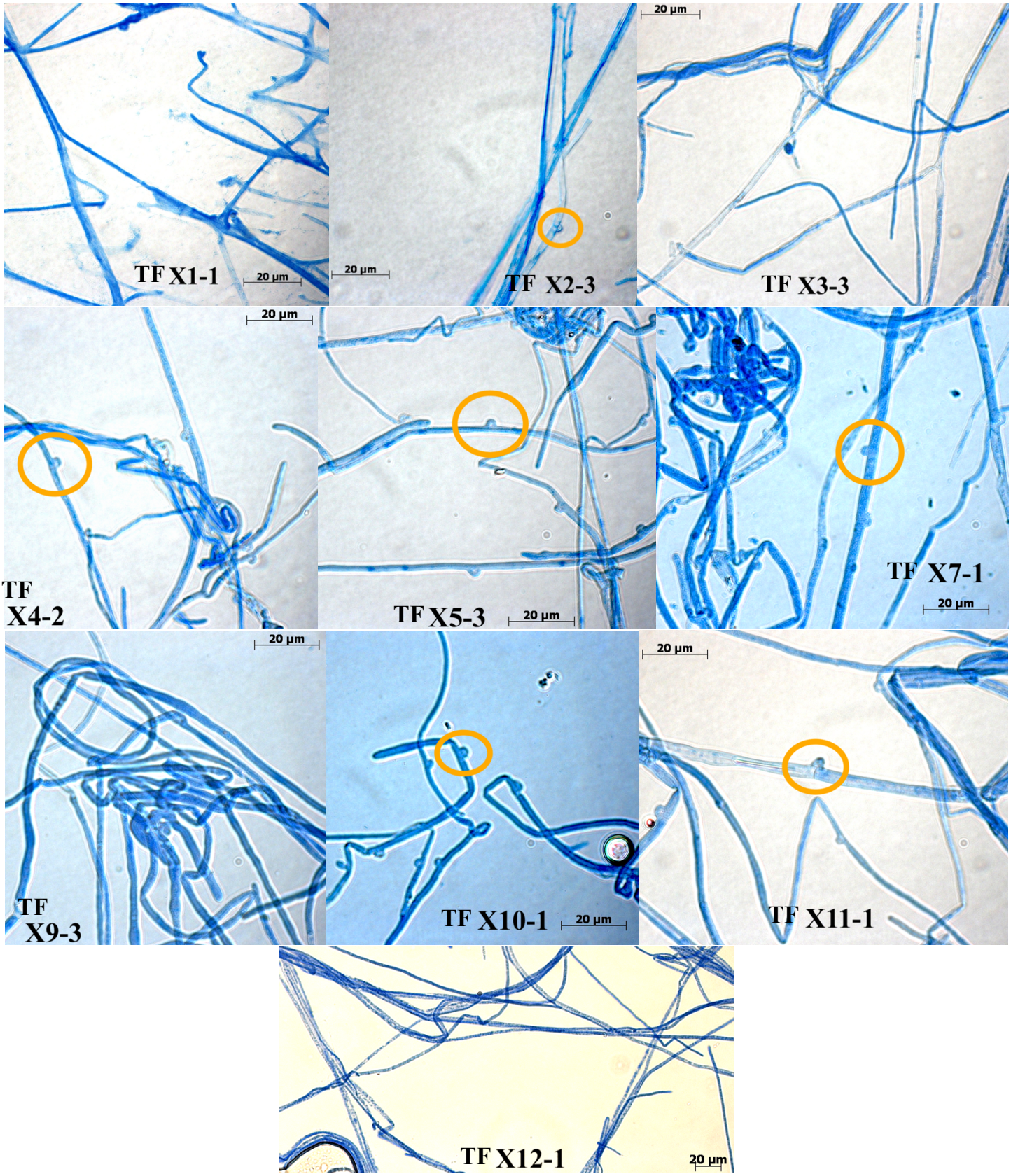

Figure S4, ***Clamp connections were observed as predicted in the crossings between populations of*** **Trichaptum fuscoviolaceum.** *Microscope photographs of the crossing experiments. Cross names are indicated at the bottom of the pictures and the number after the dashed lines indicate replicate number. A scale bar is included in every picture. Orange circles denote clamp connections. Photographs were taken using Zeiss Axioplan 2 imaging light microscope (Güttingen, Germany) with Zeiss AxioCam HRc (Güttingen, Germany).*

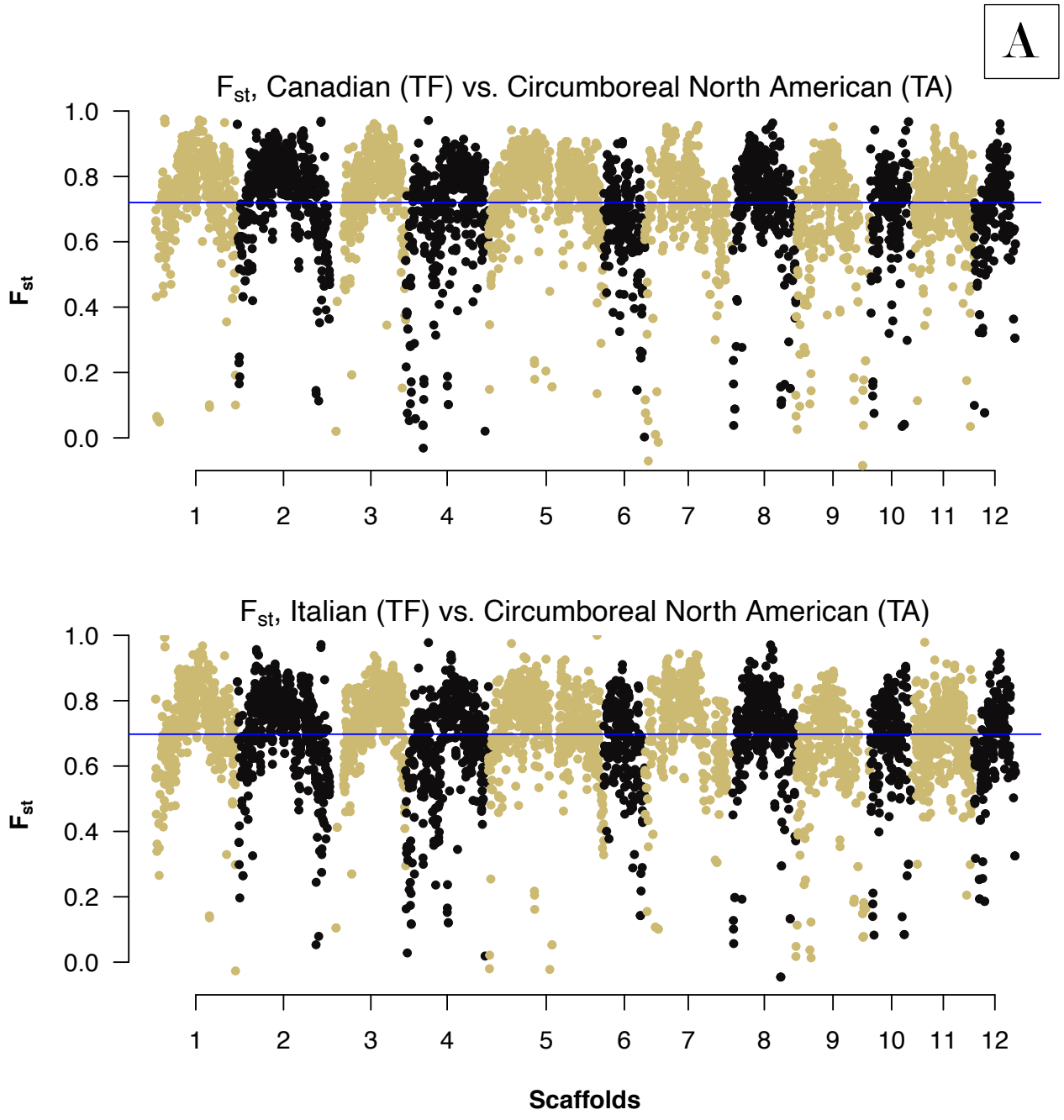
A
F_{st}, Canadian (TF) vs. Circumboreal North American (TA)
F_{st}
1.0
0.8
0.6
0.4
0.2
0.0
1
2
3
4
5
6
7
8
9
10
11
12
F_{st}, Italian (TF) vs. Circumboreal North American (TA)
F_{st}
1.0
0.8
0.6
0.4
0.2
0.0
1
2
3
4
5
6
7
8
9
10
11
12
Scaffolds

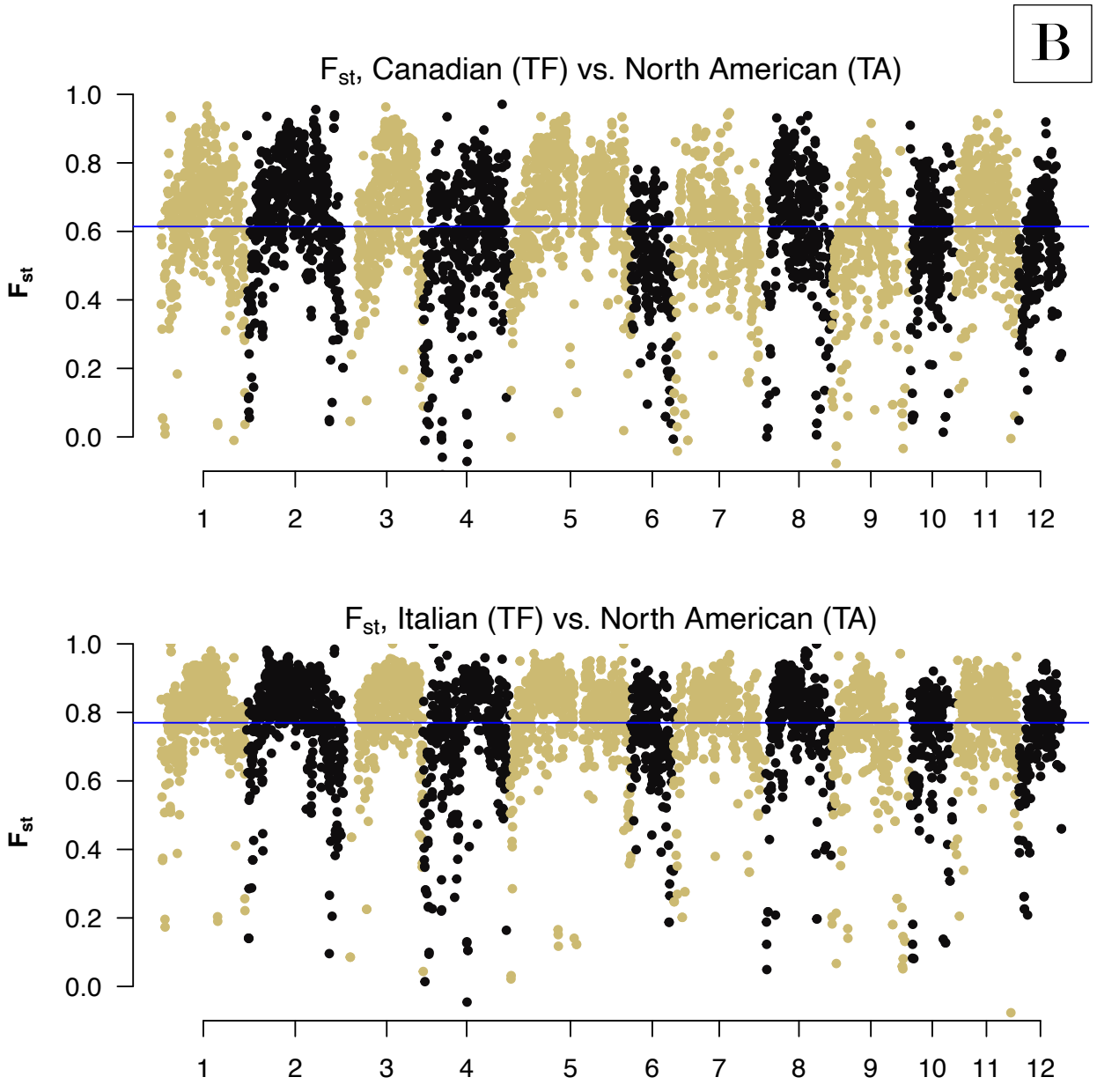
B
F_{st}, Canadian (TF) vs. North American (TA)
F_{st}
1.0
0.8
0.6
0.4
0.2
0.0
1
2
3
4
5
6
7
8
9
10
11
12
F_{st}, Italian (TF) vs. North American (TA)
F_{st}
1.0
0.8
0.6
0.4
0.2
0.0
1
2
3
4
5
6
7
8
9
10
11
12

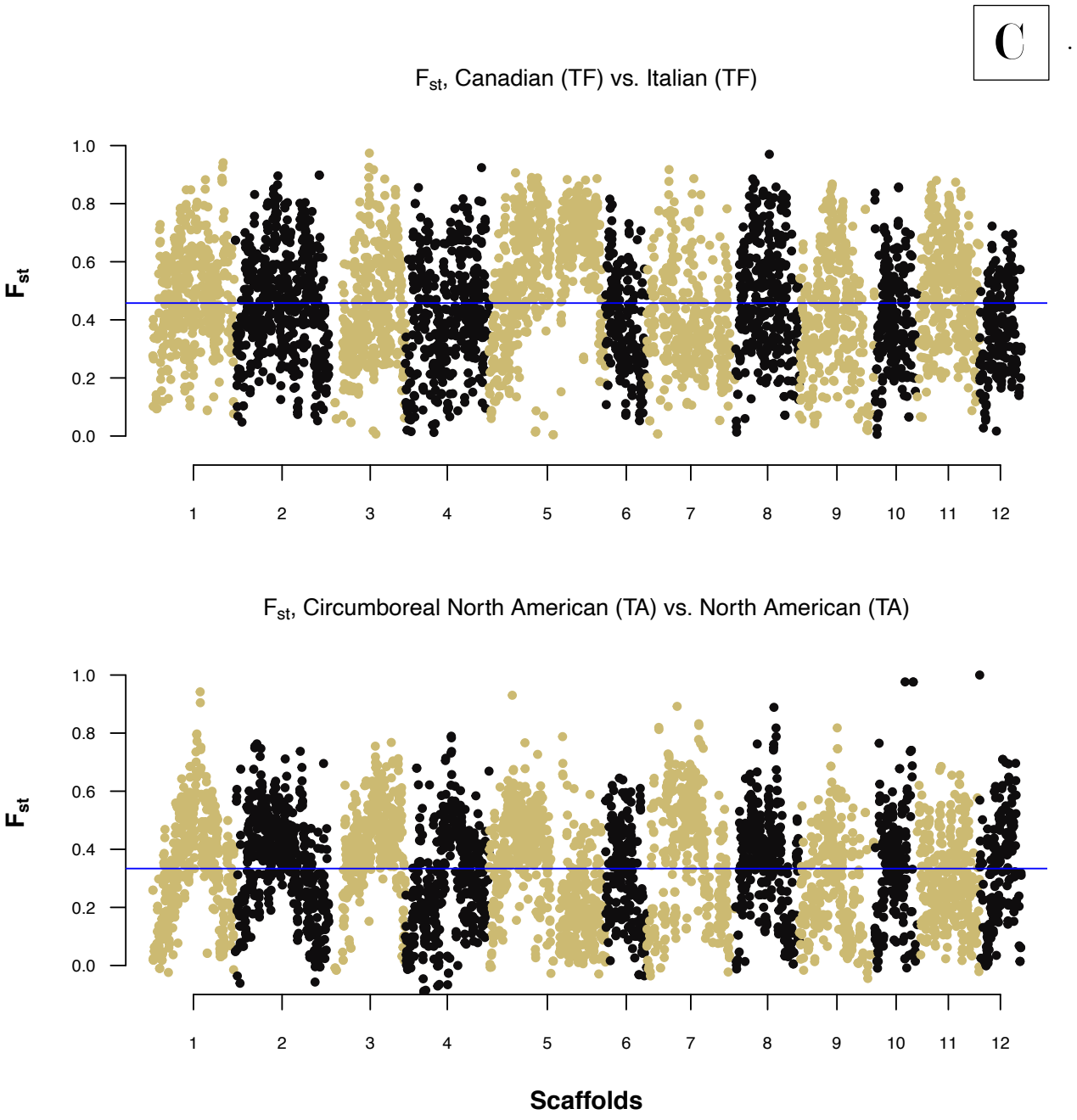

Figure S5, ***The sliding window fixation index (F_{ST}) analysis between*** **Trichaptum** ***species and populations revealed high divergence.*** *(A)* F_{ST} *between Circumboreal North American* T. abietinum *and two different* T fuscoviolaceum *populations. (B)* F_{ST} *between the North American* T. abietinum *and two different* T. fuscoviolaceum *populations. (C)* F_{ST} *between two* T. abietinum *populations and two* T. fuscoviolaceum *populations*. *The analysis is based on a nucleotide polymorphism (SNP) dataset of 3 065 109 SNPs. The x-axes represent scaffolds of the reference genome (alternating between beige and black), and the y-axes denote the* F_{ST} *value. Each point is the* F_{ST} *value within a certain window (window size of 20 000 base pairs with 10 000 base pairs overlap). The blue horizontal lines mark the mean* F_{ST} *value across the genome and the headers indicate between which populations the estimates are calculated. TF =* T. fuscoviolaceum *and TA =* T. abietinum*. The figure is made in R v4.0.2 GUI 1.72 Catalina build using RStudio v1.3.1073 and the packages qqman (Turner, 2017), tidyverse (Wickham et al., 2019) and wesanderson (Ram and Wickham, 2018).*

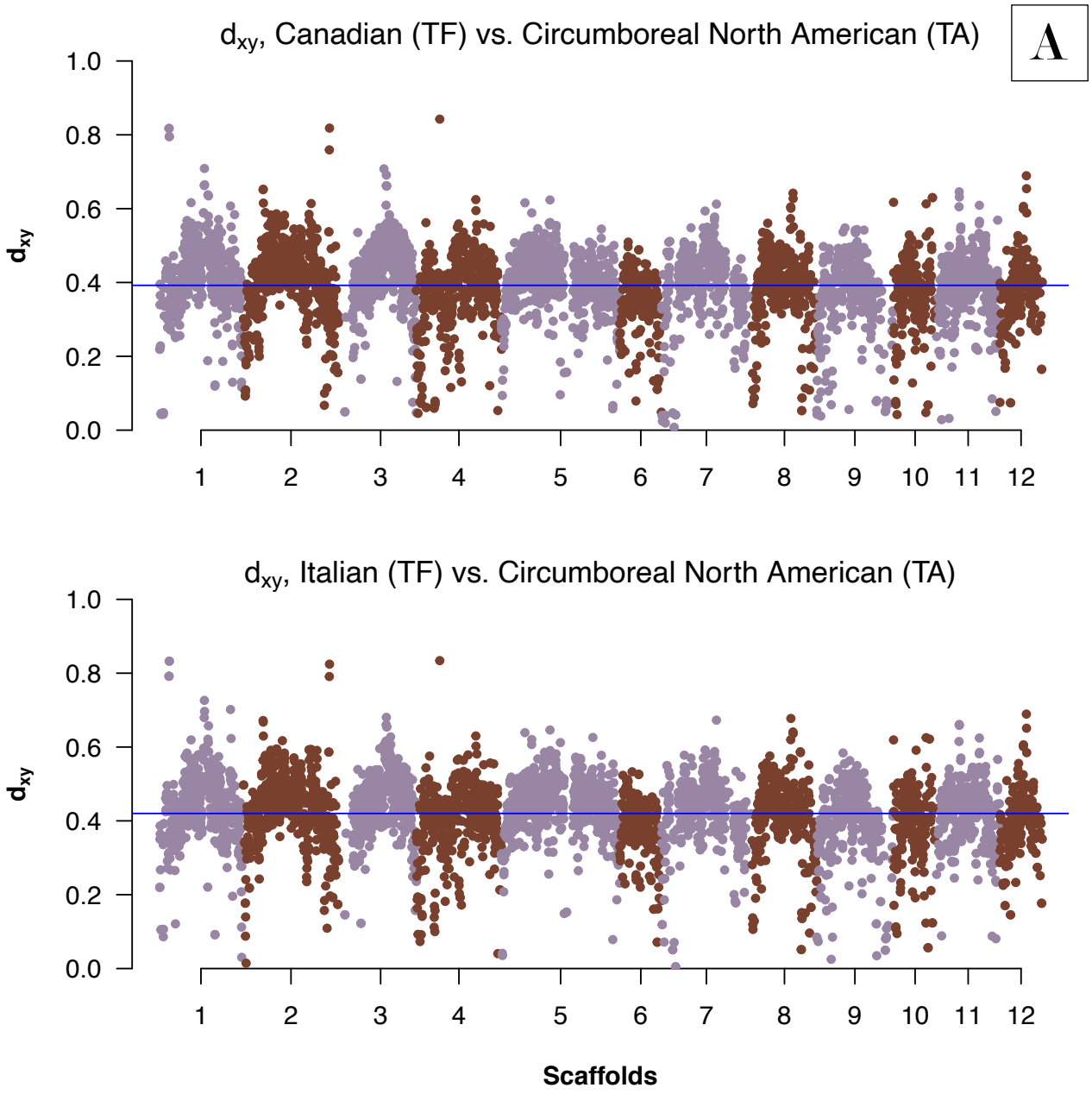
A
dxy, Canadian (TF) vs. Circumboreal North American (TA)
dxy, Italian (TF) vs. Circumboreal North American (TA)
dxy
1.0
0.8
0.6
0.4
0.2
0.0
1
2
3
4
5
6
7
8
9
10
11
12
Scaffolds

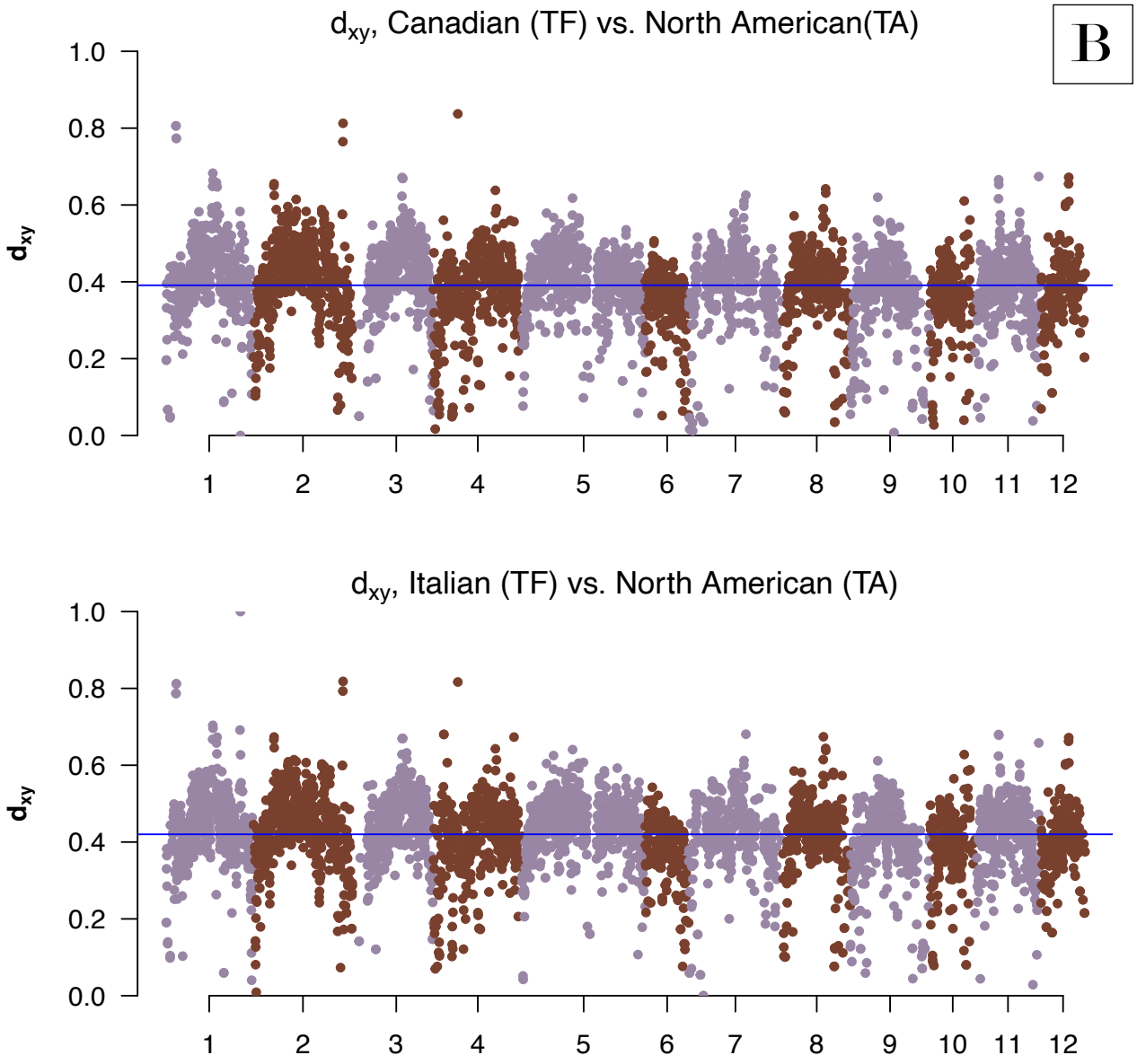
B
d_{xy}, Canadian (TF) vs. North American(TA)
d_{xy}, Italian (TF) vs. North American (TA)
d_{xy}
1.0
0.8
0.6
0.4
0.2
0.0
1
2
3
4
5
6
7
8
9
10
11
12

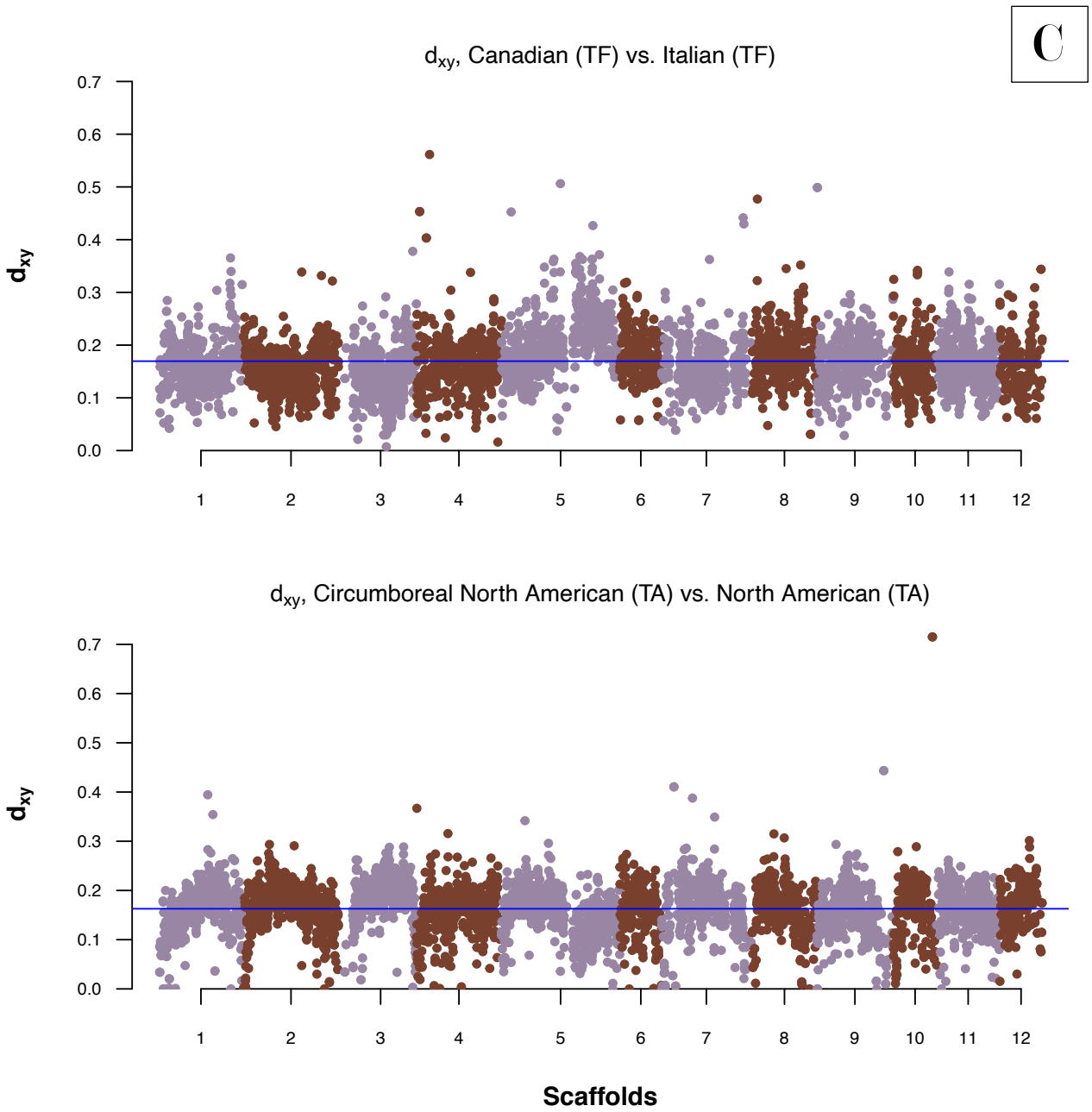

Figure S6, ***High divergence was reveled between*** **Trichaptum** ***species and populations in sliding window absolute divergence (*** d_{XY} ***) analyses.*** *(A)* d_{XY} *between Circumboreal North American* T. abietinum *and two different* T fuscoviolaceum *populations. (B)* d_{XY} *between the North American* T. abietinum *and two different* T. fuscoviolaceum *populations. (C)* d_{XY} *between two* T. abietinum *populations and two* T. fuscoviolaceum *populations. The analysis is based on a nucleotide polymorphism (SNP) dataset of 3 065 109 SNPs. The x-axes represent scaffolds of the reference genome (alternating between purple and burgundy), and the y-axes denote the* d_{XY} *value. Each point is the* d_{XY} *value within a certain window (window size of 20 000 base pairs with 10 000 base pairs overlap). The blue horizontal lines mark the mean* d_{XY} *value across the genome and the headers indicate between which populations the estimates are calculated. TF =* T. fuscoviolaceum *and TA =* T. abietinum*. The figure is made in R v4.0.2 GUI 1.72 Catalina build using RStudio v1.3.1073 and the packages qqman (Turner, 2017), tidyverse (Wickham et al., 2019) and wesanderson (Ram and Wickham, 2018).*

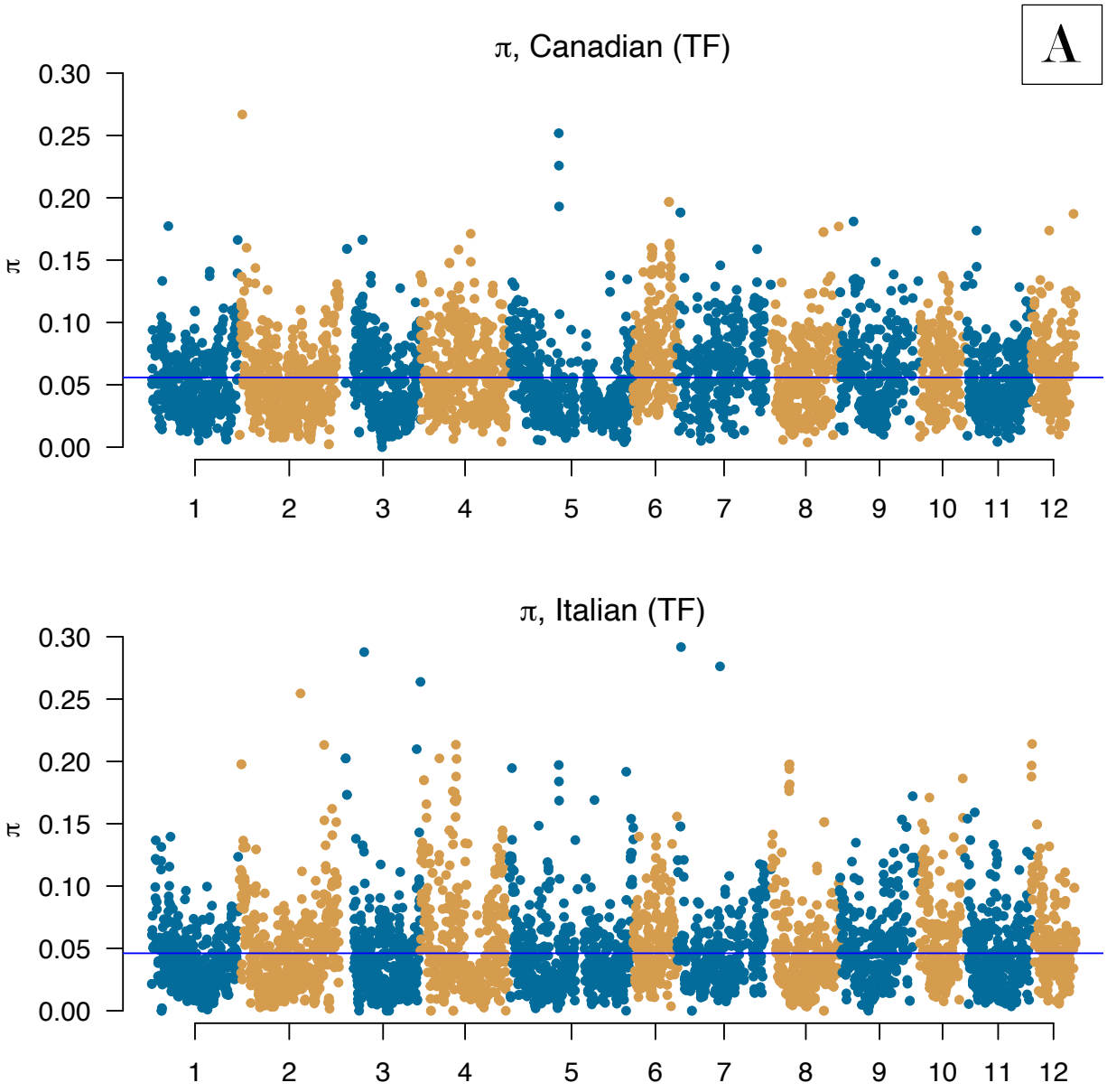
A
π, Canadian (TF)
π
0.30
0.25
0.20
0.15
0.10
0.05
0.00
1
2
3
4
5
6
7
8
9
10
11
12
π, Italian (TF)
π
0.30
0.25
0.20
0.15
0.10
0.05
0.00
1
2
3
4
5
6
7
8
9
10
11
12

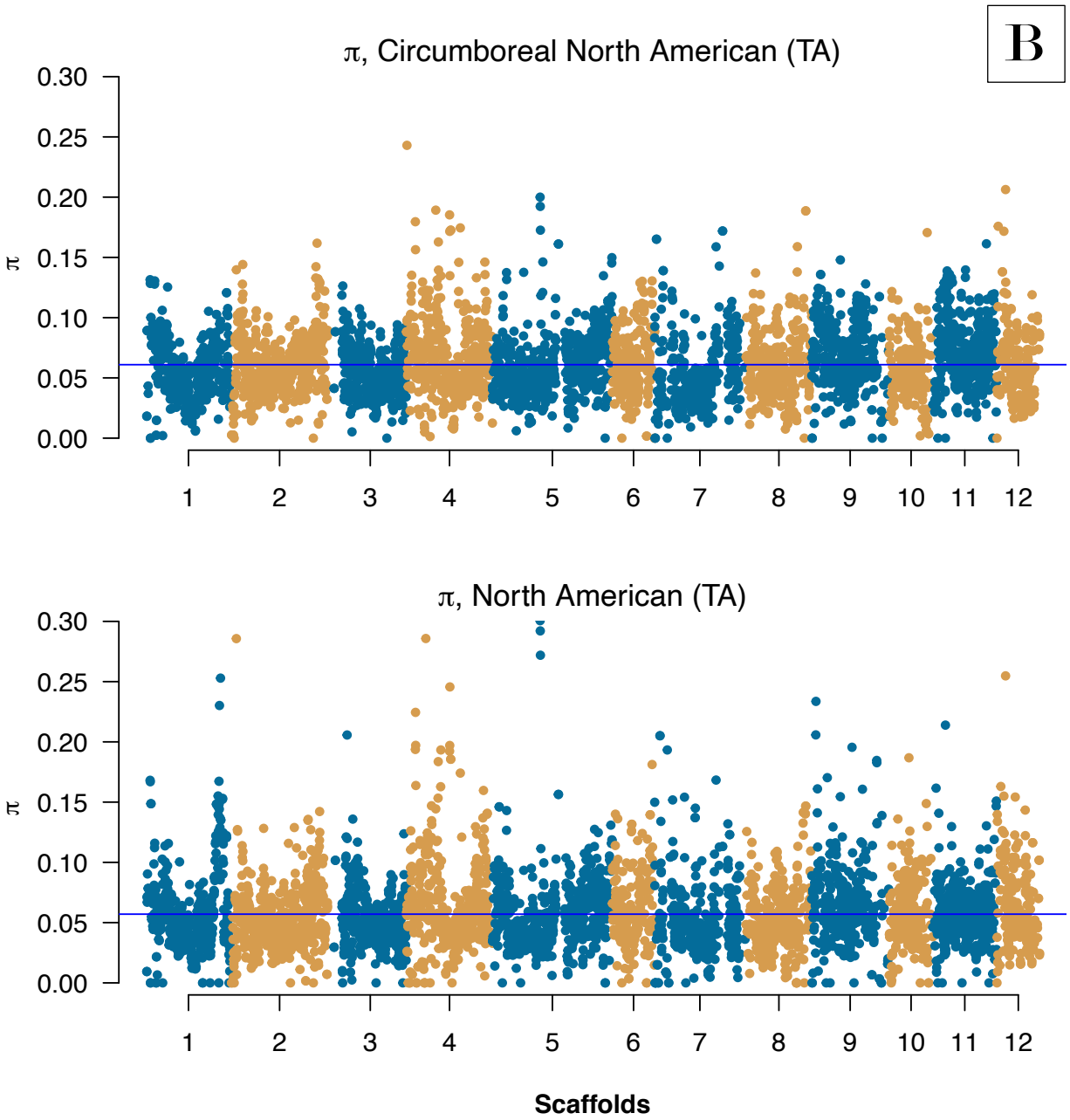

Figure S7, ***The sliding window nucleotide divergence (π) show moderate variation within populations.*** *Analysis of the* Trichaptum fuscoviolaceum *populations (A) and the* T. abietinum *populations (B) based on a nucleotide polymorphism (SNP) dataset of 3 065 109 SNPs. The x-axes represent scaffolds of the reference genome (alternating between blue and orange), and the y-axes denote the π value. Each point is the π value within a certain window (window size of 20 000 base pairs with 10 000 base pairs overlap). The blue horizontal lines mark the mean π value across the genome and the headers indicate for which populations the estimates are calculated. TF =* T. fuscoviolaceum *and TA =* T. abietinum*. The figure is made in R v4.0.2 GUI 1.72 Catalina build using RStudio v1.3.1073 and the packages qqman (Turner, 2017), tidyverse (Wickham et al., 2019) and wesanderson (Ram and Wickham, 2018).*

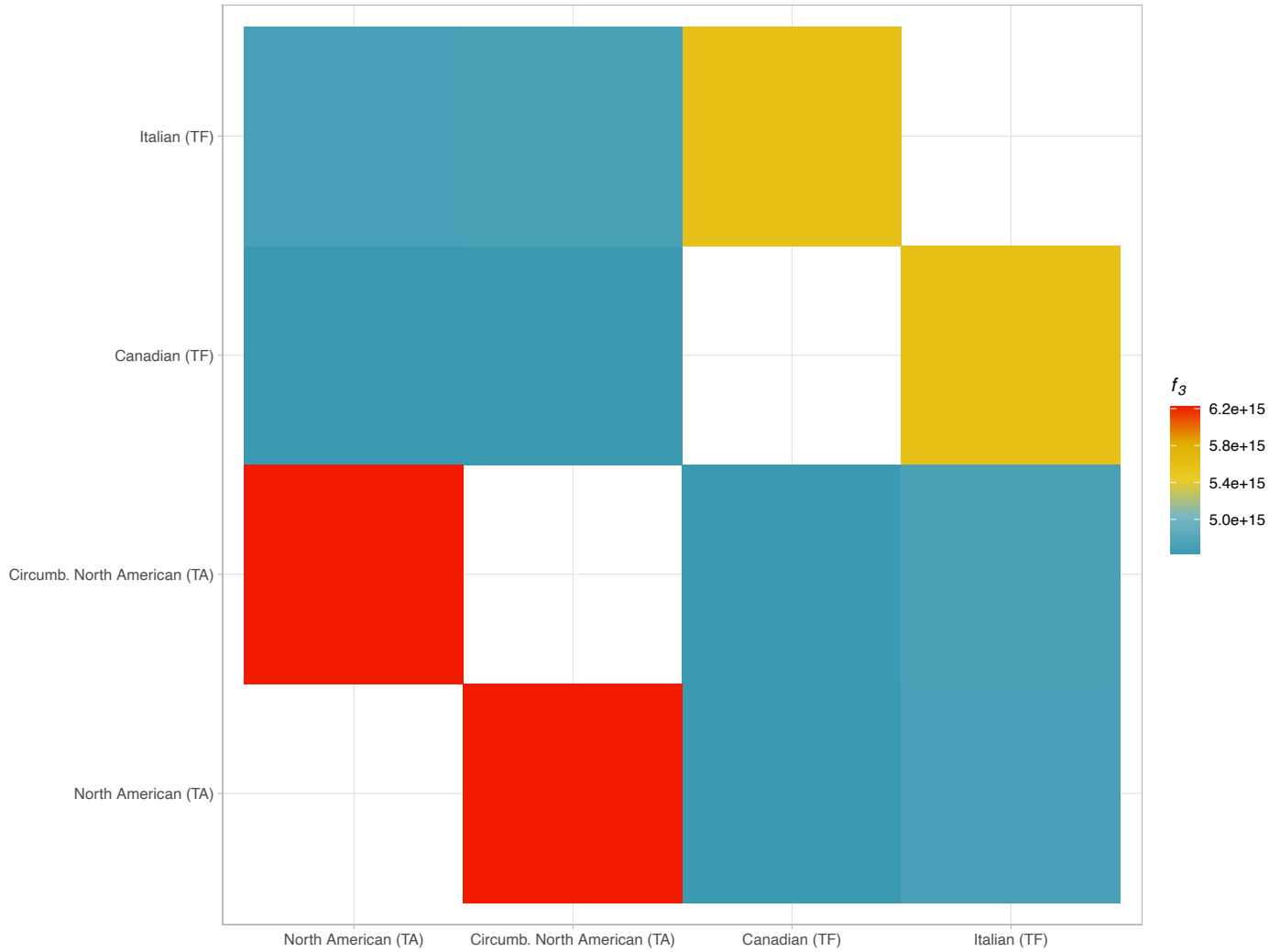

Figure S8, Trichaptum abietinum *populations split more recently than the* T. fuscoviolaceum *populations in the three-population* f-*statistic* (f_3) *with outgroup.* *The analysis is based on a single nucleotide polymorphism (SNP) dataset of 3 118 957 SNPs. The figure shows a pairwise comparison of populations colored by amount of shared evolutionary history. The analysis is based upon the phylogenetic hypothesis ((A, B), C)) in Newick tree format, where the branch lengths of A and B are estimated relative to C. All populations have been tested at position A and B, while C is kept constant as the outgroup* Trichaptum biforme. *As the legend on the right-hand side depicts, warmer colors indicate a later split (more shared genetic drift) between the two populations compared, while cooler colors indicate an earlier split (less shared genetic drift) between the populations. TF =* Trichaptum fuscoviolaceum*, TA =* T. abietinum *and Circumb. = Circumboreal. The figure is made in R v4.0.2 GUI 1.72 Catalina build using RStudio v1.3.1073 and the packages admixr (Petr, 2020), tidyverse (Wickham et al., 2019) and wesanderson (Ram and Wickham, 2018).*

Table S2, ***An overview of the 99.7% (three standard deviations) outliers from the*** f_{dM} ***genome scan.*** *The green and purple headers indicate the phylogenetic typology of the test in Newick tree format; (((P1, P2), P3), O), where P1, P2 and P3 are populations investigated for introgression and O is the outgroup. A positive* f_{dM} *value indicates more shared derived polymorphisms than expected between P2 and P3, while a negative value indicates more shared derived polymorphisms than expected between P1 and P3. The negative values are colored in blue in the* f_{dM} *column, and positive are in white. The table also denotes which scaffold the genes are in, including the start and end of the gene on that scaffold, how many sites that were used to estimate the* f_{dM} *value in the specific window, the name of the genes from the annotated genome, and a note on the function of the genes. TA* = Trichaptum abietinum *and TF* = T. fuscoviolaceum.

(((Circumboreal North American TA, North American TA), Canadian TF), *T. biforme*)						
Scaffold	**Start**	**End**	**Sites used**	f_{dM}	**Gene**	**Note**
Scaffold01	1272431	1274047	163	-0.1313	maker-Scaffold01-exonerate_protein2genome-gene-12.6	Protein of unknown function
Scaffold01	1263652	1264784	163	-0.1313	snap_masked-Scaffold01-processed-gene-12.8	Similar to RDT1: Elsinochrome reductase 1 (Elsinoe fawcettii OX=40997)
Scaffold01	1276633	1277652	163	-0.1313	snap_masked-Scaffold01-processed-gene-12.9	Similar to SPAC13G6.15c: Uncharacterized protein C13G6.15c (Schizosaccharomyces pombe (strain 972 / ATCC 24843) OX=284812)
Scaffold01	1268178	1271268	163	-0.1313	maker-Scaffold01-snap-gene-12.19	Protein of unknown function
Scaffold01	1274807	1276403	163	-0.1313	maker-Scaffold01-snap-gene-12.20	Protein of unknown function
Scaffold01	1265281	1266088	163	-0.1313	maker-Scaffold01-snap-gene-12.18	Protein of unknown function
Scaffold01	2975369	2975485	145	0.1387	maker-Scaffold01-exonerate_protein2genome-gene-29.152	Protein of unknown function
Scaffold02	891633	895671	210	-0.145	maker-Scaffold02-snap-gene-9.31	Protein of unknown function
Scaffold02	884108	889633	210	-0.145	maker-Scaffold02-snap-gene-9.30	Similar to brc1: BRCT-containing protein 1 (Schizosaccharomyces pombe (strain 972 / ATCC 24843) OX=284812)
Scaffold02	883386	884083	210	-0.145	maker-Scaffold02-snap-gene-9.29	Similar to PAXIP1: PAX-interacting protein 1 (Homo sapiens OX=9606)
Scaffold02	2355665	2357588	101	-0.139	maker-Scaffold02-snap-gene-23.33	Similar to hxpA: Hexitol phosphatase A (Escherichia coli (strain K12) OX=83333)
Scaffold03	1620126	1622452	117	0.1619	genemark-Scaffold03-processed-gene-16.4	Similar to GRC3: Polynucleotide 5'-hydroxyl-kinase GRC3 (Cryptococcus neoformans var. neoformans serotype D (strain JEC21 / ATCC MYA-565) OX=214684)

Scaffold03	1633221	1636431	117	0.1619	maker-Scaffold03-exonerate_protein2genome-gene-16.48	Similar to RDR1: Probable RNA-dependent RNA polymerase 1 (Oryza sativa subsp. japonica OX=39947)
Scaffold03	1637269	1638202	117	0.1619	maker-Scaffold03-exonerate_protein2genome-gene-16.56	Similar to SEC14: SEC14 cytosolic factor (Saccharomyces cerevisiae (strain ATCC 204508 / S288c) OX=559292)
Scaffold03	1624233	1626184	117	0.1619	maker-Scaffold03-snap-gene-16.42	Similar to DAL1: Allantoinase (Saccharomyces cerevisiae (strain ATCC 204508 / S288c) OX=559292)
Scaffold03	1632377	1632573	117	0.1619	maker-Scaffold03-exonerate_est2genome-gene-16.2	Protein of unknown function
Scaffold03	1632645	1632758	117	0.1619	maker-Scaffold03-exonerate_protein2genome-gene-16.47	Protein of unknown function
Scaffold03	1626282	1628466	117	0.1619	maker-Scaffold03-snap-gene-16.43	Protein of unknown function
Scaffold03	1631588	1632628	117	0.1619	maker-Scaffold03-snap-gene-16.54	Protein of unknown function
Scaffold03	1628643	1630494	117	0.1619	maker-Scaffold03-snap-gene-16.53	Protein of unknown function
Scaffold04	3575064	3576172	119	-0.1114	maker-Scaffold04-exonerate_protein2genome-gene-35.39	Protein of unknown function
Scaffold04	3573762	3574274	119	-0.1114	maker-Scaffold04-exonerate_protein2genome-gene-35.38	Protein of unknown function
Scaffold04	3561733	3570103	119	-0.1114	maker-Scaffold04-snap-gene-35.11	Similar to klpA: Kinesin-like protein klpA (Emericella nidulans (strain FGSC A4 / ATCC 38163 / CBS 112.46 / NRRL 194 / M139) OX=227321)
Scaffold04	3573842	3574267	119	-0.1114	snap_masked-Scaffold04-processed-gene-35.8	Protein of unknown function
Scaffold04	3570833	3571890	119	-0.1114	snap_masked-Scaffold04-processed-gene-35.7	Protein of unknown function
Scaffold04	940001	960000	120	-0.1136	No annotated genes	No annotated genes
Scaffold05	6945996	6946307	113	-0.1208	snap_masked-Scaffold05-processed-gene-69.55	Protein of unknown function
Scaffold05	6942608	6943541	113	-0.1208	maker-Scaffold05-snap-gene-69.28	Protein of unknown function
Scaffold05	6956284	6957955	113	-0.1208	maker-Scaffold05-exonerate_protein2genome-gene-69.115	Protein of unknown function
Scaffold05	6946976	6954608	113	-0.1208	maker-Scaffold05-snap-gene-69.44	Similar to abcd1: ATP-binding cassette sub-family D member 1 (Danio rerio OX=7955)
Scaffold05	6944073	6945290	113	-0.1208	maker-Scaffold05-snap-gene-69.43	Protein of unknown function
Scaffold05	6957990	6959021	113	-0.1208	maker-Scaffold05-snap-gene-69.31	Protein of unknown function

Scaffold05	712158	713655	125	0.1398	maker-Scaffold05-exonerate_protein2genome-gene-7.31	Similar to SPAC5D6.12: Uncharacterized protein C5D6.12 (Schizosaccharomyces pombe (strain 972 / ATCC 24843) OX=284812)
Scaffold05	718805	719236	125	0.1398	maker-Scaffold05-exonerate_protein2genome-gene-7.39	Protein of unknown function
Scaffold05	704321	707167	125	0.1398	maker-Scaffold05-snap-gene-7.2	Similar to STY8: Serine/threonine-protein kinase STY8 (Arabidopsis thaliana OX=3702)
Scaffold05	701713	703798	125	0.1398	maker-Scaffold05-exonerate_protein2genome-gene-7.20	Similar to pik-1: Pelle-like serine/threonine-protein kinase pik-1 (Caenorhabditis elegans OX=6239)
Scaffold05	707896	709998	125	0.1398	maker-Scaffold05-snap-gene-7.3	Similar to splB: Dual specificity protein kinase splB (Dictyostelium discoideum OX=44689)
Scaffold05	710120	711718	125	0.1398	maker-Scaffold05-snap-gene-7.16	Similar to SPAC4A8.06c: AB hydrolase superfamily protein C4A8.06c (Schizosaccharomyces pombe (strain 972 / ATCC 24843) OX=284812)
Scaffold05	713908	718057	125	0.1398	maker-Scaffold05-snap-gene-7.17	Similar to ARHGAP39: Rho GTPase-activating protein 39 (Homo sapiens OX=9606)
Scaffold05	360001	380000	136	-0.1253	No annotated genes	No annotated genes
Scaffold05	2380001	2400000	111	0.1137	No annotated genes	No annotated genes
Scaffold06	2087800	2089396	104	-0.1809	maker-Scaffold06-snap-gene-20.7	Protein of unknown function
Scaffold06	2094159	2096915	104	-0.1809	maker-Scaffold06-snap-gene-21.41	Similar to phyB: 3-phytase B (Emericella nidulans (strain FGSC A4 / ATCC 38163 / CBS 112.46 / NRRL 194 / M139) OX=227321)
Scaffold06	2088824	2091056	104	-0.1809	maker-Scaffold06-snap-gene-21.40	Similar to rpc6: Probable DNA-directed RNA polymerase III subunit rpc6 (Schizosaccharomyces pombe (strain 972 / ATCC 24843) OX=284812)
Scaffold06	2081074	2085675	104	-0.1809	maker-Scaffold06-snap-gene-21.38	Protein of unknown function
Scaffold06	2086284	2088111	104	-0.1809	maker-Scaffold06-snap-gene-21.39	Protein of unknown function
Scaffold07	3843021	3844141	167	0.1483	snap_masked-Scaffold07-abinit-gene-38.26	Protein of unknown function
Scaffold07	3848870	3850190	167	0.1483	maker-Scaffold07-exonerate_protein2genome-gene-38.89	Protein of unknown function

Scaffold07	3850825	3853362	167	0.1483	maker-Scaffold07-snap-gene-38.40	Similar to exosc3: Putative exosome complex component rrp40 (Dictyostelium discoideum OX=44689)
Scaffold07	3840869	3842531	167	0.1483	maker-Scaffold07-snap-gene-38.79	Similar to ZFAND2A: AN1-type zinc finger protein 2A (Pongo abelii OX=9601)
Scaffold07	3845137	3848851	167	0.1483	maker-Scaffold07-snap-gene-38.49	Similar to PHB2: Prohibitin-2 (Saccharomyces cerevisiae (strain ATCC 204508 / S288c) OX=559292)
Scaffold07	3853955	3856502	167	0.1483	maker-Scaffold07-snap-gene-38.51	Protein of unknown function
Scaffold07	3857642	3858990	167	0.1483	maker-Scaffold07-snap-gene-38.52	Protein of unknown function
Scaffold08	987415	988459	111	0.1333	maker-Scaffold08-snap-gene-9.25	Protein of unknown function
Scaffold08	990859	996481	111	0.1333	maker-Scaffold08-snap-gene-10.13	Protein of unknown function
Scaffold08	998636	999746	111	0.1333	maker-Scaffold08-exonerate_protein2genome-gene-10.16	Similar to ECI3: Enoyl-CoA delta isomerase 3 (Arabidopsis thaliana OX=3702)
Scaffold08	996522	997428	111	0.1333	maker-Scaffold08-snap-gene-10.18	Protein of unknown function
Scaffold08	990031	990293	111	0.1333	maker-Scaffold08-exonerate_protein2genome-gene-10.96	Protein of unknown function
Scaffold08	997701	997814	111	0.1333	trnascan-Scaffold08-noncoding-Gly_GCC-gene-10.66	Protein of unknown function
Scaffold09	980952	985182	102	-0.1463	maker-Scaffold09-snap-gene-9.12	Similar to vrtI: Oxidoreductase vrtI (Penicillium aethiopicum OX=36650)
Scaffold09	995656	999766	102	-0.1463	maker-Scaffold09-snap-gene-10.11	Similar to COQ8: Atypical kinase COQ8 mitochondrial (Saccharomyces cerevisiae (strain ATCC 204508 / S288c) OX=559292)
Scaffold10	2106777	2108857	123	-0.1314	maker-Scaffold10-snap-gene-21.55	Protein of unknown function
Scaffold10	2110415	2112040	123	-0.1314	maker-Scaffold10-exonerate_protein2genome-gene-21.42	Similar to asnS: Asparagine--tRNA ligase (Pseudoalteromonas haloplanktis (strain TAC 125) OX=326442)
Scaffold10	2113238	2116089	123	-0.1314	snap_masked-Scaffold10-processed-gene-21.23	Protein of unknown function
Scaffold10	2117353	2118482	123	-0.1314	snap_masked-Scaffold10-processed-gene-21.24	Protein of unknown function
Scaffold10	2103403	2105467	123	-0.1314	snap_masked-Scaffold10-processed-gene-21.20	Similar to lgd1: L-galactonate dehydratase (Hypocrea jecorina OX=51453)

Scaffold10	2102509	2103129	123	-0.1314	maker-Scaffold10-exonerate_protein2genome-gene-21.33	Protein of unknown function
Scaffold10	2118762	2119891	123	-0.1314	maker-Scaffold10-snap-gene-21.76	Protein of unknown function
Scaffold10	2108816	2110680	123	-0.1314	snap_masked-Scaffold10-processed-gene-21.41	Similar to cwf23: Pre-mRNA-splicing factor cwf23 (Schizosaccharomyces pombe (strain 972 / ATCC 24843) OX=284812)
Scaffold10	2100500	2101755	123	-0.1314	maker-Scaffold10-exonerate_protein2genome-gene-21.154	Similar to BAR2: Pheromone B alpha 2 receptor (Schizophyllum commune OX=5334)
Scaffold10	2112239	2112786	123	-0.1314	snap_masked-Scaffold10-processed-gene-21.42	Similar to smd1: Small nuclear ribonucleoprotein Sm D1 (Schizosaccharomyces pombe (strain 972 / ATCC 24843) OX=284812)
Scaffold10	1742972	1744147	241	0.1656	snap_masked-Scaffold10-processed-gene-17.14	Protein of unknown function
Scaffold10	1744941	1746814	241	0.1656	snap_masked-Scaffold10-processed-gene-17.15	Similar to MEL: Alpha-galactosidase (Saccharomyces mikatae OX=114525)
Scaffold10	1740426	1741739	241	0.1656	snap_masked-Scaffold10-abinit-gene-17.14	Protein of unknown function
Scaffold11	581399	585397	203	-0.1331	maker-Scaffold11-augustus-gene-5.5	Protein of unknown function
Scaffold12	1804679	1805250	173	-0.133	maker-Scaffold12-augustus-gene-18.1	Protein of unknown function
Scaffold12	1807223	1809082	173	-0.133	maker-Scaffold12-snap-gene-18.46	Similar to RED1: NADP-dependent oxidoreductase RED1 (Cochliobolus heterostrophus (strain C4 / ATCC 48331 / race T) OX=665024)
Scaffold12	1818810	1819010	173	-0.133	snap_masked-Scaffold12-processed-gene-18.17	Similar to SPAPB24D3.08c: Zinc-type alcohol dehydrogenase-like protein PB24D3.08c (Schizosaccharomyces pombe (strain 972 / ATCC 24843) OX=284812)
Scaffold12	1812320	1817407	173	-0.133	maker-Scaffold12-snap-gene-18.62	Similar to utp7: Probable U3 small nucleolar RNA-associated protein 7 (Schizosaccharomyces pombe (strain 972 / ATCC 24843) OX=284812)
Scaffold12	1809234	1811268	173	-0.133	maker-Scaffold12-snap-gene-18.61	Similar to RED1: NADP-dependent oxidoreductase RED1 (Cochliobolus heterostrophus (strain C4 / ATCC 48331 / race T) OX=665024)
Scaffold12	1802320	1804441	173	-0.133	genemark-Scaffold12-processed-gene-18.20	Protein of unknown function

Scaffold12	1882007	1884023	157	-0.1571	maker-Scaffold12-snap-gene-18.58	Similar to LAS17: Proline-rich protein LAS17 (Saccharomyces cerevisiae (strain ATCC 204508 / S288c) OX=559292)
Scaffold12	1892128	1892597	157	-0.1571	maker-Scaffold12-exonerate_protein2genome-gene-19.2	Protein of unknown function
Scaffold12	1888312	1889117	157	-0.1571	maker-Scaffold12-exonerate_protein2genome-gene-19.0	Similar to tea4: Tip elongation aberrant protein Tea4 (Schizosaccharomyces pombe (strain 972 / ATCC 24843) OX=284812)
Scaffold12	1886454	1890769	157	-0.1571	maker-Scaffold12-snap-gene-19.49	Similar to CMD1: Calmodulin (Pleurotus ostreatus OX=5322)
Scaffold12	1895963	1897078	157	-0.1571	maker-Scaffold12-exonerate_protein2genome-gene-19.138	Protein of unknown function
Scaffold12	1892859	1895135	157	-0.1571	maker-Scaffold12-snap-gene-19.50	Similar to HT1: Serine/threonine/tyrosine-protein kinase HT1 (Arabidopsis thaliana OX=3702)
Scaffold12	1897700	1898159	157	-0.1571	maker-Scaffold12-snap-gene-19.35	Protein of unknown function
(((Circumboreal North American TA, North American TA), Italian TF), *T. biforme*)						
Scaffold	**Start**	**End**	**Sites used**	**f_{dM}**	**Gene**	**Note**
Scaffold01	983792	985118	112	-0.1194	maker-Scaffold01-snap-gene-9.27	Protein of unknown function
Scaffold01	986524	993296	112	-0.1194	maker-Scaffold01-snap-gene-10.0	Similar to DODA: DOPA 4 5-dioxygenase (Amanita muscaria OX=41956)
Scaffold01	1272431	1274047	148	-0.1235	maker-Scaffold01-exonerate_protein2genome-gene-12.6	Protein of unknown function
Scaffold01	1263652	1264784	148	-0.1235	snap_masked-Scaffold01-processed-gene-12.8	Similar to RDT1: Elsinochrome reductase 1 (Elsinoe fawcettii OX=40997)
Scaffold01	1276633	1277652	148	-0.1235	snap_masked-Scaffold01-processed-gene-12.9	Similar to SPAC13G6.15c: Uncharacterized protein C13G6.15c (Schizosaccharomyces pombe (strain 972 / ATCC 24843) OX=284812)
Scaffold01	1268178	1271268	148	-0.1235	maker-Scaffold01-snap-gene-12.19	Protein of unknown function
Scaffold01	1274807	1276403	148	-0.1235	maker-Scaffold01-snap-gene-12.20	Protein of unknown function
Scaffold01	1265281	1266088	148	-0.1235	maker-Scaffold01-snap-gene-12.18	Protein of unknown function
Scaffold01	913710	915599	133	0.1251	maker-Scaffold01-snap-gene-9.5	Similar to COX17: Cytochrome c oxidase copper chaperone (Homo sapiens OX=9606)

Scaffold01	906260	907088	133	0.1251	maker-Scaffold01-exonerate_protein2genome-gene-9.29	Protein of unknown function
Scaffold01	901468	902851	133	0.1251	snap_masked-Scaffold01-processed-gene-9.31	Protein of unknown function
Scaffold01	902938	905385	133	0.1251	snap_masked-Scaffold01-processed-gene-9.39	Protein of unknown function
Scaffold01	918913	919817	133	0.1251	snap_masked-Scaffold01-abinit-gene-9.25	Protein of unknown function
Scaffold01	915247	917294	133	0.1251	maker-Scaffold01-snap-gene-9.16	Similar to GST: Glutathione S-transferase (Plasmodium vivax OX=5855)
Scaffold01	912091	912422	133	0.1251	snap_masked-Scaffold01-processed-gene-9.40	Similar to EMC4: ER membrane protein complex subunit 4 (Saccharomyces cerevisiae (strain ATCC 204508 / S288c) OX=559292)
Scaffold01	909092	910780	133	0.1251	maker-Scaffold01-snap-gene-9.4	Protein of unknown function
Scaffold01	900331	900881	133	0.1251	maker-Scaffold01-snap-gene-9.2	Protein of unknown function
Scaffold02	891633	895671	197	-0.1472	maker-Scaffold02-snap-gene-9.31	Protein of unknown function
Scaffold02	884108	889633	197	-0.1472	maker-Scaffold02-snap-gene-9.30	Similar to brc1: BRCT-containing protein 1 (Schizosaccharomyces pombe (strain 972 / ATCC 24843) OX=284812)
Scaffold02	883386	884083	197	-0.1472	maker-Scaffold02-snap-gene-9.29	Similar to PAXIP1: PAX-interacting protein 1 (Homo sapiens OX=9606)
Scaffold03	1620126	1622452	106	0.1538	genemark-Scaffold03-processed-gene-16.4	Similar to GRC3: Polynucleotide 5'-hydroxyl-kinase GRC3 (Cryptococcus neoformans var. neoformans serotype D (strain JEC21 / ATCC MYA-565) OX=214684)
Scaffold03	1633221	1636431	106	0.1538	maker-Scaffold03-exonerate_protein2genome-gene-16.48	Similar to RDR1: Probable RNA-dependent RNA polymerase 1 (Oryza sativa subsp. japonica OX=39947)
Scaffold03	1637269	1638202	106	0.1538	maker-Scaffold03-exonerate_protein2genome-gene-16.56	Similar to SEC14: SEC14 cytosolic factor (Saccharomyces cerevisiae (strain ATCC 204508 / S288c) OX=559292)
Scaffold03	1624233	1626184	106	0.1538	maker-Scaffold03-snap-gene-16.42	Similar to DAL1: Allantoinase (Saccharomyces cerevisiae (strain ATCC 204508 / S288c) OX=559292)

Scaffold03	1632377	1632573	106	0.1538	maker-Scaffold03-exonerate_est2genome-gene-16.2	Protein of unknown function
Scaffold03	1632645	1632758	106	0.1538	maker-Scaffold03-exonerate_protein2genome-gene-16.47	Protein of unknown function
Scaffold03	1626282	1628466	106	0.1538	maker-Scaffold03-snap-gene-16.43	Protein of unknown function
Scaffold03	1631588	1632628	106	0.1538	maker-Scaffold03-snap-gene-16.54	Protein of unknown function
Scaffold03	1628643	1630494	106	0.1538	maker-Scaffold03-snap-gene-16.53	Protein of unknown function
Scaffold04	956159	956359	120	-0.1136	maker-Scaffold04-exonerate_protein2genome-gene-9.61	Protein of unknown function
Scaffold04	944673	946836	120	-0.1136	genemark-Scaffold04-processed-gene-9.10	Similar to COX2: Cytochrome P450 monooxygenase COX2 (Coprinopsis cinerea (strain Okayama-7 / 130 / ATCC MYA-4618 / FGSC 9003) OX=240176)
Scaffold04	956861	958976	120	-0.1136	genemark-Scaffold04-processed-gene-9.12	Similar to COX2: Cytochrome P450 monooxygenase COX2 (Coprinopsis cinerea (strain Okayama-7 / 130 / ATCC MYA-4618 / FGSC 9003) OX=240176)
Scaffold04	951321	953201	120	-0.1136	maker-Scaffold04-exonerate_protein2genome-gene-9.55	Protein of unknown function
Scaffold04	955395	955664	120	-0.1136	maker-Scaffold04-exonerate_protein2genome-gene-9.60	Protein of unknown function
Scaffold04	946874	950562	120	-0.1136	genemark-Scaffold04-processed-gene-9.25	Similar to nps10: Adenylate-forming reductase Nps10 (Heterobasidion annosum OX=13563)
Scaffold04	953812	955239	120	-0.1136	maker-Scaffold04-exonerate_protein2genome-gene-9.213	Similar to Coq2: 4-hydroxybenzoate polyprenyltransferase mitochondrial (Drosophila melanogaster OX=7227)
Scaffold04	941265	942991	120	-0.1136	maker-Scaffold04-exonerate_protein2genome-gene-9.190	Protein of unknown function
Scaffold04	3575064	3576172	119	-0.1114	maker-Scaffold04-exonerate_protein2genome-gene-35.39	Protein of unknown function
Scaffold04	3573762	3574274	119	-0.1114	maker-Scaffold04-exonerate_protein2genome-gene-35.38	Protein of unknown function
Scaffold04	3561733	3570103	119	-0.1114	maker-Scaffold04-snap-gene-35.11	Similar to klpA: Kinesin-like protein klpA (Emericella nidulans (strain FGSC A4 / ATCC 38163 / CBS 112.46 / NRRL 194 / M139) OX=227321)
Scaffold04	3573842	3574267	119	-0.1114	snap_masked-Scaffold04-processed-gene-35.8	Protein of unknown function
Scaffold04	3570833	3571890	119	-0.1114	snap_masked-Scaffold04-processed-gene-35.7	Protein of unknown function

Scaffold04	2356438	2357580	167	0.1162	maker-Scaffold04-exonerate_protein2genome-gene-23.84	Similar to panC: Pantothenate synthetase (Moorella thermoacetica (strain ATCC 39073 / JCM 9320) OX=264732)
Scaffold04	2340374	2351183	167	0.1162	maker-Scaffold04-augustus-gene-23.58	Similar to Phenol hydroxylase (Cutaneotrichosporon cutaneum OX=5554)
Scaffold04	2346097	2347849	167	0.1162	maker-Scaffold04-snap-gene-23.59	Protein of unknown function
Scaffold04	2352453	2353590	167	0.1162	maker-Scaffold04-exonerate_protein2genome-gene-23.184	Similar to LECRK42: L-type lectin-domain containing receptor kinase IV.2 (Arabidopsis thaliana OX=3702)
Scaffold05	367059	369239	136	-0.1253	maker-Scaffold05-snap-gene-3.62	Similar to apdF: Aspyridones efflux protein apdF (Emericella nidulans (strain FGSC A4 / ATCC 38163 / CBS 112.46 / NRRL 194 / M139) OX=227321)
Scaffold05	363913	364996	136	-0.1253	genemark-Scaffold05-processed-gene-3.16	Protein of unknown function
Scaffold05	362571	363375	136	-0.1253	maker-Scaffold05-snap-gene-3.60	Similar to UK114: RutC family protein UK114 (Drosophila melanogaster OX=7227)
Scaffold05	370136	371660	136	-0.1253	maker-Scaffold05-exonerate_protein2genome-gene-3.77	Protein of unknown function
Scaffold05	361778	363285	136	-0.1253	maker-Scaffold05-snap-gene-3.74	Protein of unknown function
Scaffold05	375695	376255	136	-0.1253	genemark-Scaffold05-processed-gene-3.34	Protein of unknown function
Scaffold05	6945996	6946307	113	-0.1208	snap_masked-Scaffold05-processed-gene-69.55	Protein of unknown function
Scaffold05	6942608	6943541	113	-0.1208	maker-Scaffold05-snap-gene-69.28	Protein of unknown function
Scaffold05	6956284	6957955	113	-0.1208	maker-Scaffold05-exonerate_protein2genome-gene-69.115	Protein of unknown function
Scaffold05	6946976	6954608	113	-0.1208	maker-Scaffold05-snap-gene-69.44	Similar to abcd1: ATP-binding cassette sub-family D member 1 (Danio rerio OX=7955)
Scaffold05	6944073	6945290	113	-0.1208	maker-Scaffold05-snap-gene-69.43	Protein of unknown function
Scaffold05	6957990	6959021	113	-0.1208	maker-Scaffold05-snap-gene-69.31	Protein of unknown function
Scaffold05	2389277	2393966	111	0.1137	maker-Scaffold05-snap-gene-24.8	Protein of unknown function
Scaffold05	2480001	2500000	125	0.1398	No annotated genes	No annotated genes
Scaffold07	3843021	3844141	163	0.1162	snap_masked-Scaffold07-abinit-gene-38.26	Protein of unknown function
Scaffold07	3848870	3850190	163	0.1162	maker-Scaffold07-exonerate_protein2genome-gene-38.89	Protein of unknown function

Scaffold07	3850825	3853362	163	0.1162	maker-Scaffold07-snap-gene-38.40	Similar to exosc3: Putative exosome complex component rrp40 (Dictyostelium discoideum OX=44689)
Scaffold07	3840869	3842531	163	0.1162	maker-Scaffold07-snap-gene-38.79	Similar to ZFAND2A: AN1-type zinc finger protein 2A (Pongo abelii OX=9601)
Scaffold07	3845137	3848851	163	0.1162	maker-Scaffold07-snap-gene-38.49	Similar to PHB2: Prohibitin-2 (Saccharomyces cerevisiae (strain ATCC 204508 / S288c) OX=559292)
Scaffold07	3853955	3856502	163	0.1162	maker-Scaffold07-snap-gene-38.51	Protein of unknown function
Scaffold07	3857642	3858990	163	0.1162	maker-Scaffold07-snap-gene-38.52	Protein of unknown function
Scaffold08	987415	988459	107	0.1363	maker-Scaffold08-snap-gene-9.25	Protein of unknown function
Scaffold08	990859	996481	107	0.1363	maker-Scaffold08-snap-gene-10.13	Protein of unknown function
Scaffold08	998636	999746	107	0.1363	maker-Scaffold08-exonerate_protein2genome-gene-10.16	Similar to ECI3: Enoyl-CoA delta isomerase 3 (Arabidopsis thaliana OX=3702)
Scaffold08	996522	997428	107	0.1363	maker-Scaffold08-snap-gene-10.18	Protein of unknown function
Scaffold08	990031	990293	107	0.1363	maker-Scaffold08-exonerate_protein2genome-gene-10.96	Protein of unknown function
Scaffold08	997701	997814	107	0.1363	trnascan-Scaffold08-noncoding-Gly_GCC-gene-10.66	Protein of unknown function
Scaffold10	1742972	1744147	222	0.1555	snap_masked-Scaffold10-processed-gene-17.14	Protein of unknown function
Scaffold10	1744941	1746814	222	0.1555	snap_masked-Scaffold10-processed-gene-17.15	Similar to MEL: Alpha-galactosidase (Saccharomyces mikatae OX=114525)
Scaffold10	1740426	1741739	222	0.1555	snap_masked-Scaffold10-abinit-gene-17.14	Protein of unknown function
Scaffold11	2846866	2850623	110	0.1194	genemark-Scaffold11-processed-gene-28.8	Protein of unknown function
Scaffold11	2845048	2846438	110	0.1194	maker-Scaffold11-snap-gene-28.58	Similar to SLC25A17: Peroxisomal membrane protein PMP34 (Homo sapiens OX=9606)
Scaffold12	1804679	1805250	184	-0.1456	maker-Scaffold12-augustus-gene-18.1	Protein of unknown function
Scaffold12	1807223	1809082	184	-0.1456	maker-Scaffold12-snap-gene-18.46	Similar to RED1: NADP-dependent oxidoreductase RED1 (Cochliobolus heterostrophus (strain C4 / ATCC 48331 / race T) OX=665024)
Scaffold12	1818810	1819010	184	-0.1456	snap_masked-Scaffold12-processed-gene-18.17	Similar to SPAPB24D3.08c: Zinc-type alcohol dehydrogenase-like protein PB24D3.08c

						(Schizosaccharomyces pombe (strain 972 / ATCC 24843) OX=284812)
Scaffold12	1812320	1817407	184	-0.1456	maker-Scaffold12-snap-gene-18.62	Similar to utp7: Probable U3 small nucleolar RNA-associated protein 7 (Schizosaccharomyces pombe (strain 972 / ATCC 24843) OX=284812)
Scaffold12	1809234	1811268	184	-0.1456	maker-Scaffold12-snap-gene-18.61	Similar to RED1: NADP-dependent oxidoreductase RED1 (Cochliobolus heterostrophus (strain C4 / ATCC 48331 / race T) OX=665024)
Scaffold12	1802320	1804441	184	-0.1456	genemark-Scaffold12-processed-gene-18.20	Protein of unknown function